Column Experiments Simulating Various Scenarios for Arsenic Mobilisation in Bangladesh

Heidi Lißner

TRENT UNIVERSITY

University Of Dhaka

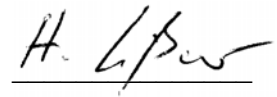## Declaration of Authorship

I certify that the work presented here is, to the best of my knowledge and belief, original and the result of my own investigations. Special assistance and information I received as well as utilized published information are properly and duly acknowledged.

Freiberg, 1st of March 2008

_____

Signature

Acknowledgements

List of Contents

List of Tables

List of Figures

List of Abbreviations

AGW	Artificial groundwater
DIC	Dissolved inorganic carbon
DOC	Dissolved organic carbon
DOM	Dissolved organic matter
Eh	Redox potential
IC-ICP-MS	Ion chromatography-inductively coupled plasma mass spectrometry
ICP-MS	Inductively coupled plasma mass spectrometry
MDL	Method detection limit
MQ	Milli-Q, ultrapure water
NDIR	Non-dispersive infrared analysis
OM	Organic matter
PE	Polyethylene
pH	pH-value
PVC	Polyvinyl chloride
R^2	R-square, coefficient of determination
rpm	Rotations per minute
SI	Saturation Index
StDev	Standard Deviation
TC	Total carbon
TIC	Total inorganic carbon
TOC	Total organic carbon
USDA	United States Department for Agriculture
WHO	World Health Organisation
XRD	X-Ray diffraction

Abstract

To study mechanisms of Arsenic (As) mobilization into the groundwater, sediments were collected from core drilling in Comilla District, Bangladesh, where 60 % of the wells exceed the international drinking water guideline for As of 50 µg/L. Sediment properties and mineralogy were investigated in the surficial silty layer, the shallow aquifer (5 to 27 m), the underlying thick aquiclude (52 m thick), the deep aquifer (79 to 83 m), and the deepest aquiclude (> 83 m) of the depth profile. The shallow aquifer sediments were grey in colour, probably due to reducing conditions, while the deeper aquifer consisted of brown sand, indicating an oxidized milieu and the presence of iron(hydr)oxides. The degradation of peat, found in 61 to 73 m, released high concentrations ammonium and phosphorus into the underlying deeper aquifer, which is associated with high contents of dissolved iron, mainly Fe(II), assuming the reductive dissolution of iron(hydr)oxides supporting As release. Batch experiments to determine the sorption and leaching mechanisms revealed a strong retention of As in the aquiclude sediments, dominated by clay and mica. Arsenic sorption rates were higher for the oxidized aquifer material than for the grey sediments in the shallow aquifer, implying As sorption on iron(hydr)oxides. The observed partial oxidation of arsenite to arsenate in the sediment-solutions mixtures suggests microbial oxidation of arsenite or the contact with oxidative soil compounds, such as MnO_2. Arsenic leaching in 0.04 M $NaHCO_3$ released very small quantities of As in solution, thus bicarbonate does not seem to contribute to As mobilization from the Bangladesh sediments. In column experiments on the competition between arsenate and phosphate for exchangeable sites has shown that both anions formed stable surface complexes, resulting in a non-exchangeable fraction; yet apparently, arsenate had a higher affinity for mineral surfaces than did phosphate. In contrast, arsenite and monothioarsenate exhibited a greater mobility through the columns, indicating weaker bonding structures. The effect of bicarbonate (0.01 to 0.1 M) on As release from the mineral phases As_2O_3 and As_2S_3 demonstrated a bicarbonate dependent dissolution of As_2S_3, while the solubility of As_2O_3 seemed unaffected. The results from As_2S_3 dissolution for a pH range from 3 to 12 indicated that under anoxic conditions, increasing pH promoted the dissolution rate and thereby also regulated the formation of arsenic-sulphur species.

1. Objectives

Bangladesh is highly affected by arsenic contamination in drinking water, and millions of people still suffer from arsenic poising. The conditions that lead to As mobilization in Bangladesh groundwater are understood only in a general sense, but the origin of arsenic is still not clear. The aim of this study is to understand and elucidate how different processes and mechanisms may influence and enhance arsenic mobility in Bangladesh's aquifers.

The objects of the study were to:

- Log the stratigraphy of an 84 m deep drilling as a basis for the establishment of a test field, with 7 wells tapping different aquifers in different depths.
- Determine associations between sediment properties (e.g., mineralogy, content of organic matter, iron, manganese, and phosphorus…) and arsenic contents to identify triggers for arsenic mobilization.
- Determine the sorption capacity of the different lithological units for arsenite, arsenate, and phosphate in different solutions.
- Observe the sorption behaviour of specific anions (AsO_3^{3-}, AsO_4^{3-}, AsO_3S^{3-}, and PO_4^{3-}) on the sediment surface in column experiments, as well as how far competitive sorption with phosphate ($AsO_4^{3-} \leftrightarrow PO_4^{3}$) plays a role in arsenic mobilization. In addition, the formation of As-S species (thioarsenates) was observed in this artificial groundwater environment.
- Investigate the influence of carbonate on arsenic sorption and mobilization from different mineral phases (Pyrite (FeS_2), Orpiment (As_2S_3), and arsenic trioxide (As_2O_3)) as well as the detection of potential influence of arsenic carbonate complexation on arsenic dissolution.

The detection of arsenic species beyond inorganic arsenite and arsenate was performed by ion chromatography, coupled on-line to inductively coupled plasma spectrometry (IC-ICP-MS) at Trent University in Peterborough, Canada.

The results of the recent case study offer a better understanding of the behaviour of arsenic in the environment, mobilization and possibly retardation mechanisms, as well as arsenic speciation in groundwaters as an issue of global relevance, particularly with regard to arsenic hotspots in Asia.

2. Introduction

2.1. Bangladesh – Groundwater environment with high arsenic concentrations

The Bengal Basin, within southern, central and eastern Bangladesh, is highly affected by geogenic arsenic contamination of groundwater. From 1970 to 2000, at least 3-4 million hand-pumped tube wells were installed in the Bengal Basin, politically supported and financed by the World Bank (RAVENSCROFT et al., 2005). This massive shift in drinking water consumption to groundwater was intended to provide an alternative to surface water contaminated with pathogens, thereby reducing the incidence of water-borne diseases.

The first adverse health effects of this operation were observed in the 1980s in West Bengal. In 1993, chronic health problems related to arsenic were diagnosed in Bangladesh in the form of the so-called "Black Foot disease", skin cancer, and deaths. What first seemed a blessing became, 25 years later, the "greatest mass poisoning in history" (KINNIBURGH and SMEDLEY, 2001; RAVENSCROFT et al., 2005; SMEDLEY and KINNIBURGH, 2002).

Today, it is known that particularly in groundwaters from the Holocene alluvium of the Ganges, Brahmaputra, and Meghna river system, As concentrations locally exceed the World Health Organisation (WHO) guideline value for drinking water (10 µg/L As) by up to 200 times. Roughly 45 % of all wells exceed the WHO standard by one to two orders of magnitude. As levels in 27 % of wells are above the national drinking water standard of 50 µg/L (GAUS et al., 2003). The maximum As concentrations occur in depths of 20 to 40 m while low As concentrations prevail at shallow depths of 10 m below the surface, as well as between depths of approximately 100 to 200 m. Thus, groundwater from Pleistocene and older aquifers is largely free of arsenic (RAVENSCROFT et al., 2005). However, typically, tube wells were drilled to depths of 20 to 70 m and in most cases tap the Holocene aquifers.

Today, there is extensive literature on arsenic health effects in Bangladesh (AKTER and NAIDU, 2006; BISSEN and FRIMMEL, 2003a; BISSEN and FRIMMEL, 2003b; DPHE, 1999; SMEDLEY and KINNIBURGH, 2002) and 40,000 cases of arsenicoses have already been diagnosed. Arsenic contamination in groundwater poses a long-term risk for chronic arsenic poisoning, because groundwater provides 90 % of drinking water and a large majority of irrigation supply. It is estimated that 30 millions people rely on As-contaminated groundwater (SMEDLEY and KINNIBURGH, 2002).

2.2. Geology of the Bengal Basin

The arsenic problem in Bangladesh is the result of As-mobilization from As-rich minerals (e.g. arseno-pyrite, FeAsS) in the Himalayas under natural conditions (geogenic).

These minerals are basically bound in sedimentary or magmatic rocks which underlie a combination of natural processes, such as erosion, weathering, sedimentation, and transport. Geological characteristics for the Bangladesh sediments are (AKTER and NAIDU, 2006):

- river drainage from the rapidly-weathering Himalayas;
- quickly-buried, organic-bearing and relatively young Holocene sediments resulting in reducing condition in the sediments;
- reductive dissolution of iron -, aluminium-, and manganese(hydro)oxides with adsorbed As;
- and very low, basin-wide hydraulic gradients.

The Bengal Basin belongs to one of the largest deltas in the world. For approximately 11,000 years, high rates of sediments have been eroded and transported by the Ganges Brahmaputra Meghna system from a wide area of the rapidly-weathering Himalayas and from the Indo-Burman range, resulting in the formation of the submarine Bengal Delta in the south of Bangladesh ($1,500 \times 10^9 \, m^3$ sediment in the last 7,000 years) (AHMED et al., 2004; ALAM et al., 2003; RAVENSCROFT et al., 2001). Today, the Ganges Brahmaputra Meghna river system still produces the greatest total sediment load of any river system in the world, with especially high levels during the annual monsoon season.

Most likely, there are multiple source areas for the geogenic arsenic contamination. These may include the Gondwana coal of the Rajmahal basin (up to 200 ppm As), the arsenic mineral lollingite and pyrite found to be associated with pegmatites in the mica-belt of Bihar (0.12-0.018 % As in mineralized rocks), the pyrite-bearing shale from the Proterozoic Vindhyan range (0.26 % As), the gold belt of the Son Valley (As in bedrock 2.8 % - 1000 ppm), the isolated outcrops of the sulphides in the Darjeeling Himalayas (up to 0.8 % As), or outcrops in the upper reaches of the Ganges River system (ACHARYYA et al., 2000).

The Bengal Basin mainly consists of alluvial and deltaic floodplains, which can be divided into five main geomorphologic units, represented in Figure 2.2.1. They include:

- the slightly elevated alluvial Plio-Pleistocene terraces of the Barind and Madhupur Tracts, which interrupt the flat topography of Bangladesh west of the Meghna and north of the Ganges;
- mountain-front fan deltas of the Tista and Brahmaputra;
- fluvial floodplains of the Ganges, Brahmaputra, Meghna, and Tista Rivers;
- the delta plain of the lower Ganges, Brahmaputra, and Meghna river system south of the Ganges-Meghna valleys;
- and subsiding basins within the eastern Ganges tidal delta and the Shylet basin (SMEDLEY and KINNIBURGH, 2002).
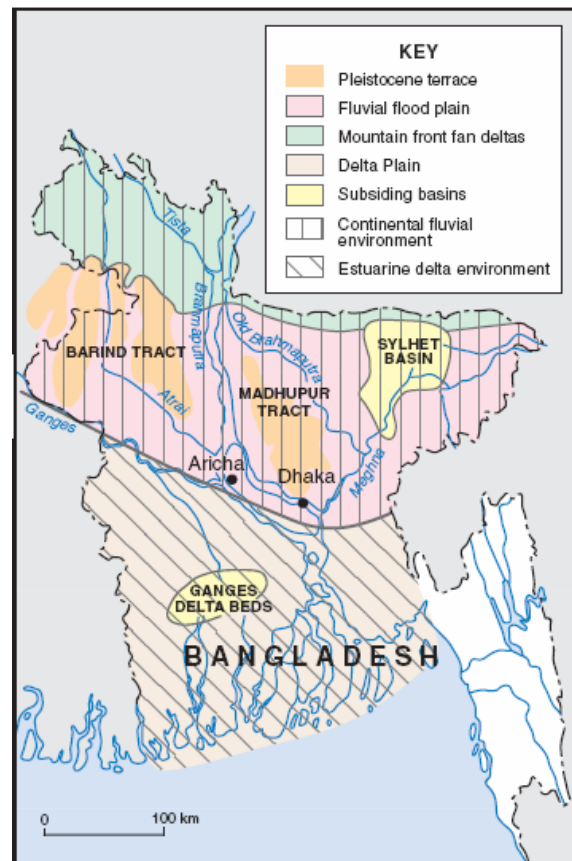
Figure 2.2.1 Main geomorphologic units of the GBM delta system (KINNIBURGH AND SMEDLEY, 2001)

The Bengal Basin is surrounded by the Chittagong Hill Tracts in the east, the Shillong Plateau (Precambrian Shield) in the northeast, and the Precambrian basement complex (Indian Shield) in the west (ACHARYYA and SHAH, 2004).

The two major alluvial aquifer units comprise sediments from Holocene, Pleistocene, and Plio-Pleistocene (see table 2.2.1).

Table 2.2.1 Main stratigraphic units in Holocene/ Plio-Pleistocene in Bangladesh

Stage	Formation	Lithology	Notes
Late Pleistocene-Holocene	Chandina Formation Dhamrai Formation	Upward fining, grey micaceous, medium and coarse sand to silt with organic mud and peat.	Forms major aquifers beneath recent floodplains. Probably < 150 m thick.
Lower Pleistocene	Madhupur Clay Barind Clay	Red-brown to grey, silty-clay; residual deposits; kaolinite and iron oxide.	Often absent beneath Holocene floodplains. Thickness 6 to 60 m.
Plio-Pleistocene	Dihing Formation Dupi Tila Formation	Yellowish-brown to light grey, medium and coarse sand to clay; very weakly consolidated; depleted in mica and organic matter.	Forms major aquifers beneath Holocene the terraces and hills, and deeper aquifers beneath the Holocene floodplains hundreds to thousand of metres thick (up to 6375 m).

After ALAM et al. (1989) and RAVENSCROFT et al. (2005)

The Pleistocene aquifer system consists of Madhupur and Barind clay overlying Dupi Tila sands. Groundwater from Pleistocene and older aquifers is largely free of arsenic (RAVENSCROFT et al., 2005). Sediments from the Plio-Pleistocene and the early Holocene, and sediments which can be found in depths of more than $100 - 200$ m are considered to release low As concentrations into groundwater (< 5 µg/L and usually < 0.5 µg/L). This is due to oxidation and exposition of the sediment during phases of marine regression. Bangladesh´s capital, Dhaka, is situated in the southern part of the Madhupur Tract and withdraws groundwater from these older sediments; thus, no arsenic problem appears (RAVENSCROFT et al., 2001; SMEDLEY and KINNIBURGH, 2002).

During mid-Holocene ($10,000 - 7,500$ years ago), the GBM river system discharged up to two and a half times more sediment than in present times. High arsenic concentrations in the groundwater in the Ganges delta and some low-lying areas in the Bengal basin are mainly restricted to these Holocene alluvial aquifers at shallow and intermediate depths (max. As values in 20 to 40 m) (AHMED et al., 2004). Arsenic is preferentially enriched in fine-grained and organic-rich sediments, where it is bounded to Fe(III)-, Al(III)-, and Mn(II/IV)-hydroxide-coated sand grains, organic matter (up to 6 % by weight), and clay minerals (ACHARYYA et al., 2000; ACHARYYA and SHAH, 2004; BISSEN and FRIMMEL, 2003b). The

rapid burial of young, organic-rich sediments, combined with low flushing rates due to basin-wide low hydraulic gradients, causes aquifer conditions to be mainly reducing. Particularly in groundwaters from the Holocene alluvium of the Ganges, Brahmaputra, and Meghna river system, As concentrations locally exceed 200 times the WHO guideline value for drinking water of 10 µg/L of As.

Sediments in Bangladesh do not appear to have exceptionally high As concentrations (2 to 20 mg/kg) compared to the average crustal concentration worldwide (2 to 6 mg/kg). Thus, the release mechanisms for As must work in a very effective way.

2.3. Distribution of arsenic in Bangladesh

The most As-rich areas are located in the central and southern parts of the country (Figure 2.3.1). Especially in areas located in the south and southeast, extremely high As concentrations are found exceeding 250 µg/L. High As concentrations can generally be found in the lower catchment areas of the Ganges, Brahmaputra, and Meghna river system, particularly in areas close to the lower Meghna Estuary, where 80 % of wells exceed the 50 µ/L concentration limit for arsenic. Areas located in the uplifted north-central areas and in the northwest are less affected, some even showing As concentrations below the WHO drinking water standard (< 10 µg/l) (AHMED et al., 2004). But within the broad distribution pattern of As, occurrence of As-enriched waters remains very patchy on a regional scale.
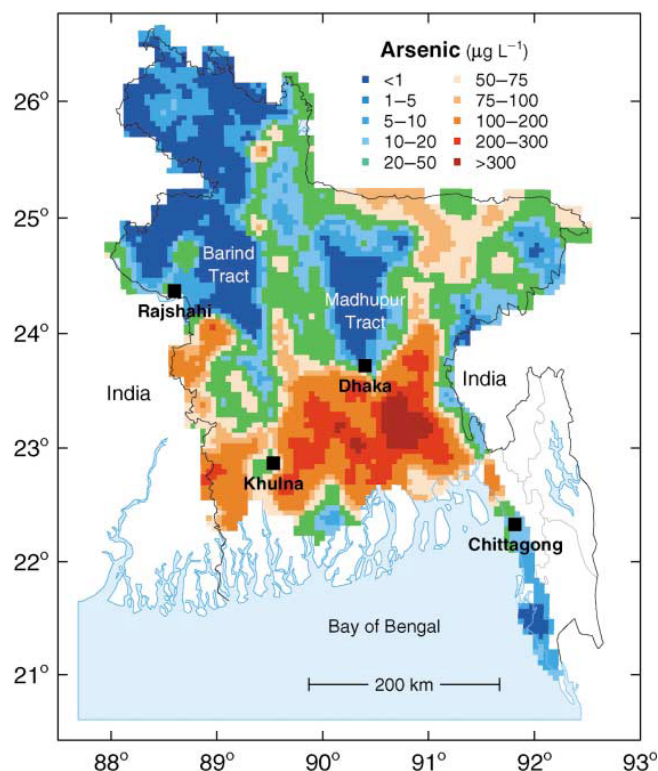
Figure 2.3.1 Distribution of As concentration in groundwater from tube wells < 150 m depth (SMEDLEY and KINNIBURGH, 2002)

With regard to depth, the highest As concentrations occur between 20 and 40 m, whereas groundwater from dug wells (< 10 m) and from depths greater than 150 m is either nearly As-free, or contains very low As concentrations (< 10 µg/L). Another aspect playing a major role in As distribution is the subsurface geology, with its facies showing characteristics of the alluvial deposits, i.e. age, mineralogy, organic matter, and iron oxides (see chapter Geology of the Bengal Basin). Arsenic is generally mobilised from tube wells tapping the fine-grained mid-Holocene aquifers, while those placed in the coarser sediments of the early Holocene and in Plio-Pleistocene aquifers show almost no As contamination (AHMED et al., 2004).

2.4. Groundwater composition and chemistry

The oxidation of organic matter, combined with hydrolyses of feldspar and the weathering of mica representing the dominant processes in the evolution of the groundwater chemistry (AHMED et al., 2004). The groundwater beneath the Holocene floodplains is generally a Ca-HCO_3 or Ca-Mg-HCO_3 type with a relatively high mineralization (conductivity 500 – 1000 µS/cm), tending towards Na-Cl type water near the coast. High-arsenic groundwater is typically characterised by high concentrations of HCO_3^- (320 to 600 mg/L), PO_4^{2-} (up to 8.75 mg/L), Fe(tot) (0.4 – 15.7 mg/L), and Mn (0.02 – 1.86 mg/L), and low concentrations of SO_4^{2-} (< 3mg/L), Cl^- (< 60 mg/L), and NO_3^- (< 0.22 mg/L), except for some local variations. The distribution of the major cations, such as Ca^{2+} (21-122 mg/L), Mg^{2+} (14-41 mg/L), Na^+ (7-150 mg/L), and K^+ (1.5-13.5 mg/L), varies depending on depth and region (AHMED et al., 2004).

The groundwater is predominantly anoxic and mostly strongly reducing. Locally, CH_4 production can take place. Organic matter in the alluvial Holocene sediments is considered as the source of the dissolved organic carbon (DOC). The pH is close to or greater than 7. A negative correlation has been observed between arsenic and sulphate concentrations in groundwaters due to reducing conditions that force arsenic mobilization and SO_4^{2-} reduction ($SO_4^{2-} \rightarrow S^{2-}$) (AHMED et al., 2004; RAVENSCROFT et al., 2001; SMEDLEY and KINNIBURGH, 2002).

In groundwaters from the affected areas, arsenic concentrations were seen to vary within a very wide range (< 0.5 to ca. 3,200 µg/L). Arsenite is reported to have a modal proportion of 50-60 % of total arsenic (SMEDLEY and KINNIBURGH, 2002) and even to be the dominant species, with about 67-99 % of T-As in most groundwaters (AHMED et al., 2004). Arsenic correlations with high-iron groundwaters and other water quality parameters, such as bicarbonate, sulphate, phosphate, and redox sensitive elements (iron, manganese, ammonium, and nitrite), may appear locally but are not sufficient for general assumptions (KINNIBURGH and SMEDLEY, 2001).

Strong reducing conditions in Bangladesh's aquifers with near-neutral pH, the increased concentrations of dissolved sulphide, and the predominance of arsenite may also favour the formation of As-S species.

2.5. Mobilization of arsenic in groundwater

Redox potential (Eh) and pH are the dominant factors controlling As speciation, thus also As mobilization into groundwater (Figures 2.5.1 and 2.5.2). High As concentrations are always associated with reducing conditions (low redox conditions) induced by rapid burial of the alluvial and deltaic organic-rich sediments (SMEDLEY and KINNIBURGH, 2002). Under reducing conditions at pH below 9.2, arsenic occurs predominantly in the form of uncharged arsenite species $H_3AsO_3^0$, which preferably stays in solution. Under oxidising conditions and a pH of less than 6.9, the charged arsenate species $H_2AsO_4^-$ is predominant, while at higher pH, $HAsO_4^{2-}$ becomes dominant. These anionic complexes can be adsorbed on the exchangeable sites of iron(hydr)oxides, clay minerals, etc., which limits their mobility. The charging of the As-complex strongly affects the bio-availability, mobility, and toxicological characteristics of arsenic. The mobile arsenite is considered to be much more toxic than arsenate and to have much stronger affects on organisms. The dissolution of iron(hydr)oxides under strongly acidic and alkaline conditions can cause the mobilization of adsorbed arsenite and arsenate (ANDERSON et al., 1976).
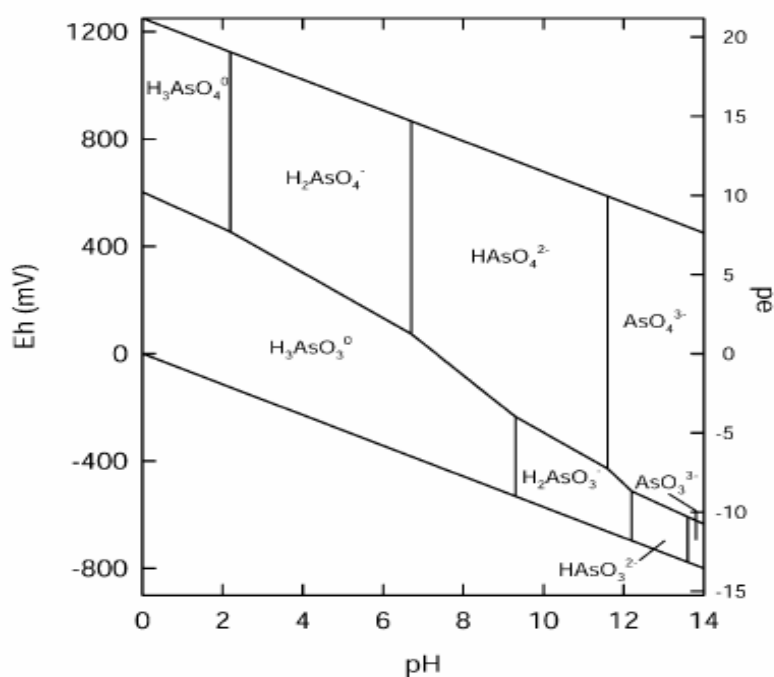
Figure 2.5.1 Eh-pH diagram for aqueous As species in the system As-O$_2$-H$_2$O at 25°C and 1 bar total pressure (KINNIBURGH AND SMEDLEY, 2001)
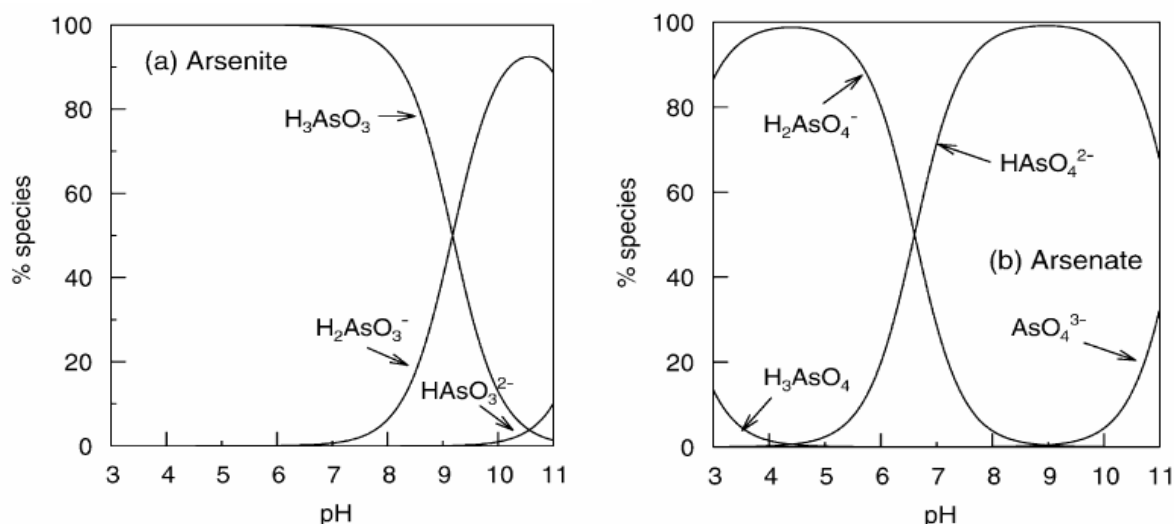
Figure 2.5.2 (a) Arsenite and (b) arsenate speciation as a function of pH (ionic strength of about 0.01 M) (KINNIBURGH AND SMEDLEY, 2001)

The sorption of arsenite and arsenate on iron(hydr)oxides strongly depends on the ratio solid : liquid phase, as well as on the type and size of the surface of the specific minerals. A highly nonlinear sorption isotherm is responsible for low As concentration in groundwater, even if the As loading on the sediment is comparatively high (KINNIBURGH and SMEDLEY, 2001). But even small disturbances in this equilibrium can lead to the release of high quantities of As from the mineral phase into the groundwater. These disturbances can result from competitive interactions with sorption sites of iron(hydr)oxides by naturally occurring ligands, including phosphate, sulphate, carbonate, silicate, and dissolved organic matter (ANDERSON et al., 1976; KINNIBURGH and SMEDLEY, 2001; LUXTON et al., 2006).

Figure 2.5.3 summarises the development of arsenic-contaminated groundwater, emphasising the reduction of arsenate to arsenite as the main mechanism. Low topographic gradients result in very low basin-wide hydraulic gradients, particularly in the young sediments of Pleistocene terraces and the Holocene floodplains. These sediments are poorly flushed and contain higher As concentrations than the well-flushed, older sediments, which are almost As-free (KINNIBURGH and SMEDLEY, 2001). A field study reported the immobilization of arsenic by pyrite. Pyrite can incorporate arsenic under certain conditions whereby As is removed from the groundwater (RAVENSCROFT et al., 2001).
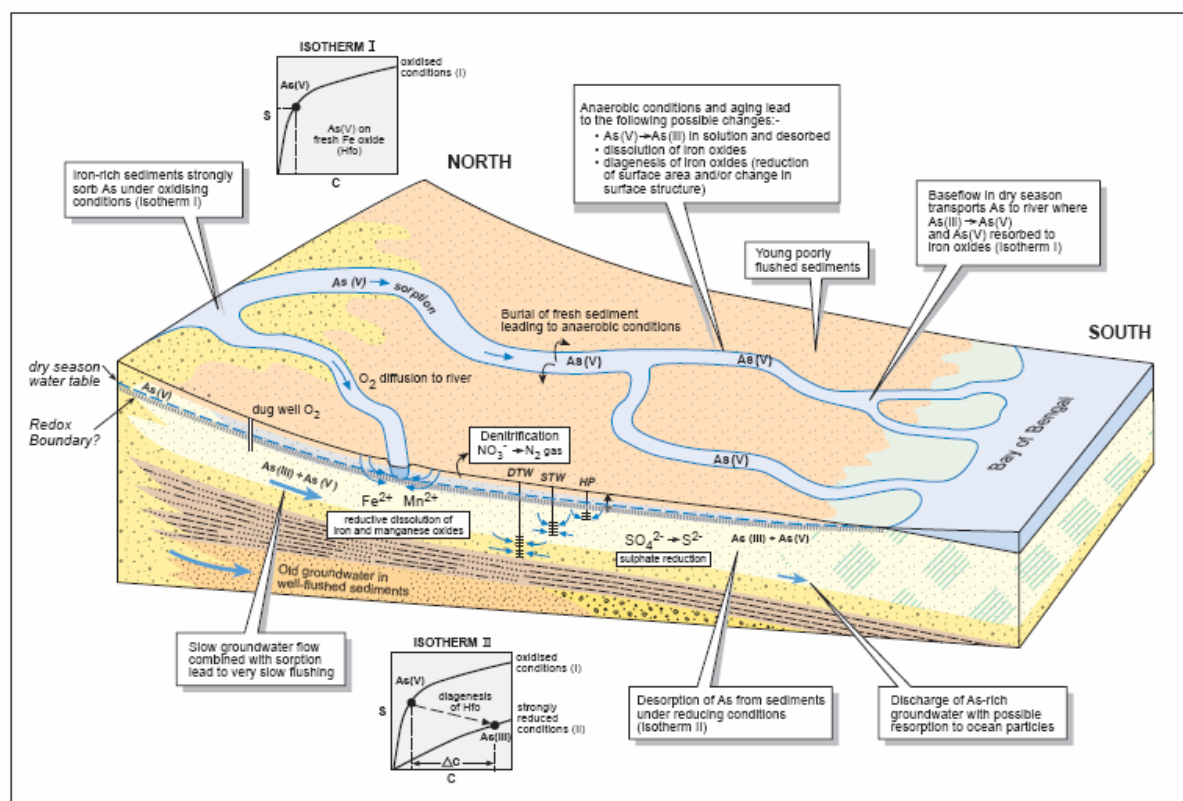
Figure 2.5.3 Principal geogechemical processes involved in the developement of arsenic-contaminated groundwater (KINNIBURGH and SMEDLEY, 2001)

Three main mechanisms that could possibly explain the release of As from the sediment and the pollution of the groundwater in Bangladesh have been postulated in different studies (ACHARYYA et al., 2000; RAVENSCROFT et al., 2005; RAVENSCROFT et al., 2001; SMEDLEY and KINNIBURGH, 2002).

1) One theory suggests the **oxidation of arsenic-bearing pyrite in the alluvial sediments** after water table drawdown by massive extraction, especially of irrigation water. Consequently, oxygen enters the previously anoxic aquifer sediment, pyrite is oxidized, and arsenic is released in the form of arsenate (RAVENSCROFT et al., 2001). However, several studies reject this theory as a mechanism for As contamination in Bangladesh (HARVEY et al., 2002; KINNIBURGH and SMEDLEY, 2001; RAVENSCROFT et al., 2001). Firstly, there is no spatial correlation between the distribution of arsenic concentrations and irrigation intensity. Moreover, the observed concentration of sulphate does not match with that of arsenic in the Bangladesh groundwater. If oxidation of sulphide minerals leads to the release of high amounts of arsenic, the concentration of sulphate should correlate with the high arsenic concentration. Finally, the low As concentration in groundwater withdrawn from the shallow aquifers (< 10 m) indicates that no oxidation of

arsenic-bearing pyrite can cause the arsenic problem. These shallow sediments are exposed to atmospheric oxygen and would be most polluted.

2) Intensive groundwater irrigation began in the mid-1970s with a simultaneous increase in the application of fertilizer phosphate, particularly within the last 15 years. It has been therefore suggested that the excessive use of **fertilizer phosphate displaces arsenic from FeOOH as a result of competitive anion exchange** (ACHARYYA et al., 2000). In addition, both elements, As and P, form similar anions ($H_2AsO_4^-$, $HAsO_4^{2-}$ and $H_2PO_4^-$, HPO_4^{2-}) that strongly adsorb to iron(hydr)oxides, hence the reduction of iron(hydr)oxides would cause their joint release. Furthermore the microbial degradation of organic matter (OM) (peat and human organic waste) mobilizes phosphate into groundwater (MCARTHUR et al., 2004). Phosphate shows a similar sorption behaviour to arsenate, making it a significant competitive anion. RADU et al. (2005) postulated that phosphate contributes more to arsenate desorption than carbonate, even when present in much lower concentrations than phosphate. ACHARRYA et al.(2000) reported the leaching of up to 150 µg/L total As from Fe-coated quartz grains in sandy aquifers after adding 1 mM KH_2PO_4. But again, the effectiveness of this mechanism was questioned in different studies. The distribution patterns of both arsenic and phosphate application did not interfere with each other. In areas with high fertilizer application, the groundwater was found to be essentially free of arsenic and phosphorus. Furthermore, arsenic concentrations were rather low in very young waters that should have contained the highest phosphate and arsenic concentrations (HARVEY et al., 2002; KINNIBURGH and SMEDLEY, 2001; RAVENSCROFT et al., 2001). Another study (MANNING and GOLDBERG, 1996) has shown that a concentration of 5 mg/L (approximate upper limit for Bangladesh groundwater) phosphorus would desorb not more than 2 µg/L of arsenic sorbed to mineral surfaces.

3) The third hypothesis is the microbiologically mediated **reductive dissolution of arsenic-rich iron(hydr)oxides**, which is now the most widely accepted explanation for arsenic mobilization in the groundwaters of the alluvial aquifers in the Bengal basin (KINNIBURGH and SMEDLEY, 2001; MCARTHUR et al., 2004; NICKSON et al., 2000; RAVENSCROFT et al., 2005; SMEDLEY and KINNIBURGH, 2002; ZHENG et al., 2004). Arsenic, particularly arsenate, is strongly sorbed onto iron(hydr)oxides, which is preferentially entrapped in organic-rich, fine-grained deltaic sediments. The oxidation of sedimentary organic matter

and the microbiological consumption of oxygen lead to reduction of sulphate, nitrate, manganese, and finally to the reductive dissolution of iron(hydr)oxides (e.g. FeOOH).

$$8FeOOH + CH_3COOH + 14H_2O \rightarrow 8Fe^{2+} + 16HCO_3^- + 12H_2O \tag{1}$$
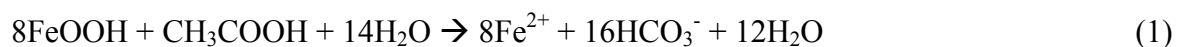
which is accompanied by the mobilization of the strongly adsorbed arsenate ($E_h < 200$ mV under neutral and acidic conditions) (AKAI et al., 2004). This process subsequently reduces arsenate to arsenite, shown by the fact that arsenite is the predominant dissolved arsenic species (ACHARYYA and SHAH, 2004; AHMED et al., 2004; RAVENSCROFT et al., 2001). Discussions are still taking place as to whether the trigger reaction for this process is the reduction of arsenite and arsenate, followed by the desorption of arsenite from iron(hydr)oxides (AHMED et al., 2004), or if arsenate dissolves after dissolution of iron(hydr)oxides and is later reduced in solution (VAN GEEN et al., 2004). Furthermore, the Fe(III) oxides can undergo diagenetic changes leading to the desorption of adsorbed arsenic (SMEDLEY and KINNIBURGH, 2002). In Bangladesh, the dissolved iron content in the groundwater is very high (values up to 30 mg/L) and high-arsenic concentrations are often associated with high-iron concentrations

It has been pointed out in several studies that there is seldom a good correlation between arsenic and iron concentrations in groundwater. These inconsistencies may indicate that Fe dissolution is not always the main mechanism for significant As release into the groundwater. Poor correlations could also arise from the re-precipitation of iron or the re-adsorption of arsenic onto fresh iron(hydr)oxides exposed by dissolution (APPELO et al., 2002; NICKSON et al., 1998; NICKSON et al., 2000; RAVENSCROFT et al., 2001; VAN GEEN et al., 2004).

The degradation of OM is known to be the redox driver for iron(hydr)oxide reduction, which consequently also reduces sorbed arsenate to arsenite and releases it into the groundwater. The required degradable organic carbon can derive from the sediments or the surface. As suggested by HARVEY et al.(2002), intensive groundwater irrigation can draw down young organic carbon from the surface into the aquifer system (e.g. human waste from latrines), thereby inducing reducing conditions and accelerating the arsenic release (HARVEY et al., 2002; MCARTHUR et al., 2004). OM was also transported with the fluvial sediments in the rivers and generally exposed to oxic degradation during transport before deposition. Following it was enriched in fluvial sands (total organic carbon (TOC)

< 0.5 %) and organic-rich horizons. The oxic degradation leaves OM that is cellulose-rich and unfavourable for bacterial metabolism in the sediments. Its contribution to iron(hydr)oxide reduction is therefore considered to be negligible (MCARTHUR et al., 2004; MCARTHUR et al., 2001; RAVENSCROFT et al., 2005).

Peat beds represent another source for OM, even though no peat was found in several studies (HARVEY et al., 2002; SWARTZ et al., 2004). They are very common beneath the Old Meghna Estuarine Floodplain in Greater Comilla and can contain high contents of OM (e.g. 6 % TOC in NICKSON et al., 1998). The age of wood, peat and other organic debris found in Bangladesh sediments from depths of 20 to 70 m is estimated to be 5,000 a to 7,000 a BP. The degradation of peat (much OM) is often associated with the presence of high concentrations of ammonium and phosphorus in the groundwater (MCARTHUR et al 2001).

Using surface complexation models, APPELO et al.(2002) proposed **the release of arsenic from sediments by dissolved carbonate as an alternative mechanism**. APPELO et al. hypothesized that increasing carbonate concentrations ((bi-)carbonate ions) might be responsible for the mobilization of sorbed As from iron(hydr)oxides into the groundwater, either by competitive sorption between the carbonate and arsenate anions (ligand exchange) or by formation of arsenic-carbonate complexes. ANAWAR et al. (2004) assumed that leaching of bicarbonateis supposed as important mechanism for arsenic mobilization in bicarbonate dominated reducing aquifers in Bangladesh.

Several authors (MENG et al., 2000; NEUBERGER and HELZ, 2005; RADU et al., 2005) questioned these theoretical assumptions. They concluded that increasing carbonate concentrations have a relatively low influence on the adsorption of arsenite and arsenate on iron(hydro)oxides. RADU et al. (2005) pointed out that the competitive aspect between carbonate and arsenic is low with regard to the total concentration of adsorbed As. Phosphate, known as a competitive anion, has a comparatively higher effect on desorption of As from the sediment.

KIM et al. (2000) suggest the direct interaction between HCO_3^- and arsenic sulphide minerals (such as orpiment, As_2S_3) and sulfosalts, and propose that As forms stable aqueous As(III)–carbonato complexes ($[As(CO_3)_2^-]$, $[AsCO_3^+]$, and $[As(CO_3)(OH)_2^-]$), thereby dissolving sulphide minerals. KIM et al. (2000) hypothesized that these complexes have a strong influence on the effective leaching of arsenic in anaerobic systems, and that carbonation of arsenic sulphide minerals is the major process causing As mobilization into groundwater (KIM

et al., 2000). Significant concentrations of sulfide-bound As in the environment would be necessary for this mechanism to become predominant (RADU et al., 2005). NEUBERGER and HELZ (2005) pointed out that naturally occurring carbonate concentrations are too low to enhance arsenite solubility by HCO_3^-. They showed the formation of only a single and moderate stable As(III)-carbonate complex, $As(OH)_2CO_3^-$ ($As(OH)_3^0 + HCO_3^- = As(OH)_2CO_3^- + H_2O$, pK = 0.57 ± 0.15), to be responsible for increasing Arsenite solubility in the presence of carbonate. The small constant suggests that As(III)-carbonate complexes will be negligible at carbonate concentrations found in nature (NEUBERGER and HELZ, 2005). The complexes $As(CO_3)_2^-$ and $AsCO_3^+$, proposed by KIM et al.(2000), were found to be unstable and vulnerable to hydrolysis (TOSSELL, 2005).

2.6. Thioarsenates

It has long been known that the formation of soluble arsenic sulphur complexes plays an important role in aquatic reducing environments. Since arsenic is known to be more mobile under reducing conditions and that it has a high affinity to sulphur compounds, the geochemical interaction between As and reduced sulphur species (H_2S or HS^-) may play an important role for the mobility and toxicity of arsenic in sulphate reducing environments.

The most abundant arsenic – sulphur species that are formed in sulphidic solutions are monomeric species. Theoretically, three thioarsenites (H_3AsO_2S, H_2AsOS_2, H_2AsS_3) and four thioarsenates (H_3AsO_3S, $H_3AsO_2S_2$, H_3AsOS_3, H_3AsS_4) exist. They are highly sensitive to oxygen and pH (particularly tri- and tetrathioarsenate). Further their formation depends on the As:S ratio in the solution. There are two processes describing the formation of the homologue series of thioarsenates ($AsO_xS_{4-x}^{3-}$). Either they can be formed by reaction of arsenite (AsO_3^{3-}) with elemental sulphur under alkaline conditions or by alkaline dissolution of As-bearing sulphide minerals, e.g. Orpiment (As_2S_3) and Realgar (As_4S_4). The mechanism of oxidation in a reducing environment still remains unclear. The occurrence of thioarsenic species is limited to a pH ranging from near neutral to alkaline. Acidifying samples containing arsenic and sulphide (As-S species) leads to precipitation of arsenic sulphides, e.g. in form of Orpiment (WALLSCHLÄGER and STADEY, 2007).

There is no confirmation for the formation of As-S species in Bangladesh's groundwaters yet. A recent study (GAULT et al., 2005) pointed out that there is no evidence for other significant As species next to arsenite and arsenate, which can represent an important form of dissolved arsenic in groundwaters with moderate sulphide concentrations.

3. Materials and Methods

3.1. Site description

The study site is located on the property of the Upazila health complex in Titas/Daudkandi (Comilla District) approximately 80 km away from Dhaka and is situated approximately 5.5 m above mean sea level (Figure 3.3.1). In Comilla 65 % of the wells exceed the As concentration of 50 µg/L (the national guideline for drinking water).
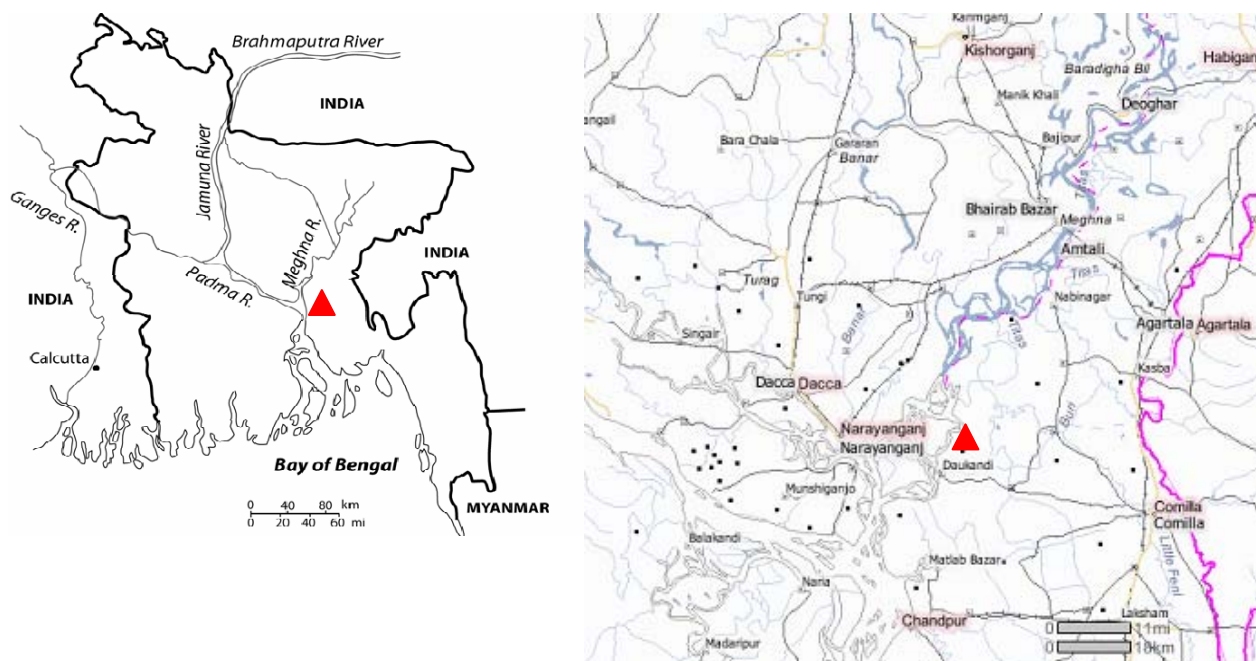
Figure 3.1.1 Location of the study site in Daudkandi (23.5970 North, 90.7963 East) (maps: BREIT et al. 2006 and www.cartographic.com)

On-site analyses of the tube well (40 m depth) investigated in November 2006 at the health complex have shown that the groundwater chemistry at the test field has a comparatively low mineralization compared to the general groundwater composition in Bangladesh (for comparison see chapter 2.4.). The pH is near neutral (7.06). Conductivity and redox potential were measured with 154 µS/cm and 90 mV. The groundwater is dominated by Ca^{2+} (28.1 mg/L) and DIC (HCO_3^-, 29.2 mg/L) and can be defined as a Ca-HCO_3-type (Table 3.1.1). Arsenic concentrations of about 84 µg/L were observed and thus exceeded the drinking water guidelines massively.

Table 3.1.1 Groundwater chemistry with the major cations and anions at the study site in Daudkandi/Comilla

Na^+	K^+	Ca^{2+}	Mg^{2+}	NH_4^+
8.98	1.43	28.1	7.00	0.49
F^-	Cl^-	PO_4^{3-}	DIC	DOC
0.22	9.8	0.99	29.2	0.21

Conc. in mg/L

3.2. Drilling and collection of sediments samples

The core drilling was done by rotary drilling and cable percussion 30 m from the test field. A total of 37 samples were collected in 2" and 4" PVC liners from below the artificial filling of the hospital site (upper 3 m) to a final depth of 84 m (Figure 3.2.1). The drilling was cored and stratigraphically logged. The majority of samples were retrieved as undisturbed core samples the PVC liners were sealed immediately with paraffin wax. In a glove bag the liners were divided in subsamples and packed in nitrogen-filled polyethylene bags to avoid contact with the atmosphere. Samples of broken liners or unconsolidated material that was not retained in the liner were refilled in bags immediately at the drilling site. Samples were further used for analyses carried out in Dhaka, Freiberg, and Peterborough. An overview over the investigations of the sediment properties in different depths is represented in Table 3.2.1.
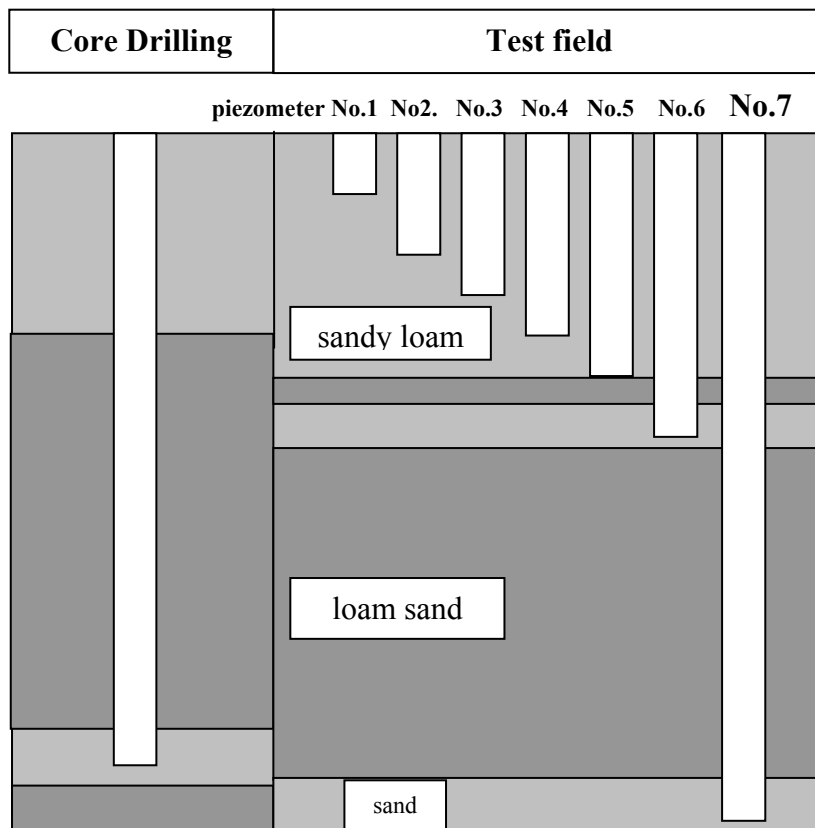
Figure 3.2.1 The boreholes are located in a few meter distances from the core drilling and show a slightly different stratigraphy. The core drilling and the deepest piezometers tap the upper aquifer.

The test field for further monitoring (5.2 m * 15.7 m) was set up in approximately 30 m horizontal distance where seven individual sampling wells were installed at 9 m, 15 m, 21 m, 26 m, 27 m (tapping the upper aquifer), 35 m (in a sand layer lens immediately below the major upper aquifer), and 85 m (in the shallow aquifer) (Figure 3.2.1). Drilling of the piezometers 1 to 6 was carried out using the local "hand-flapper" method. The "hand-flapper" method works with the inflow of water (enriched in bentonite) in the borehole and the generation of a low-pressure in a PVC pipe that was inserted in the borehole. The hand is used as a check valve to suck a sediment-laden slurry out of the pipe. After removing the material out of the hole the depth can be extended up to the length of the PVC pipe (VAN GEEN et al., 2004). The seventh and deepest borehole was drilled using manual rotary drilling. None of the 7 boreholes were cored. Screens were installed at the end of the boreholes with 1.5 m (boreholes 1 to 5), 3.1 m (borehole 6), and 6.3 m (borehole 7) length. The sediment slurry was continuously monitored to control for changes in stratigraphy.

The stratigraphy of the test field and the core drilling showed slight variations in the dominant sediment layers probably caused by inhomogeneous deposition of alluvial sediments during the last thousands of years.

Table 3.2.1 Overview experiments on Bangladesh sediments with sampling depths and sample numbering, including investigations on sediment properties, leaching and sorption experiments in different solutions as well as samples taken for column experiments.

LAYER	from [m]	to [m]	average [m]	Sample No.	grain size distribution	mineralogy	pH	Calcite	organic C (ignition loss)	TC (TIC/TOC)	hot HCl (As, Fe, Mn, P)	Aqua Regia (As, P)	AGW	MQ, NaOH, NaHCO3	MQ, NaOH NaHCO3 (N2)	AGW	MQ	Columns
1	3	3.7	3.3	**A1, 1**	x		x	x	x			x						
	4.6	5.2	4.9	**A2, 2**	x	x	x	x	x	x		x						
	6.1	6.7	6.4	**3**	x		x	x	x	x		x						
	7.6	8.2	7.9	**4**	x		x	x	x			x						
	9.1	9.7	9.4	**5**	x	x	x	x	x	x		x						
	10.7	11.3	11	**6**	x		x	x	x									
	12.2	12.8	12.5	**7**	x		x	x	x		x	x	x	x	x		x	
	13.7	14.3	14	**8**	x		x	x	x									
	15.2	15.8	15.5	**9**	x		x	x	x									
2	16.7	17.3	17	**10**	x		x	x	x			x						
(shallow	18.3	18.9	18.6	**11**	x		x	x	x									
aquifer)	19.5	20.1	19.8	**13/14**	x		x	x	x									
	20.7	21.3	21	**15/16**	x		x	x	x	x	x	x	x	x	x		x	x
	21.9	22.5	22.2	**17/18**	x		x	x	x									
	23.1	23.7	23.4	**19/20**	x		x	x	x			x						
	24.3	25	24.6	**21/22**	x		x	x	x									
	25.6	26.2	25.9	**23/24**	x	x	x	x	x	x	x	x	x	x	x		x	
	26.8	27.4	27.1	**25**	x		x	x	x	x		x						
	27.4	28	27.7	**26**	x		x	x	x									
	28	28.6	28.3	**27**	x		x	x	x	x	x	x	x					
	33.5	34.1	33.8	**28**	x		x	x	x	x	x	x	x					
3	34.1	34.7	34.4	**29**	x	x	x	x	x	x		x						
	42.6	43.2	42.9	**30**	x		x	x	x		x	x						
	43.2	43.8	43.5	**31**	x		x	x	x									
	60.9	61.5	61.2	**32**	x	x	x	x	x	x	x	x	x	x	x		x	
	64.5	65.1	64.8	**34**	x		x	x	x									
4	79.1	82.2	80.6	**RD**	x		x	x	x	x	x	x	x	x	x	x	x	x
(deeper	82.2	82.8	82.5	**35**	x	x	x	x	x	x		x						
aquifer)	82.8	83.4	83.1	**36**	x		x	x	x									
5	83.7	84.3	84	**37**	x	x	x	x	x	x	x	x	x	x	x		x	

A – material from hand auger, RD – material from rotary drilling, (N2) – anoxic conditions

3.3. Basic investigations of sediment properties

3.3.1. Sieve analyses, organic C, Calcite, and pH in Dhaka, Bangladesh

The first part of analyses was carried out at the Geology Department at Dhaka University and included sieve analyses, the determination of organic carbon, content of calcite, and pH. The named analyses were done for each sample to get detailed information about their depth distribution.

To separate the sand fraction from silt and clay ≈ 50 g of sediment sample was washed through a sieve with a mesh size of 0.063 mm (wet-sieving). The weight of the sieves was known. The sieve with the remaining sand fraction was dried in the furnace (≈ 60 °C) and the quantity of sand could be estimated (weight$_{sieve+sand}$ - weight$_{sieve}$ = weight$_{sand}$). Following, the residue in the sieves were used for dry-sieving with separation into fine, medium, and coarse sand. Different sieves with a specific mesh size (0.063 mm-0.2 mm-0.63 mm) were fixed onto a sieving machine, with the biggest mesh and the dry residue on top. After dry-sieving the quantity of each fraction can be calculated in the same way as for wet-sieving. Differentiation between clay and silt fraction was done in Freiberg.

A very simple method to estimate the amount of organic substances in sediment samples is the so-called ignition loss. The sample (≈ 20 g) was heated in a high-temperature furnace using a porcelain crucible, first at 110°C to remove the water content and afterwards at 550°C for at least 5 h. For cooling, the porcelain crucible containing the sample was left in a desiccator until it reached room-temperature. The loss of weight after heating refers to the rate of organic substances in the sediment including organic carbon and thus higher value is expected in comparison to the measured inorganic carbon with NDIR detection. The total inorganic carbon (TIC) in Calcite ($CaCO_3$) was calculated using mass balance.

To measure the pH of the soil, 25 ml of either 0.01 M $CaCl_2$ or distilled water were added to 10 g of sediment. The solution was agitated and had to stand for 1 h before pH-measuring.

The quantity of calcite in the sediment was determined with the "Carbonate bomb" as described by MUELLER and GASTNER (1971). The sediment (≈ 7.5 g) was filled in the reaction container of the "bomb". The screw closure contained an installed manometer and a small flask for acids which was filled with 6N HCl. In presence of $CaCO_3$ the sediment sample reacts with the acid and forms CO_2. Reaction time was about 15 minutes after which the pressure on the manometer was read as linear indicator for the amount of CO_2 transformed.

3.3.2. Grain size distribution, TIC/TOC/TC, XRD, and total As in Freiberg, Germany

Complementary analyses for grain size distribution as well as analyses for total inorganic carbon (TIC)/total carbon (TC), mineralogical composition by XRD, and total As were performed and organised in Freiberg by Elke Süß (sampling depths see Figure 3.2.1).

Total carbon (TC) was determined by oxidative combustion of 100 to 200 mg air-dried, homogenized sample material in a high temperature furnace at 1300 °C with subsequent NDIR detection of the resulting CO_2 on a multi EA 2000 (analytic Jena, Germany) from M. and B. Hahnewald (Chair of Soil and Water Conservation, TU Bergakademie Freiberg). Total inorganic carbon (TIC) was analyzed with the same device by detection of the resulting CO_2 after sample acidification with approximately 15-20 mL 40 % phosphoric acid in a separate reaction chamber. An oxygen carrier stream was used to purge the CO_2 from the reaction chamber to the detector. The complete system was rinsed with oxygen, to avoid the influence of atmospheric CO_2. Water vapour was removed from the combustion gas stream prior detection by filtering through a pipe filled with quartz wool to avoid interferences with water-vapor, which absorbs IR radiation at the same wavelength as CO_2. Total organic carbon (TOC) was calculated as the difference of TC and TIC. According to the manufacturer, the detection limit is approximately 0.1 mass %. For the calculation of TOC all results determined as < MDL were replaced by 0.3 * MDL.

For the determination of OM the results for TOC, the difference between TC and TIC, was multiplied with the factor 1.724 (SCHEFFER and SCHACHTSCHABEL, 2002).

Particle size distribution of constant mass dried sediment aliquots (fraction < 63 μm) was determined with the gravitational photosedimentometer of the manufacturer Retsch (Fotosedimentograph FS1, Retsch GmbH, Haan, Germany) according to the method described in STAUDINGER et al. (1986). Dispersion of the sediment was achieved in 1 mM (0.45 g/L) tetrasodium pyrophosphate solution (tetrasodium pyrophosphate decahydrate, $Na_4P_2O_7$ $10H_2O$, pro analysis, Merck) and by storing in an ultrasonic bath for 5 min to avoid particle agglomeration. Particle size and its distribution were calculated with the Software GRAINTEST. Bulk densities of the sediment aliquots for calculating the grain size with the Stokes Law were determined in duplicate with pycnometer (ISO 1183-1:2004).

The proportions of the soil separates clay, silt and sand were classified using the USDA soil textural class system. The textural class names were defined by the USDA textural triangle according to their textural composition (Appendix A.1 and B.1).

Mineralogy of the freeze-dried sediment samples (A2, 5, 24, 29, 32, 35, 37, Table 3.2.1) was determined by powder X-ray diffraction (XRD, Dr. R. Kleeberg, TU Bergakademie Freiberg,

Department of Mineralogy) using the diffractometer URD-6 (Seifert-FPM) equipped with a Co-anode and a graphite monochromator. The diffraction patterns were measured in a range of 5 to 80 °2Theta in a step width of 0.03 °2Theta (5 sec/step). Identification of the mineral phases is based on the data material from the database DDView2004. Phase quantification was done by the Rietveld method (program BGMN/Autoquan). Depending on the mineral structure the detection limit is between 0.5 and 5 M %.

The microwave-assisted aqua regia digestion (microwave system Start 1500, MLS, Leutkirch, Germany) was done at the Department of Hydrogeology following the method described in Kopp (2005). Approximately 0.3 g dry sediment were diluted in a mixture of 2 ml nitric acid (65 %, suprapure, Merck), 6 ml hydrochloric acid (32 %, puriss. p. a., Riedel de Haën), and 2 mL UPW. After a 30 minute pre-reaction under a fume hood the digestion was performed in a microwave (Start 1500, MLS GmbH) using a slightly modified temperature-wattage program (Table 3.2.2.1). Total arsenic and phosphorus in these aqua regia digests were determined by Dr. Britta Planer-Friedrich at Trent University, Canada, by ICP-MS (for general performance parameters see also chapter 3.2.2.1).

Table 3.2.2.1 Temperature-performance program used for closed-vessel microwave digestion

step	time [min]	electrical power [W]	temperature [°C]	description
S1	8:00	1000	120	heating-up to final operating temperature
S2	10:00	1000	170	
S3	15:00	1000	170	operating at constant temperature level
vent	20:00	0	70	cooling down

3.3.3. Leaching with artificial groundwater (AGW), hot HCl leach, and leaching/sorption experiment on Bangladesh sediment in Peterborough, Canada

The samples used in all experiments described in the following were taken from different depths according to their variations in stratigraphic features (e.g. grain size, colour, organic carbon) (Figure 3.3.3.1).
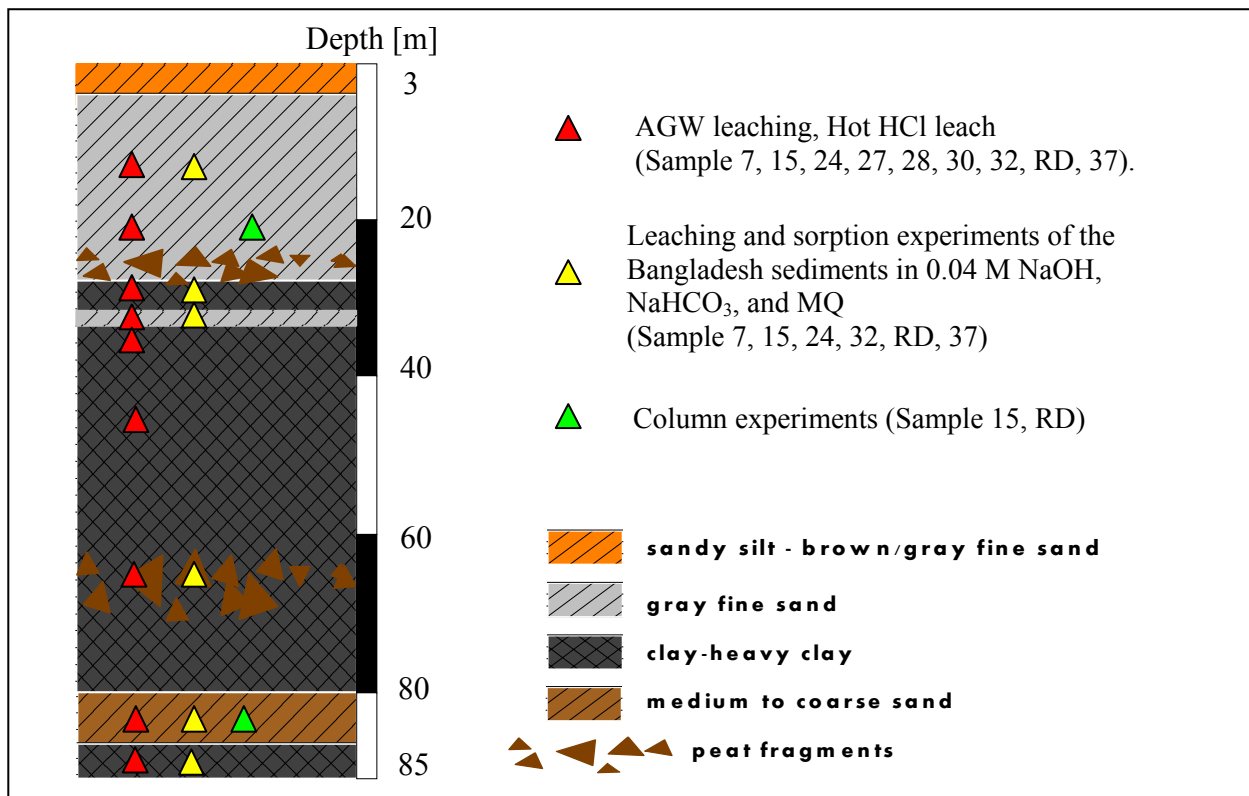
Figure 3.3.3.1 Stratigraphical sketch of the well with sampling points and numbers (see also Table 3.2. 1) of the different experiments. Sediment description was taken from the litholog.

For all experiments Sarstedt Filtrapur S plus 0.2 µm syringe filters, 20 ml BD Syringes with BD Luer-Lok Tip (USA) and for pipetting Fisherbrandt Finnpipettes II (USA) were used. Before measuring the pH the pH-electrode (I.Q. 140 pH meter, USA) was calibrated using 2-3 buffer solutions (pH 4, 7, 10). All solutions, except the artificial groundwater (AGW), were prepared with MQ (Milli-Q element, Ultrapure Ionex Cartridge, Millipore). For preparation of the artificial groundwater (AGW), deionised water was used.

3.3.3.1. AGW leach

The estimation of the weakly bound concentration of As, P, Fe, and Mn was done with an artificial groundwater (AGW) leaching. The chemical composition of the AGW (2.5 M $NaHCO_3$ (Caledon, Canada), 2.5 M $CaCO_3$ (Fisher Scientific, USA), and 2.5 M $MgCl_2*6 H_2O$ (Caledon, Canada)) was adapted from groundwater chemistry data of the test field (Table 3.1.1). The suspensions used for

the experiments on weakly bound elements contained ≈ 1 g sediment and 20 ml AGW in 50 ml centrifuge tubes (Sarstedt, USA). The filtered suspension was analysed after 1, 3, and 6 days shaking (21 rpm, GFL 3040, Rotating Shaker, Burgwedel, Germany). A colorimeter (DR890 of Hach®, Germany) was used to determine the extracted concentration of Fe and Mn. The methods are listed in Table 3.3.3.2.1. The concentration of dissolved As and P was analysed without dilution by Inductively-Coupled Plasma Mass Spectrometry (ICP-MS).

Table 3.3.3.2.1 Colorimetric methods (HACH manual)

Ion	Method	Concentration range/std. deviation	Interferences
Fe_{tot}	FerroVer method	0 – 3 mg/L 0.03 ± 0.017 mg/L	Ca, Mg > 10 g/L as $CaCO_3$; high S^{2-}; extreme pH values; Cl^- > 185 g/L
Mn_{tot} low range	PAN method	0 – 0.700 mg/L 0.007 ± 0.013 mg/L	Mg > 300 mg/L as $CaCO_3$ hardness 1:20

3.3.3.2. Hot HCl leach

The quantity of As, P, Fe, and Mn that is moderately bound on the sediment surface was extracted with a hot HCl leach. This leaching method targets As, P, Fe, and Mn that is associated with poorly crystallized and amorphous iron(hydr)oxides and Mn oxides, acid volatile sulphides, and carbonates (HARVEY et al., 2002; HORNEMAN et al., 2004; HUDSON-EDWARDS et al., 2004; VAN GEEN et al., 2004). The leachings were performed by adding ≈ 250 g of air-dried sediment in 15 ml centrifuge tubes. Then, 5 ml of 1.2 N HCl (Fisher Sc., USA) were added to it. The tubes were heated in a water bath at 80°C for 30 min (HORNEMAN et al., 2004). After leaching, the suspensions were filtered and diluted for total analyses (As, P, S) by ICP-MS. Fe and Mn was determined by colorimeter.

3.3.3.3. Leaching and sorption experiment with Bangaldesh sediments in NaHCO₃, NaOH and MQ

Another experiment included the leaching and sorption behaviour of the Bangladesh sediment in 0.04 M NaOH (Fisher Sc., USA), 0.04 M NaHCO₃, and MQ as well as capacity tests spiking arsenate or arsenite (Table 3.3.3.3.1). All samples were prepared under anoxic conditions in the glove box. After weighting the sediment samples (6 g) in a 50 ml centrifuge tube 45 ml of the prepared solution (purged with N₂, with or without arsenic spike) was added to it. The tubes were

shaken (21 rpm) for 72 h, the samples filtered and immediately analysed for As species by IC-ICP-MS. Until analyses for total As concentrations, the samples were stored in the fridge.

Table 3.3.3.3.1 Overview leaching and sorption experiments on Bangladesh sediment.

Depth [m]	Solutions	Experiments
12	in 0.04 M NaOH, NaHCO$_3$, and MQ	
27	in 0.04 M NaOH, NaHCO$_3$, and MQ	
28	in 0.04 M NaOH, NaHCO$_3$, and MQ	1. Solution without spike
61	in 0.04 M NaOH, NaHCO$_3$, and MQ	2. Solutions with spike 1ppm arsenite
81	in 0.04 M NaOH, NaHCO$_3$, and MQ	3. Solutions with spike 1ppm arsenate
84	in 0.04 M NaOH, NaHCO$_3$, and MQ	

3.3.3.4. Sorption capacity tests on Bangladesh sediment

Within this first experiment increasing concentrations of arsenite and arsenate (25, 50, 75, 100, 150, 200, 250, 500 ppb) were added to 1 g of sediment in 20 ml AGW. The experiment was carried out with material from 81 m depth (RD). IC-ICP-MS analyses were performed after a 2 and 7 days equilibration time in the overhead shaker (21 rpm).

Because of higher expected sorption capacities of the sediment a second sorption capacity experiment with increasing concentrations arsenite, arsenate, and phosphate (0.5, 1, 2.5, 5, 10, 20 mg/L) was investigated in 50 ml MQ and with ≈ 100 mg sediment. In this experiment sediment from 6 different depths was used (7, 24, 27, 32, RD, and 37; Table 3.2.1). Each sediment was spiked with 6 different concentrations of arsenite, arsenate, and phosphate (6 x 6 x 3 = total of 120 samples). After 2 days shaking time (21 rpm) the samples were filtered and analyzed by ICP-MS.

3.5. Simulation of natural groundwater conditions in column experiments

3.5.1. Experimental design

The aim of this experiment was to observe the sorption behaviour of specific anions (AsO_3^{3-}, AsO_4^{3-}, AsO_3S^{3-}, PO_4^{3-}, and S^{2-}) on the sediment surface as well as how interactions between different anions such as the competition for exchangeable sites ($AsO_4^{3-} \leftrightarrow PO_4^{3}$) and the formation of As-S species can influence the mobilization of sorbed arsenic.

Sodium phosphate ($Na_2HPO_4*7H_2O$) and sodium arsenate ($Na_2HAsO_4*7H_2O$) were obtained from Sigma-Aldrich Chemical Co. (USA), sodium meta-arsenite ($NaAsO_2$) from J.T. Baker (USA). A monothioarsenate standard was synthesized in the laboratories of Trent University and used for the experiments (WALLSCHLÄGER and STADEY, 2007).

Natural groundwater conditions as they may appear in the Bangladesh aquifers were simulated in these column experiments. As CaCO$_3$ did not dissolve in concentrations of 2.5 mM (SI = 0.92), the AGW composition was changed to only 2.5 M NaHCO$_3$ and 2.5 M MgCl$_2$ without CaCO$_3$. Data

from groundwater analyses of the study area were used to get information about major ions, pH, conductivity, and natural occurring arsenic and phosphate concentrations so that the composition of the AGW used in these experiments represented similar conditions (Table 3.1.1). A total As concentration of 2.6 µM (0.2 mg/L) was used which is within the range of total As from analyses of the test field as well as typical for As-contaminated groundwaters in Bangladesh. Phosphate was assumed to have a concentration of 32 µM (1 mg/L). The column experiments were conducted with sediments from two aquifer units in 21 m and 81 m depth (Table 3.2.1). The material from the shallow aquifer is reduced fine sand, grey in colour, whereas the material from the deeper aquifer is oxidized coarse sand with a brownish colour.

The column setup with the flow direction of the artificial groundwater (AGW) is presented in Figure 3.5.1.1 The adsorption experiments were performed with a stock solution (AGW) of 2.5 mM $NaHCO_3$ and 2.5 mM $MgCl*6H_2O$ which was prepared in a 20 L PE storage container and afterwards filled into 1 L PE bottles (a). The bottles were stored in the dark to avoid photooxidation. New stock solutions were prepared every 1 to 2 days. Solutions were pumped with a flow rate of ≈ 0.15-0.2 ml/min by use of a Masterflex L/S pump with a cartridge pump head system (Cole Parmer, USA) (b). The columns were preconditioned by pumping only the stock solution (As-free) through the column with the sediment (c). The preconditioning started the day before the beginning of the adsorption experiment. After preconditioning, solution 1 (stock solution + first spike) was pumped through the column until equilibration of the solution with the sediment. Thereby the sorption behaviour of arsenate and monothioarsenate was monitored in experiment 3. Afterwards, a second solution (solution 2, stock solution + second spike) was pumped through the column to determine the effects of anion competition ($AsO_4^{3-} \leftrightarrow PO_4^{3-}$) on As mobilization (experiment 1) and the sorption behaviour of As species (experiment 2 and 3). The effluent was then collected continuously in 15 ml centrifuge tubes over a time period of ≈ 8 h (d). The time intervals for the sampling increased with duration of the experiment from 5 min in the first 30 min to 1 h after 5h after starting the experiment. Short time steps in the beginning guaranteed the registration of small changes in the AGW composition after sediment-solution contact with the time. A total of ≈ 25 samples for each column were collected. Pre-tests were done in advance and the samples analysed for total As and P to estimate the developing of concentrations. So it was possible to know which time steps could be interesting for species analyses in the main experiment. Hence, only a selection of samples were analysed immediately following the experiment by IC-ICP-MS or refrigerated until total analyses of As and P with ICP-MS. The pH of the stock solution was monitored at the beginning of the experiment and final pH measurements were taken at the effluent of the column.
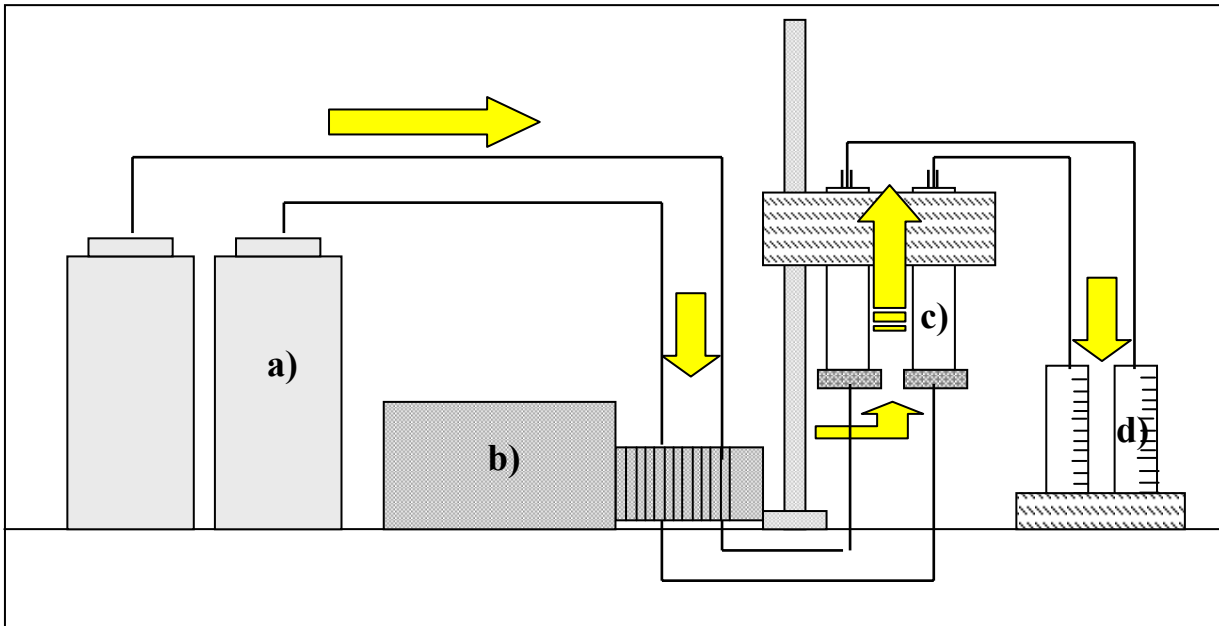
Figure 3.5.1.1 Instrumental design of column experiments. The initial solution is pumped (Masterflex L/S peristaltic pump with cartridge pump head system (b)) out of the storage bottles (a) through the columns (c) which were filled with ≈ 1 g of sediment in the upper part and. The effluent was then collected in centrifuge tubes (d) for further analyses.

The design of a single column is shown more detailed in Figure 3.5.1.2. The construction is based on an ion exchanger (length 6.2 cm, diameter 0.8 cm). After removing the ion exchanger material the PE column was cleaned with 2 % HNO_3 and distilled water. The column was then dry-packed with ≈ 1 g sediment. One filter plate was installed on both sides of the sediment to avoid the discharge of soil particles with the solution out of the column. The sediment was filled in the upper part of the column to support a uniform hydraulic gradient/pressure underside the filter plate. To prevent the generation of a preferential flow through small cracks in the sediment the water flows against the gravitation from the bottom to the top. To connect the column with the tubing two adapters made of pipette tips were attached on both ends of the column.
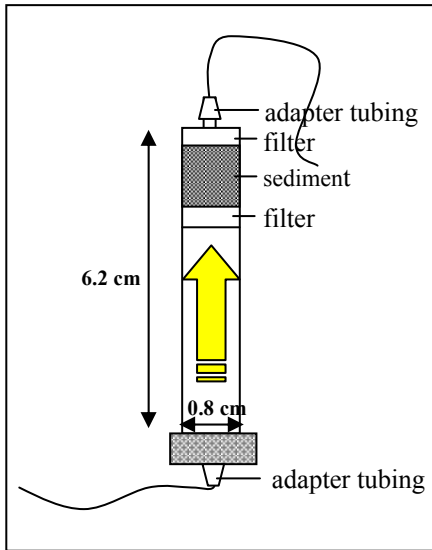
Table 3.5.1.1 Composition stock solution and concentration spike

Composition AGW (stock solution)		
NaHCO$_3$, MgCl$_2$*6H$_2$O [mM]	2.5	
pH	7.8-8.5	
Conductivity [µS]	650-800	

Concentrations spike	[mg/L]	[µM]
arsenic	0.2	2.6
phosphorus	1.0	32
sulfide	0.8	25
monothioarsenate	0.2	2.6

Figure 3.5.1.2 Design of a single column with flow direction

The calculation of the adsorbed and desorbed concentrations was done by graphically integrating sections (B and D) of the effluent breakthrough curves as shown in Figure 3.5.1.3. The following formulas were used to determine the adsorbed and desorbed concentrations:

total As/P pumped through column: $A = C_0 \times V_{tot}$

As/P adsorbed: $C = A - B$

As/P desorbed: $D_{des} = D - E$

As/P remained in pore water: $E = V_0 \times C_0$

C_0: concentration spike (e.g. 200 µg/L As)

V_{tot}: total volume pumped through column

V_0: pore volume (0.9 ml)
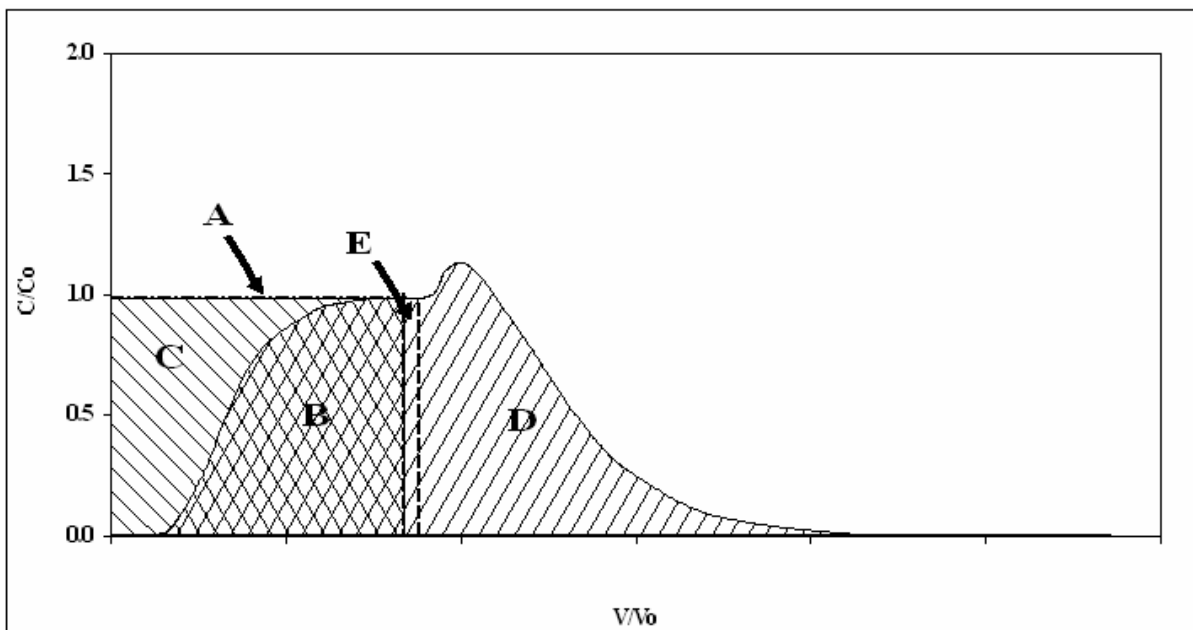
Figure 3.5.1.3 Schematic graphic of the effluent breakthrough curve used for calculating the quantity of As and P adsorbed and desorbed.

3.5.2. Column experiments

The column experiments primarily comprehend 3 parts. An overview is listed in table below (Table 3.5.2.1).

Table 3.5.2.1 Within 3 different experiments the sorption behaviour of specific anions (AsO_3^{3-}, AsO_4^{3-}, AsO_3S^{3-}, PO_4^{3-}, and S^{2-}) and their influence on arsenic mobility was investigated.

	Solution 1	Solution 2
First experiment: As-P speciation		
1. $AsO_3^{3-}/AsO_4^{3-} \rightarrow PO_4^{3-}$	AsO_3^{3-}/AsO_4^{3-}	PO_4^{3-}
2. $PO_4^{3-} \rightarrow AsO_3^{3-}/AsO_4^{3-}$	PO_4^{3-}	AsO_3^{3-}/AsO_4^{3-}
Second Experiment: Arsenate-Monothioarsenate speciation		
1. AsO_4^{3-}	AsO_4^{3-}	
2. AsO_3S^{3-}	AsO_3S^{3-}	
3. AsO_4^{3-} and AsO_3S^{3-}	$AsO_4^{3-} + AsO_3S^{3-}$	
Third Experiment: As-S(-II) speciation		
1 $AsO_3^{3-}/AsO_4^{3-} \rightarrow S(-II)$	AsO_3^{3-}/AsO_4^{3-}	S(-II)
2. $S(-II) \rightarrow AsO_3^{3-}/AsO_4^{3-}$	S(-II)	AsO_3^{3-}/AsO_4^{3-}

The first experiment simulated the impact of fertilizer phosphate on arsenic mobility and the displacement of either As or phosphate from the sediment surface after addition of the other anion.

In a second experiment the adsorption behaviour of monothioarsenate and arsenate was conducted. Arsenate, monothioarsenate (0.2 mg/L) and a mix of both (0.1 mg/L each) was added to the AGW solution and samples were taken with increasing time intervals (see experimental design) until equilibration of sediment and solution.

The addition of arsenic (arsenite and arsenate) and sulphide to the sediment system was performed in the third experiment. Sulphide released from natural occurring sulphide minerals may form thioarsenates under changing redox conditions and influence the arsenic release into the groundwater.

3.5.3. First experimental setup

Initially, the experimental setup was conducted with columns of a larger dimension (Figure 3.5.3.1).

Figure 3.5.3.1 Experimental design of first column experiment

These columns were made of glass, had a diameter of 3.3 cm, a height of 35 cm, and were filled with material from rotary drilling (oxidized sand in deeper aquifer ≈ 282 g). The flow rate of 0.18 ml/min and the total column volume of 195 ml resulted in 3.5 to 4.5 pore volumes/day. To protect the sediment from the effect of light they were wrapped in aluminium foil. In the upper 5 cm the column was filled with quartz and glass wool to avoid the discharge of soil particles out of the column. The principle for the AGW flow is the same as already described for the "little" column experiments in chapter 3.5.1, except that the PE storage container had a volume of 3 L. The AGW (2.5 mM $MgCl_2*6H_2O$, $NaHCO_3$, and $CaCO_3$) was treated with CO_2 gas to dissolve undissolved $CaCO_3$. The resulting clear solution with a pH below 6 was subsequently purged with compressed air to raise the pH up to 7 to 7.5.

Before starting the competitive sorption tests the columns were equilibrated with the AGW. 10 columns were prepared and the spike of each was as follows:

- 2x Arsenite (200 µg/L), 2x Arsenate (200 µg/L)
- 1x mixture Arsenate/Arsenite (100 µg/L:100 µg/L)

- 2x Phosphate (2000 µg/L), 2x Hypophosphite (2000 µg/L)
- 1x mixture Phosphate/Hypophosphate (1000 µg/L:1000 µg/L)

In the second part of the experiment phosphate and hypophosphite should have been added to the columns which were initially treated with arsenate and arsenite.

During the experiment samples of the effluent were collected continuously and analyses for total As and P as well as for As-species. Furthermore on-site parameters (pH, conductivity, redox, and oxygen) were frequently determined. After 30 days still no breakthrough of arsenite, arsenate, phosphate, and hypophosphite was observed in the effluent. According to sorption tests, which were conducted with Bangladesh sediments and literature data the sorption capacity of the sediment was calculated to be too high (see chapter 4.1.5) for the size of these columns and the filling of 282 g sediment. After 30 days the adsorbed As concentration was calculated with only 9 µg/g, thus there were still free sorption sites. Therefore this experiment was stopped because sorption and desorption tests would have taken too long and the setup for a smaller and more efficient experimental design was planned.

3.6. *Laboratory experiments for arsenic mobilization depending on carbonate concentration*

In a number of experiments, arsenic sorption and mobilization from different mineral phases were investigated in the presence and absence of carbonate to detect a potential influence of arsenic carbonate complexation on arsenic dissolution as described before (see chapter 2.5.). The dissolution behaviour of arsenic bond to sulfur or oxygen atoms within the aquifer material was studied using the pure mineral phases Orpiment (As_2S_3, Alfar Aesar, USA) and Arsenic Trioxide (As_2O_3, Sigma, USA) as As-bearing minerals. Binding in the system Fe-S-As was studied on Pyrite (FeS_2, Alfar Aesar, USA). All experiments were prepared under anoxic conditions in a N_2-purged glove box to avoid the contact with atmospheric oxygen.

A centrifuge tube with 25 mg solid (As_2S_3, As_2O_3, or FeS_2) was filled with 50 ml of N_2-purged solution ($NaHCO_3$ and $NaOH$). $NaHCO_3$ and $NaOH$ were added with increasing concentrations of 0.01 M, 0.04 M, and 0.1 M. To observe the sorption behaviour of arsenic on FeS_2 additionally 1 mg/L arsenite/arsenate was added to the samples. The suspension had to shake (20 rpm) for 48 h in a rotating shaker. After this time the suspension was filtered (0.2 μm) and prepared for IC-ICP-MS analyses in the glove box. High As concentrations were expected in the filtrate from As_2S_3 and As_2O_3 dissolution; therefore the samples had to be diluted up to 50 times with N_2-purged deionized water before analyses. No dilution was required for the FeS_2-samples. The pH of the liquid was measured before addition of the solid, after addition of the solid, and as well as at the end of the experiment.

Another experiment included the dissolution of As_2S_3 in MQ and in 0.04 M $NaHCO_3$ under different pH conditions (range pH: 3-12) to check for potential pH-dependent influence of arsenic-carbonate complexation. A total of 20 samples with 25 mg solid were prepared. Ten samples were used for the dissolution in MQ and 10 for the dissolution in 0.04 M $NaHCO_3$. After adding the MQ and $NaHCO_3$ the pH of the liquid was adjusted with 0.1 M NaOH (1.9 M NaOH for pH 11 and 12) and 0.1 HNO_3 (Fisher Sc.). Finally, the tubes were filled to 50 ml. These suspensions remained in the glove box for the total duration of the experiment. Species analyses were done 7 times for $NaHCO_3$ and 8 times for MQ over a time period of almost 2 months (Table 3.6.1). Each time, 1 ml sample was filtered (0.2 μm), then collected in another centrifuge tube and prepared for analyses. Additionally, total analyses were done for the last 2 analyses. The samples had to be diluted by 2 to 50 times with N_2 purged MQ for ICP-MS and IC-ICP-MS analyses. The pH was measured in the suspension directly after adding the MQ/$NaHCO_3$ to the solid and after each sampling. Because of

experimental problems the sampling of As_2S_3 in MQ for species analyses at day 0 was retarded compared to As_2S_3 in $NaHCO_3$ what may influence the results for As_2S_3 dissolution on that day. Theoretical dissolution of As_2S_3 was modeled with PhreeqC-2 (version 2.14.03) at pH ranging from 2 to 13 using the database WATEQ4F.

Table 3.6.1 Days of sampling for arsenic species after dissolution of As_2S_3 in MQ and NaHCO3

	As_2S_3+MQ	As_2S_3+NaHCO3
Start:	*30/07/2007*	*31/07/2007*
1 analysis	30/07/07 (day 0)	31/07/07 (day 0)
2 analysis	31/07/07 (day 1)	02/08/07 (day 2)
3 analysis	02/08/07 (day 3)	04/08/07 (day 4)
4 analysis	04/08/07 (day 5)	07/08/07 (day 7)
5 analysis	07/08/07 (day 8)	14/08/07 (day 14)
6 analysis	14/08/07 (day 15)	05/09/07 (day 36)
7 analysis	05/09/07 (day 37)	19/09/07 (day 51)
8 analysis	19/09/07 (day 52)	

3.7. Analytical methods and instrumentation

The methods for total arsenic concentrations and arsenic speciation used in this study were established by Dirk Wallschläger at Trent University (see also Wallschläger and Stadey (2007) for more instrumental details). Total arsenic concentration was determined by ICP-MS using the dynamic reaction cell (DRC) technology (Elan DRC 6100+, Perkin-Elmer, Shelton, CT) with O_2 as reaction gas (Table 3.7.1). Oxygen was used to avoid interferences of As^+ (m/z 75) with $ArCl^+$ ($Ar^{40}Cl^{35\ +}$: m/z 75, $^{75}As^{16}O^+$ m/z = 91) caused by the use of argon plasma for ionisation. For arsenic speciation the ICP-MS was coupled to the IC (AEC) (Table 3.7.2) (WALLSCHLÄGER and STADEY, 2007).

Table 3.7.1 Instrumental parameters for ICP-MS detection (WALLSCHLÄGER and STADEY, 2007):

instrument	Elan DRC 6100+, Perkin-Elmer, Shelton, CT
plasma rf power	1,400 W (1,550 W for As only)
nebulizer gas flow rate	0.8 to 0.9 L/min
nebulizer	TR-30-C3 (Meinhard, Santa Ana, CA)
spray chamber	cyclonic (Glass Expansion, Hawthorn East, Victoria, Australia)

Table 3.7.2 Instrumental parameters for IC (AEC) Separation (WALLSCHLÄGER and STADEY, 2007):

columns	IonPac AS-16/AG-16 4-mm (10-32) (Dionex, Sunnyvale, CA)
eluent	NaOH (0.1 mol L^{-1}) at 1.2 mL min^{-1}
gradient	0-7 min 20 mmol L^{-1} 7-17 min 20-100 mmol L^{-1} 17-25 min 100 mmol L^{-1} 25-28 min 20 mmol L^{-1}
typical retention times	AsO_3^{3-}, 217 ± 9 s; AsO_4^{3-}, 840 ± 27 s; $AsO_3S_3^-$, 935 ± 23 s $AsO_2S_2^{3-}$, 1036 ± 20 s; $AsOS_3^{3-}$, 1141 ± 25 s; AsS_4^{3-}, 1201 ± 22 s
sample volume	0.5 mL
suppression	ASRS-Ultra 4-mm (Dionex), 400 mA current, 5 mL min^{-1} water (external mode)

For total analyses an internal standard of 5 µg/L ^{103}Rh, ^{115}In, ^{192}Ir, and ^{204}Tl was added to the samples to monitor and compensate any drift in the sensitivity of the instrument. Standards were controlled against the analytical reference material TM-DWS (National Water Research Institute, Environment Canada) with nominal a concentration of 72.5 µg/L. Duplicate samples with and without spikes were run to determine possible matrix influences. Sensitivity changes of the instrument were also observed with repetitive measurements of calibration standards within each individual run. The instrument was calibrated with mixed As and P standards for ICP-MS analyses. Mixed arsenite, arsenate, phosphate, and sulphate standards were used for IC-ICP-MS measurements. The calibration standard for sulphide had to be analysed separately to avoid the complexation with arsenic. The quantification of thioarsenates was done with the arsenate calibration curve. The concentration of As, S, and P after IC-ICP-MS analyses was quantified by estimating the peak area of the chromatogram (Origin60).

Detection limits for total analyses were calculated as three times the standard deviation of the average blank (3*MQ) concentration: ≈ 0.2 µg/L for As and ≈ 0.3 µg/L for P. Detection limits for arsenic species were reported with ≈ 0.01 µg/L under the conditions of maximum S sensitivity (WALLSCHLÄGER and STADEY, 2007), but not measured during the experiments.

4. Results

4.1. Basic investigations of sediment properties

4.1.1. Lithology and mineralogy

From sediment observations in the test field a lithological log was generated (Appendix A.2), containing main sediment properties (e.g. sediment type, color, peat content, etc.). Referring to the litholog, the sediments underlying the Daudkandi area could be divided into five units.

Layer 1:   3 – 6 m sandy silt and brown to grey fine sand

Layer 2:   6 – 27 m reduced grey fine sand and silt, in 26 m peat fragments (shallow aquifer)

Layer 3:   27 – 79 m silty clay to clay, in 61 to 73 m peat fragments, lens of coarser sediment (fine sand) in 34 m

Layer 4:   79 – 83 m channel of oxidized brown fine to medium sand (deeper aquifer)

Layer 5:   > 83 m clay to heavy clay

The upper 3 m of sediments building the earth bank for the hospital were not investigated. Laboratory sediment texture analyses, results shown in Figure 4.1.1.1, confirmed the division of the profile into the described five layers.

The soil type of layer 1 is mainly silt (89 %) with 11 % clay and no sand. Layer 2 (4.6 to 27.4 m depth), the shallow aquifer, is dominated by the sand fraction. Silt and clay occurred in a minor fraction of 15 to 48 % and 1 to 3 %, respectively. At the bottom of layer 2 sand increased and formed sandy loam to loamy sand which are looser in texture, single grained and slightly cohesive when moist. The third layer (27.4 m to 79.1 m), a 50 m thick aquiclude, consisted of higher proportions of finer soil fractions, particularly silt (46 to 91 %) and clay (4 to 44 %). Silt loam represents the dominant soil textural class in the upper layer 3. The observed silty clay in 34.4 and 61.2 m depth is very sticky and very plastic when wet, and forms very hard aggregates when dry. Layer 4 (79.1 to 83.4 m) consisted of particularly loose and single-grained material with sand as the main soil fraction and was defined as the deeper aquifer. In 77.6 m, the classified sand contained only 1 % clay and 19 % silt. With increasing depth the proportion of silt increased (loamy sand to sandy loam at the bottom). The deepest layer (L5, > 83.4 m), the aquiclude underlying the deeper aquifer, was fine-grained, contained no sand and was classified as silty loam. The sieve loss did not exceed 10 % of the initial sample weight.
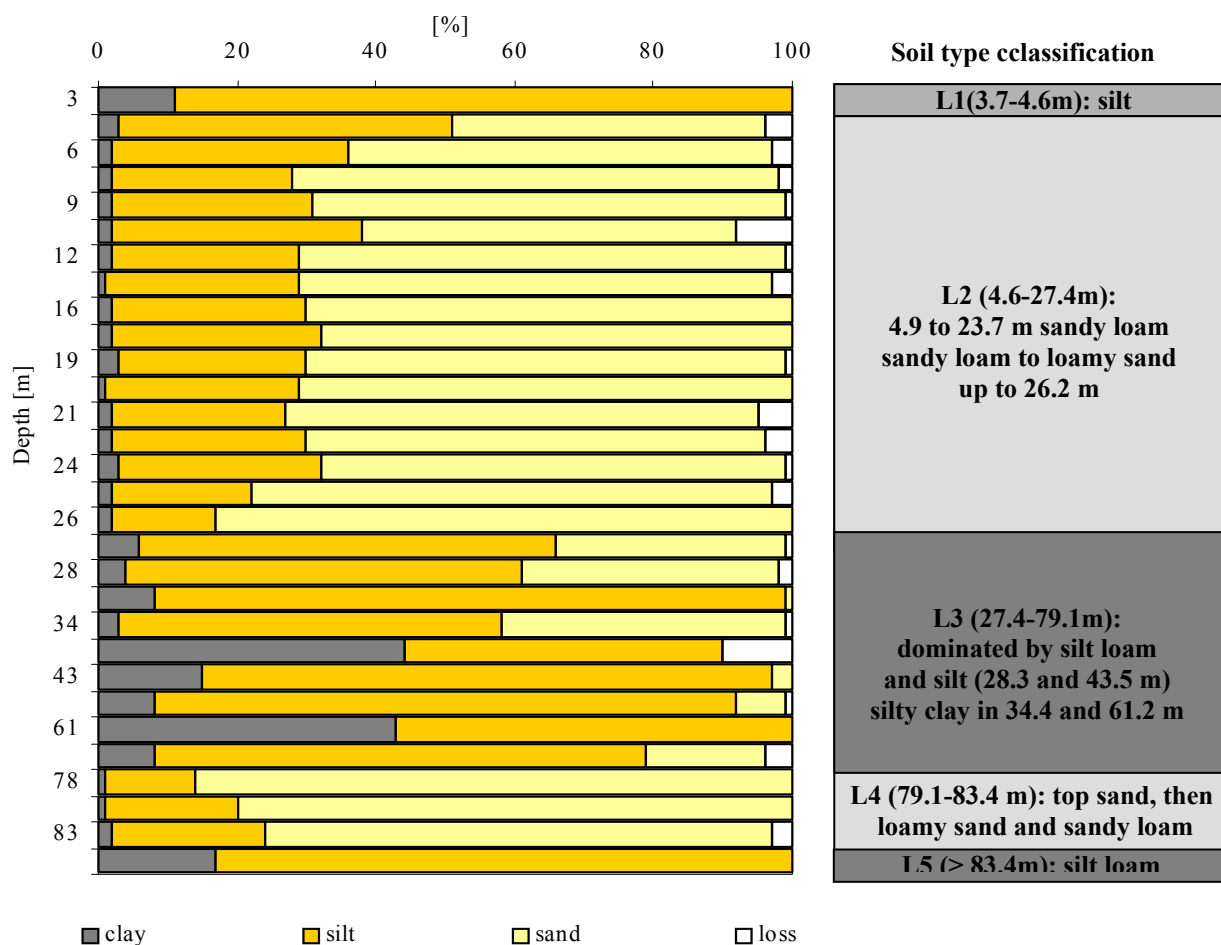
Figure 4.1.1.1 Particle size analyses according to the soil type classification of the United States Department for Agriculture (USDA; Brady and Well, (2005))

The mineralogy determined by XRD (Figure 4.1.1.1) showed quartz and feldspars (plagioclase and alkali feldspars) as the dominant minerals in the two aquifers (L2, L4) and in L1. Mica (muscovite, just in L4 traces of biotite), chlorites, and rutil were observed in minor contents. The aquicludes showed an even distribution of mica, clay minerals (dominated by smectite and kaolinite, vermiculite in minor), and quartz, where clay reached 49 % in 61 m depth. The aquicludes also showed higher chlorite contents compared to the aquifers, and feldspar and rutil just in traces. In the clayey layer in 84 m depth traces of siderite were found indicating reducing conditions in this bottom layer.

Table 4.1.1.1 Summary of mineralogical characteristics of the Bangladesh sediments. XRD analyses were done with sediment samples from 7 different depths which represent the mineralogical composition of the particular layer.

Layer	Depth [m]	Sample Depth [m]	Mineralogy	
			major	minor
L1	3-6	5	quartz (51.1 %), feldspar (28.25 % - k-feldspar and Plagioclase)	phyllosilicates: clays (in sum 4.7 %), mica mainly muscovite (7.4 %)
L2	6-27	9	quartz (55.8 %), feldspar (23.86 % - k-feldspar and Plagioclase)	phyllosilicates: clays (in sum 6.1 %), mica mainly muscovite (7.6 %)
		26	quartz (71.1 % - highest quartz content in the depth profile), feldspar (20.1 % - k-feldspar and Plagioclase)	phyllosilicates: no clays, mica (4.6 %, mainly muscovite)
L3	27-79	34	quartz (25.7 %), mica (23.5 %), clay minerals (24.7 %)	feldspar (14.2 %)
		61	clay (49.3 %), feldspar)	mica (19.4 %), quartz (14.9 %), and feldspar (8.24 %
L4	79-83	83	quartz (59.9 %), feldspar (28.6 % - k-feldspar and Plagioclase)	phyllosilicates: mica (5.3 %), clay (1.5 %, mainly kaolinite)
L5	> 83	84	quartz (28.1 %), mica (23.4 %), clay minerals (30.0 %)	feldspar (7.7 %), special feature - 2.1 % Siderite (Iron carbonate)

4.1.2. pH-value, carbon and calcite contents in the deep-core drilling sediments

The pH-values were determined in MQ and $CaCl_2$ as measure for soil acidity. The difference between pH values measured in MQ and $CaCl_2$ may serve as an indicator for the exchange capacity of the sediment. pH values measured in $CaCl_2$ are comparable with the natural occurring pH in the sediment-groundwater contact zone.

The pH for $CaCl_2$ and MQ was in the range of 5.66 to 7.09 and 6.10 to 7.58. In both cases the pH increased with depth and reached a maximum (7.09 and 7.58) in the upper part of the aquiclude (L3) in 44 to 54 m depth, whereas lowest values (5.66 and 6.10) were found in 61 to 65 m depth (see figure 4.1.2.1). A pH-increase was again observed in the sediment taken from the deeper aquifer unit (oxidized fine sand, layer 4) in 77 to 83 m depth. In all samples slightly higher pH values were determined in MQ, as visible in Figure 4.1.2.1. For the different layers (1 to 5) differences ($pH_{MQ} - pH_{CaCl}$) were calculated with 0.4 (± 0.10), 0.3 (± 0.15), 0.4 (± 0.08), 0.2 (± 0.05), and 0.1.
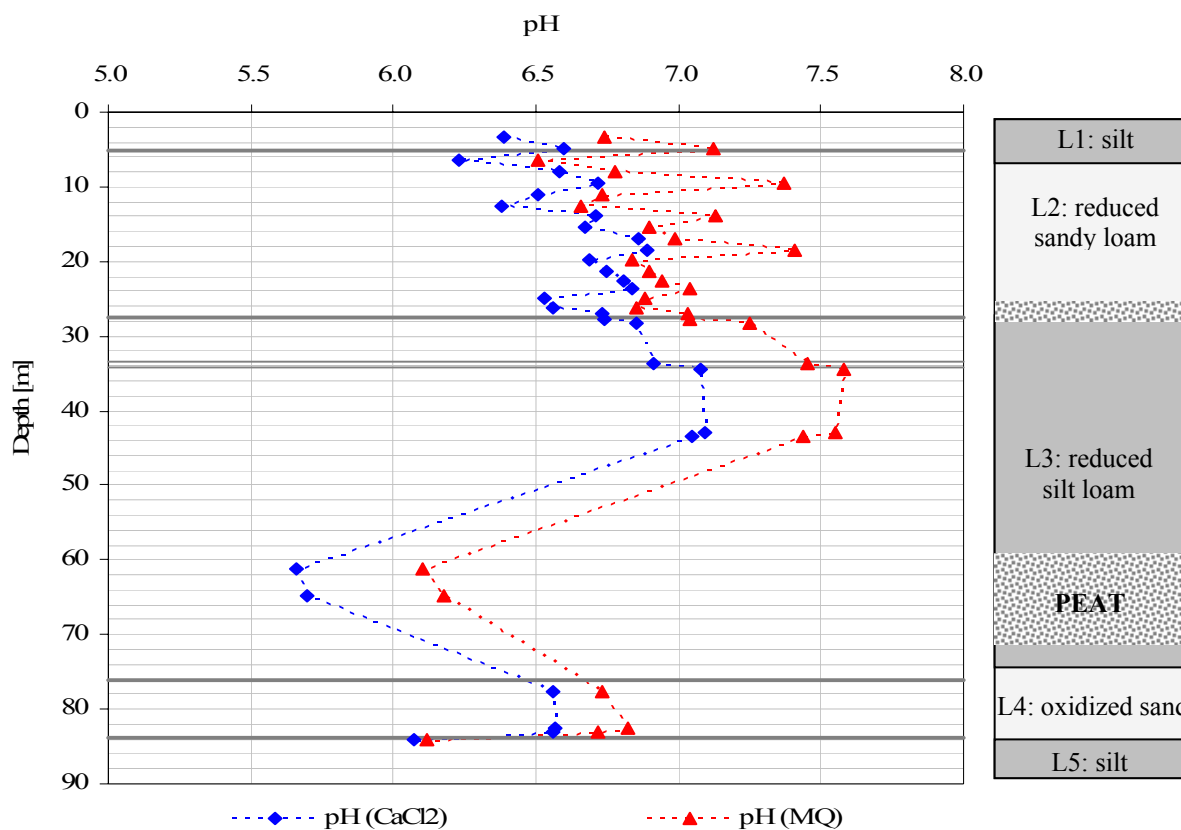
Figure 4.1.2.1 Sediment pH-values determined in CaCl₂ and MQ for the deep-core drilling sediments (3 m to 84 m depth).

Calcite and organic matter can act as potential sorption sites for arsenic. Organic matter is also the redox driver for the reductive dissolution of arsenic-rich hydrous iron oxides. Thus, the depth distribution of carbon from different sources, which includes inorganic carbon, e.g. calcite, but also organic carbon, comprised in organic matter material, is of great interest when discussing arsenic mobility in a depth profile and thus subject of the present investigations. The results for carbon and organic matter analyses (TC, TIC, TOC, OM, and Calcite) are summarized in Table 4.1.2.1 All measured TIC values were below detection limit (0.1 wt%), except sample 28 in 33.8 m depth (0.16 wt%).

Table 4.1.2.1 Summary of total (TC), total inorganic (TIC), and total organic carbon (TOC), organic matter (OM), and Calcite concentrations determined on the deep-core drilling sediments.

Layer	Sample No.	Depth [m]	TC wt%	TIC wt%	TOC wt%	OM (TOC) wt%	OM (Ignition Loss) wt%	Calcite wt%	TIC (CaCO₃) wt%
1	A2	**5**	0.28	0.00	0.28	0.47	0.53	0.00	0.00
2	3	**6**	0.40	0.00	0.40	0.68	0.42	0.00	0.00
	5	**9**	0.17	0.00	0.17	0.29	0.31	0.00	0.00
	15 16	**21**	0.13	0.00	0.13	0.22	0.29	0.00	0.00
	23 24	**26**	0.08	0.00	0.08	0.14	0.11	0.00	0.00
	25	**27**	0.28	<0.10‡	0.25	0.43	0.99	0.65	0.08
3	27	**28**	1.02	<0.10	0.99	1.71	1.56	1.40	0.17
	28	**33**	0.99	0.16	0.83	1.43	0.99	1.05	0.13
	29	**34**	0.79	<0.10	0.76	1.30	2.33	1.00	0.12
	32	**61**	4.92	<0.10	4.89	8.42	4.00	1.60	0.19
4	R	**78**	0.19	0.00	0.19	0.33	0.49	0.00	0.00
	35	**83**	0.16	0.00	0.13	0.22	0.39	0.00	0.00
5	37	**84**	1.48	<0.10	1.48	2.55	3.22	1.40	0.17

‡ for TOC calculation (TC-TIC) TIC-values < MDL (i.e. <0.10 wt%) were substituded by 0.3×MDL

TIC calculated from the content of calcite was low and only measurable in the aquicludes (0.08 to 0.19 µg/g). Because of negligible TIC values TC primarily consists of TOC. Vertical profiles of the main parameters TC, OM (TOC and ignition loss), and calcite are shown in Figure 4.1.2.2.

The same depth distribution was observed for these parameters, i.e. low values in the shallow and deeper aquifer (L2 and L4) in 5 to 26 m and 79 to 83 m depth with values below 0.4 wt% TC (TIC = 0, < 0.7 wt% OMTOC, Calcite = 0) and increasing values in the sandy loam (L3 and L5) with maximum values of 4.9 wt% TC (TIC < MDL, 0.76 wt% TOC, 8.4 wt% OM (TOC)) in 61 m depth. In contrast, the pH showed higher values in the aquifers (L2 and L4) and a minimum in the clayey layer (pH 5.6 in 61 m) as shown in Figure 4.1.2.2.
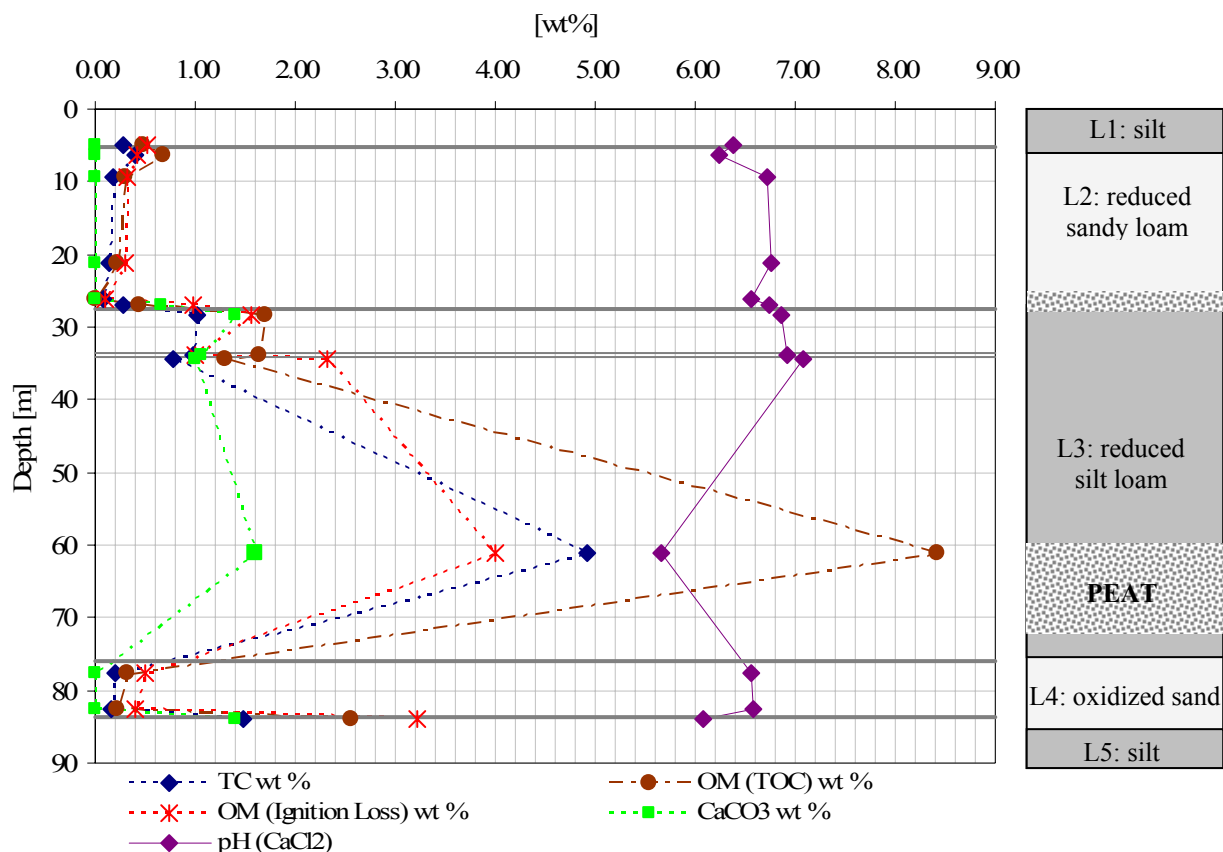
Figure 4.1.2.2 Depth distribution of total carbon, organic matter (TOC and ignition loss), Calcite (CaCO₃), and pH.

4.1.3. Determination of leachable As, P, Fe, and Mn in hot HCl and AGW, and microwave digestion to determine total arsenic and phosphorous contents

The concentrations of As, P, Fe, and Mn leachable in hot HCl are listed in Table 4.1.3.1 Arsenic ranged from 0.3 µg/g (12 and 81 m depth) to 3.8 µg/g (84 m.). Higher As concentrations were leached in the aquicludes (L 3 and 5) in 28, 43, 61, and 84 m depth. P concentrations leachable in hot HCl reached a maximum in 21 m depth (600 µg/g) and then decreased to 80 µg/g at the bottom layer (84 m depth). The leachable Fe fraction varied over a wide range with maximum values of 2.2 to 23.2 mg/g in 28, 43, and 84 m and its lowest concentrations in shallow depths (L2, 12 and 21 m) with 4.44 and 4.92 mg/g. Mn showed a similar distribution pattern (Table 4.1.3.1) with lowest concentrations in 12 m depth (52 µg/g) and highest contents in 27 m depth (476 µg/g). The depth distribution of the hot HCl-leachable As, P, Fe, and Mn is shown Figure 4.1.3.1.

Table 4.1.3.1Concentration of As, P, Fe, and Mn leachable in hot HCl in Bangladesh sediments from deep-core drilling. Standard deviation of As and P in (%).

Layer	Sample No.	Average Depth [m]	As [µg/g]	P [µg/g]	Fe(tot) [µg/g]	Mn [µg/g]
2	**7**	12	0.3 (± 9)	189 (± 9)	4920	56
	15	21	0.5 (± 14)	543 (± 7)	4440	52
	24	26	0.9 (± 10)	368 (± 13)	10480	186
3	**27**	28	3.1 (± 5)	600 (± 13)	22000	476
	28	34	1.9 (± 3)	410 (± 8)	12700	156
	30	43	3.1 (± 6)	324 (± 10)	23200	324
	32	61	2.5 (± 5)	102 (± 11)	18100	324
4	**RD**	81	0.3 (± 7)	87 (± 13)	5400	172
5	**37**	84	3.8 (± 10)	80 (± 4)	23100	282
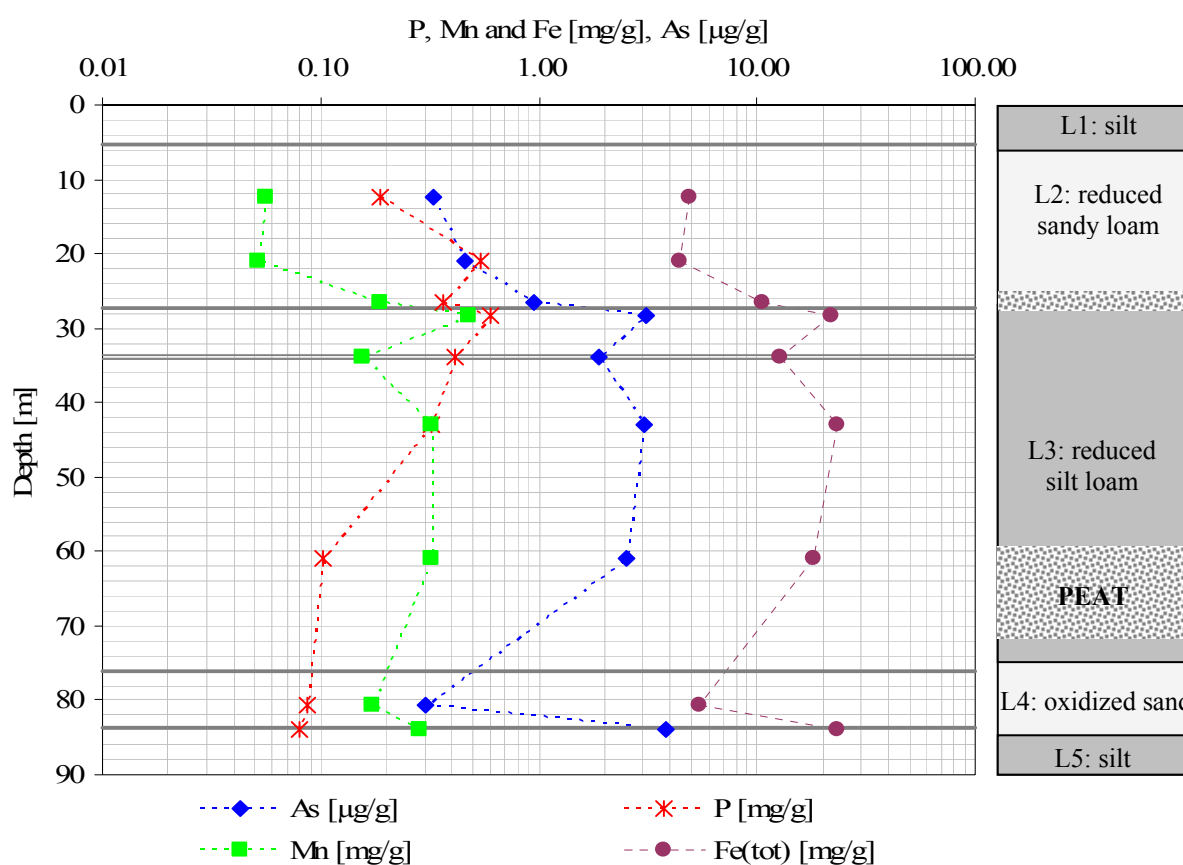
Figure 4.1.3.1 Depth distribution of hot HCl-leachable As, P, Fe, and Mn

As, Mn, and Fe associated with the solids have shown a similar distribution in the depth profile, with a concentration peak in 28 m depth (top of aquiclude, L3). In 34 m depth (lens of coarser material, sand 41 %, in L3) the concentration drops and increases again in the underlying aquiclude (L5). The oxidized sandy layer (deeper aquifer in 81 m depth) showed comparatively low values for leachable As, Mn, and Fe. At the top of the thick aquiclude of layer 3 As and Fe had their maximum values with 3.8 µg/g and 23.1 mg/g.

Spearman Rank correlations for the leachable metals with organic matter and calcite were only significant for arsenic (Table 4.1.3.2). Arsenic, iron, and manganese showed significant correlations among each other, whereas correlations with P and clay were not significant. The plot for the correlation with the developed linear regression line is shown for As and Mn and As and Fe in Figure 4.1.3.2.

Table 4.1.3.2 Spearman Rank Correlation between As and Fe, Mn, OM, CaCO₃, P and Clay

		Fe	**Mn**	**OM (TOC)**	**CaCO₃**	**P**	**Clay**
As	Correlation Coefficient	0.883	0.745	0.700	0.813	0.033	0.8721
	P-Value	0.013	0.035	0.048	0.021	0.925	0.0811
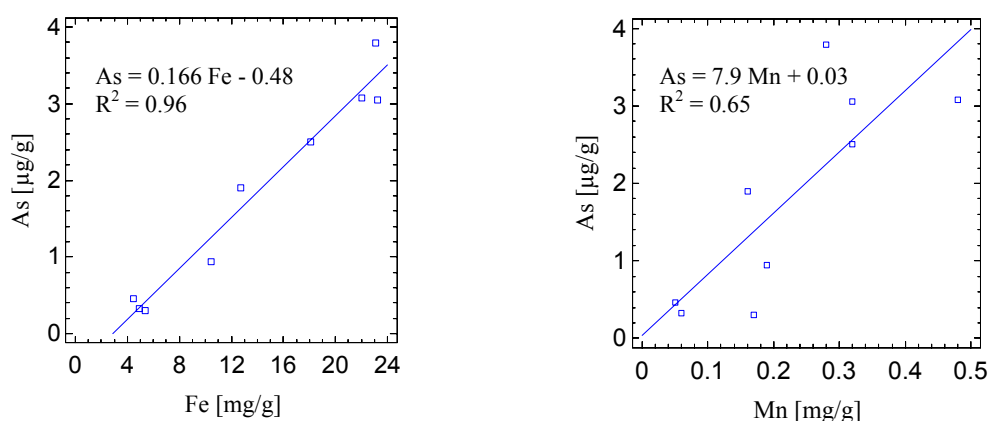
Figure 4.1.3.2 Variation in hot HCl leachable As with Fe and Mn in the Bangladesh sediments

Total As and P concentrations determined in microwave digests by ICP-MS are represented in Figure 4.1.3.3 and Figure 4.1.3.4. They have shown remarkable higher concentrations than those from hot HCl leach. The ratios of As and P contents in hot HCl leaching compared to microwave digests are listed in Table 4.1.3.3.

Table 4.1.3.3 Ratios (hot HCl leach/microwave digestion) of P and As concentrations derived from microwave digestion and hot HCl leach.

Sample Description	Average Depth [m]	Ratio P (%)	Ratio As (%)
7	12	51	2.7
15	21	84	2.6
24	26	162	6.4
27	28	66	3.1
28	34	49	1.8
32	61	15	0.8
RD	81	20	0.6
37	84	18	1.4
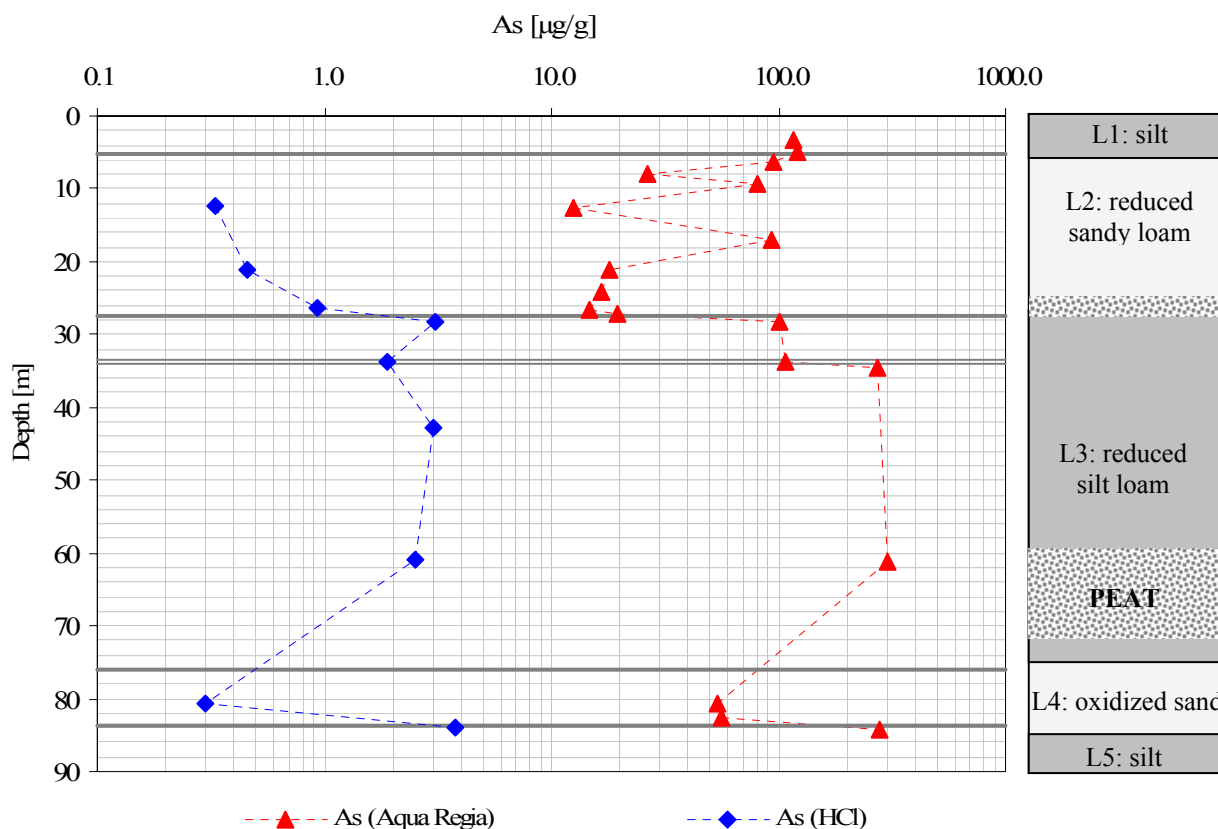
Figure 4.1.3.3 Total As concentration in after Aqua Regia and hot HCl analysed with ICP-MS.

Compared to the HCl leach (0.3 to 3.8 µg/g As) the As concentration in the microwave digests varied between 12 and 302 µg/g. Higher As values in the aquicludes (L3 and L5) as well as a decrease within the deeper aquifer in 79 to 83 m depth were observed comparable to the results for the hot HCl leach. Also the depth distribution of P determined in the microwave digests is similar to that from the hot HCl leach, with their lowest concentrations of 227 µg/g and 283 µg/g (27 m and 83 m depth) in the aquifers above the clayey layers (Figure 4.1.3.4). Additional sampling points near the surface (sample nos. 1 to 6, Table 3.2.1) showed high P contents of 1913 µg/g, particularly in 8 m depth (L2, sandy loam).

Typical As concentrations for groundwater sediments in Bangladesh are in the range of 1 to 30 µg/g (NICKSON et al., 1998). Other authors reported that they extracted up to 10 µg/g in aquifer and aquiclude materials (AHMED et al., 2004; HARVEY et al., 2002; KINNIBURGH and SMEDLEY, 2001; SWARTZ et al., 2004; VAN GEEN et al., 2004). Therefore, the measured As concentrations (probably also P) in microwave digests are apparently above realistic values and are not further discussed. The reason for this discrepancy is unknown.
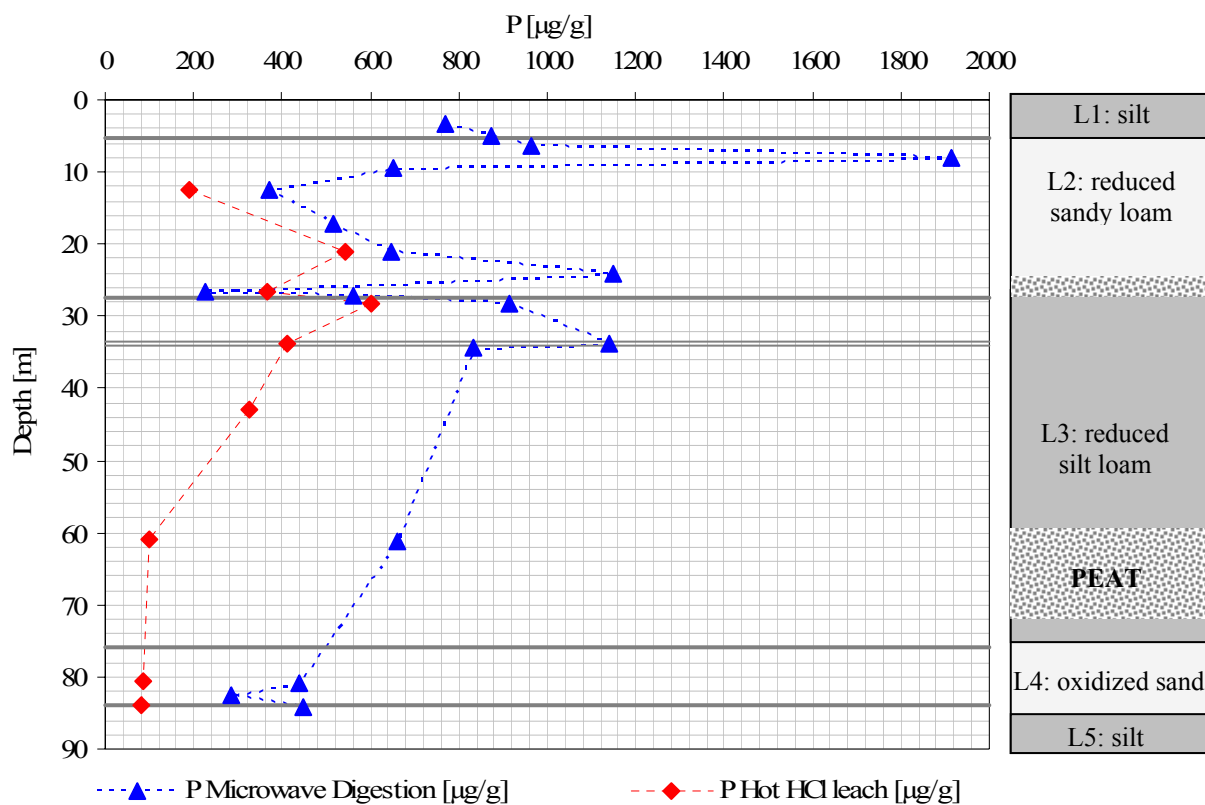
Figure 4.1.3.4 Comparison of phosphorous concentrations determined in microwave digests and hot HCl leaches

Leaching with AGW only released low quantities of Mn and Fe, but no As and P from the sediment, indicating that equilibrium exists between the sediment and the natural groundwater. The values for Fe in the sediment were negligible with 0 to 1.07 µg/g. For the Mn distribution a similar pattern as for the hot HCl leach was observed. Maximum values of 3.5, 5.5 and 13.6 µg/g were detected at the top of L3 (thick aquiclude), in 61 m depth and the top of L5. In the layers with higher proportions of sand (aquifers L2 and L4) Mn concentrations were close to zero.
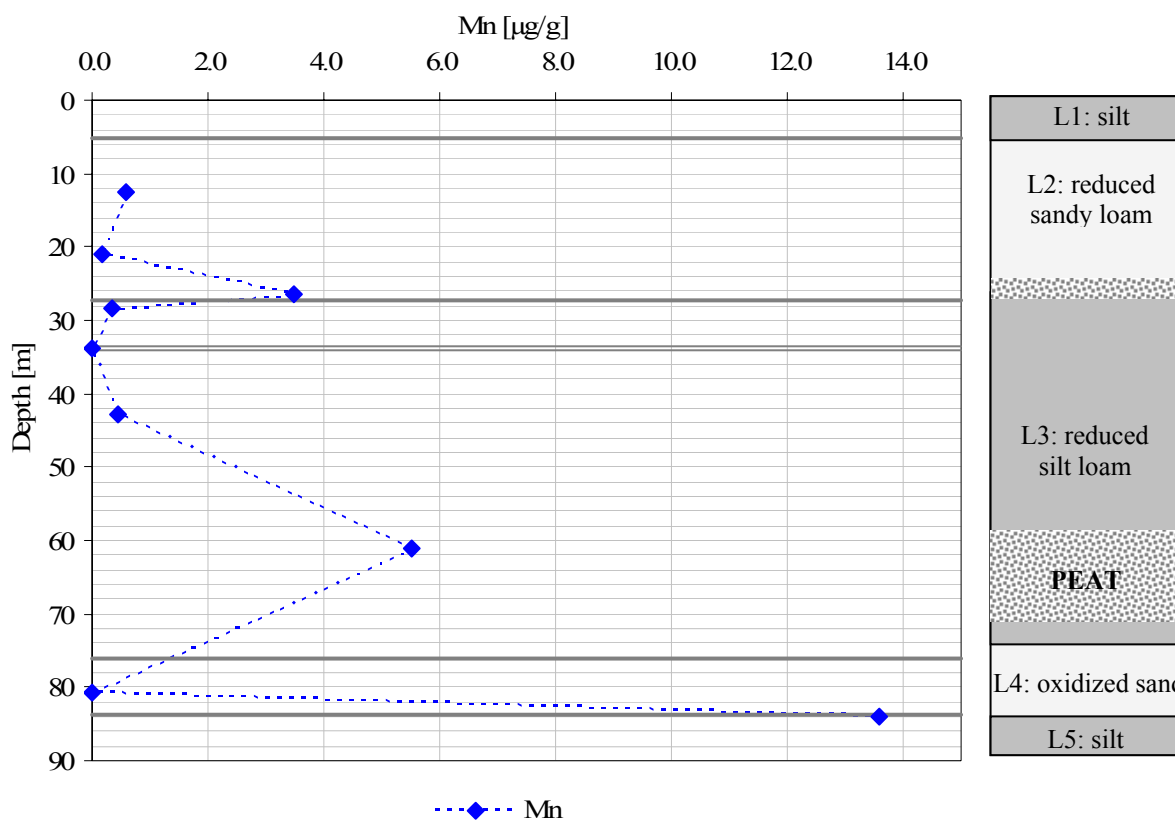
Figure 4.1.3.5 Dissolved Mn concentration after leach with artificial groundwater (AGW)

4.1.4. Leaching and sorption experiments on Bangladesh sediments in $NaHCO_3$, NaOH, and MQ

Extraction experiments under anoxic conditions were carried out to determine the concentration of arsenic which can be mobilized from the sediments by solutions of various chemical compositions. As source solutions MQ (pH 7.1), 0.04 M NaOH (pH 12.3), and 0.04 M $NaHCO_3$ (pH 8.8) were chosen. NaOH targets As that is bound to iron(hydr)oxides and OM, while $NaHCO_3$ was used to simulate the effect of bicarbonate (HCO_3^-) on As exchange from exchangeable sites. To exclude the influence of pH and bicarbonate MQ was used for comparison. Further also the sorption behaviour of arsenite and arsenate in these sediment-solution mixtures was investigated. A total concentration of 1.11 mg/L of both, arsenite and arsenate, was chosen for the sorption experiments and the adsorption of arsenic was measured after 72 h equilibration time. Sediment samples from 12, 26, 28, 61, 81, and 84 m depth were subjected to these extraction and sorption experiments, depicted in Table 3.2.1. Leachable As from the sediments with MQ, NaOH, and $NaHCO_3$ are shown in Table 4.1.4.1 The leaching of As from the solid phase was only effective in NaOH at a pH of 12.2 to 12.4, where the extracted As ranged from minimum values of 0.2 µg/g in 12 m depth to 2.1 µg/g in 61 m depth. Thus, leached As concentrations in NaOH resemble those of the hot HCl leach (comparison in Figure 4.1.4.1). Leachable As concentrations in NaOH were specified as arsenate for all samples. Generally it can be assumed that leachable As is highest in the thick

aquiclude (L3, silt loam) and lowest at the top of the shallow aquifer (L2, sandy loam) and in the deeper aquifer (L4, sand). Differences, particularly in 84 m depth can result from inhomogeneities of the analysed material as well as from the efficiency of each leaching to attack different bonds between As and the solid phase. Almost no arsenic was detected in the leachates of MQ and $NaHCO_3$ (only 0.1 µg/g in 26 and 28 m in $NaHCO_3$).

Table 4.1.4.1 Leaching and sorption of arsenic in MQ, 0.04 M NaOH, and 0.04 M $NaHCO_3$. Bangladesh sediments were taken from 6 different depths in 12, 26, 28, 61, 81, and 84 m. Adsorbed As in µg/g and % represents As that was adsorbed to the solid phase after adding arsenite and arsenate (1.11 mg/L) to the sediment. The pH was measured after shaking.

Laye	Sample No.	Depth[m]	Solution	pH	Leached As		Adsorbed As			
							Arsenite		Arsenate	
					µg/L	[µg/g]	[µg/g]	(%)	[µg/g]	(%)
2	7	12	MQ	8.7	4	0.0	6.4	76	2.6	31
			NaOH	12.4	27	0.2	1.9	22	1.3	15
			NaHCO3	8.9	1	0.0	6.7	81	4.9	59
	24	26	MQ	8.1	3	0.0	6.9	83	5.9	71
			NaOH	12.3	188	1.4	0.3	4	-0.1	-1
			NaHCO3	8.8	18	0.1	7.4	89	6.2	74
3	27	28	MQ	8.0	2	0.0	8.1	97	8.2	98
			NaOH	12.3	234	1.8	1.1	13	0.9	11
			NaHCO3	8.7	8	0.1	8.0	96	7.6	91
	32	61	MQ	5.4	5	0.0	7.4	89	8.3	99
			NaOH	11.1	283	2.1	4.3	51	2.2	27
			NaHCO3	8.1	3	0.0	8.1	97	8.2	98
4	RD	81	MQ	6.8	0	0.0	7.6	91	8.1	97
			NaOH	12.4	53	0.4	0.9	11	0.9	11
			NaHCO3	9.0	2	0.0	5.6	67	5.7	68
5	37	84	MQ	7.1	0	0.0	8.2	98	8.3	100
			NaOH	12.2	56	0.4	2.7	32	2.3	28
			NaHCO3	8.6	0	0.0	8.3	100	8.1	97
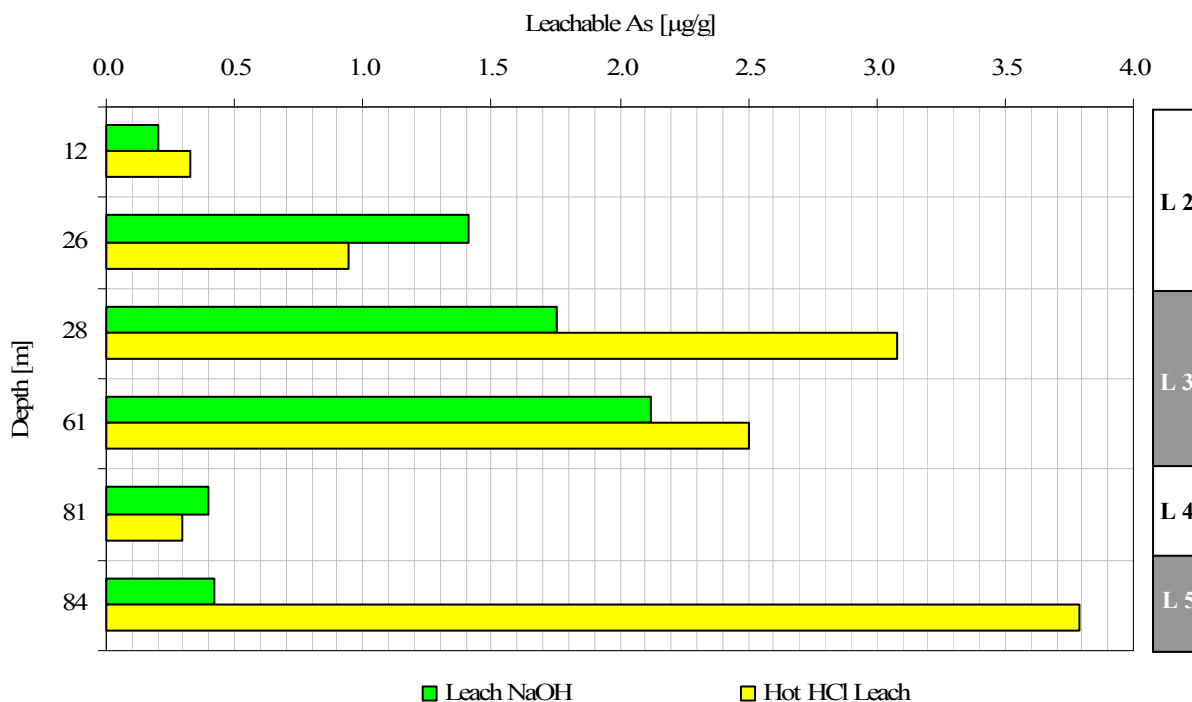
Figure 4.1.4.1 Comparison of leachable As in NaOH and hot HCl from Bangladesh sediment. The scale on the right represents the stratigraphical layers (aquifers: L2, L4; aquicludes: L3, L5).

Dissolved arsenic concentrations in MQ, NaHCO$_3$, and NaOH after addition of arsenite and arsenate respectively are displayed in the figures below (Figures 4.1.4.2, 4.1.4.3 and 4.1.4.5). The grey bars indicate the As concentrations that were adsorbed from the initial spike to the sediment, including also the leachable fractions As (see also Table 4.1.4.1). The adsorption of As was most efficient in MQ and NaHCO$_3$, where As was almost completely adsorbed, particularly in L3, L4 and L5. Lowest As sorption was observed in NaOH at high pH.

In MQ (pH 5.4 to 8.7) the adsorbed As concentration ranged between 6.4 µg/g (12 m) and 7.6 µg/g (84 m) after adding arsenite and 2.6 µg/g (12 m) to 8.3 µg/g (61 and 84 m) after addition of arsenate. Thus sorption increased with the depth of the samples and was highest in 28, 61, 81, and 84 m depth with 97, 89, 91, and 98 % after addition arsenite and 98, 99, 97, and 100 % after addition arsenate (L3, L4, and L5) (see also Figure 4.1.4.2). In 12 and 26 m depth the sorption of As seemed to be less after adding arsenate, because still 69 and 29 % of the initial spike remained in solution.
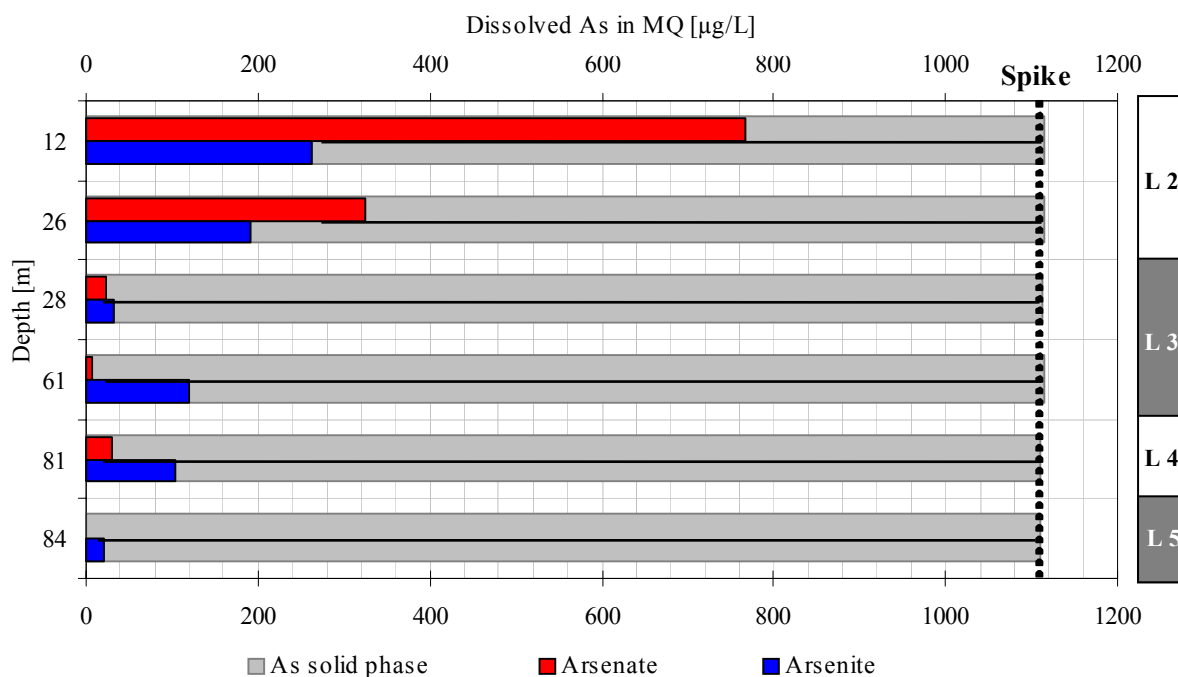
Figure 4.1.4.2 Dissolved and adsorbed As concentrations in MQ after addition of arsenite and arsenate. The solid phase comprises As associated with the sediments, i.e. adsorbed concentration (from 1.11 mg/L As spike) and the leached As [µg/L] from the solid phase (Table 4.1.4.1).

Arsenic sorption (arsenate and arsenite) in $NaHCO_3$ (pH 8.1 to 9.0) was highest in the aquicludes (L3 and L5; Figure 4.1.4.3). More than 90 % of the initial spikes of arsenic were adsorbed in these layers with predominantly silty texture. Samples from 12, 26, and 81 m depth showed lower sorption capacities with 59 %, 74 %, and 68 % (4.9, 6.2, and 5.7 µg/g) adsorbed As after addition of arsenate. Adsorbed As concentrations from both spikes were similar in 61, 81, and 84 m. Further in 12, 26, and 28 m depth 22 %, 15 %, and 5 % less As was adsorbed after addition of arsenate (Figure 4.1.4.3).

The differences of As sorption in both solutions, MQ and $NaHCO_3$, after addition of either arsenite and arsenate are emphasized in Figure 4.1.4.4. The differences were highest in 12 and 26 m depth (L2, sandy loam), where As seemed to be stronger adsorbed after addition of arsenite than of arsenate to the sediment. In samples below 26 m the adsorption behaved similar. Arsenic sorption after addition of arsenate was enhanced in the sediments from 61 and 81 m (0.9 and 0.5 µg/g more arsenate), but only in MQ. It is also visible that As sorption was highest in L3 and L5 (MQ and $NaHCO_3$) and in L4 (only MQ).

Dissolved As in NaHCO3 [µg/L]
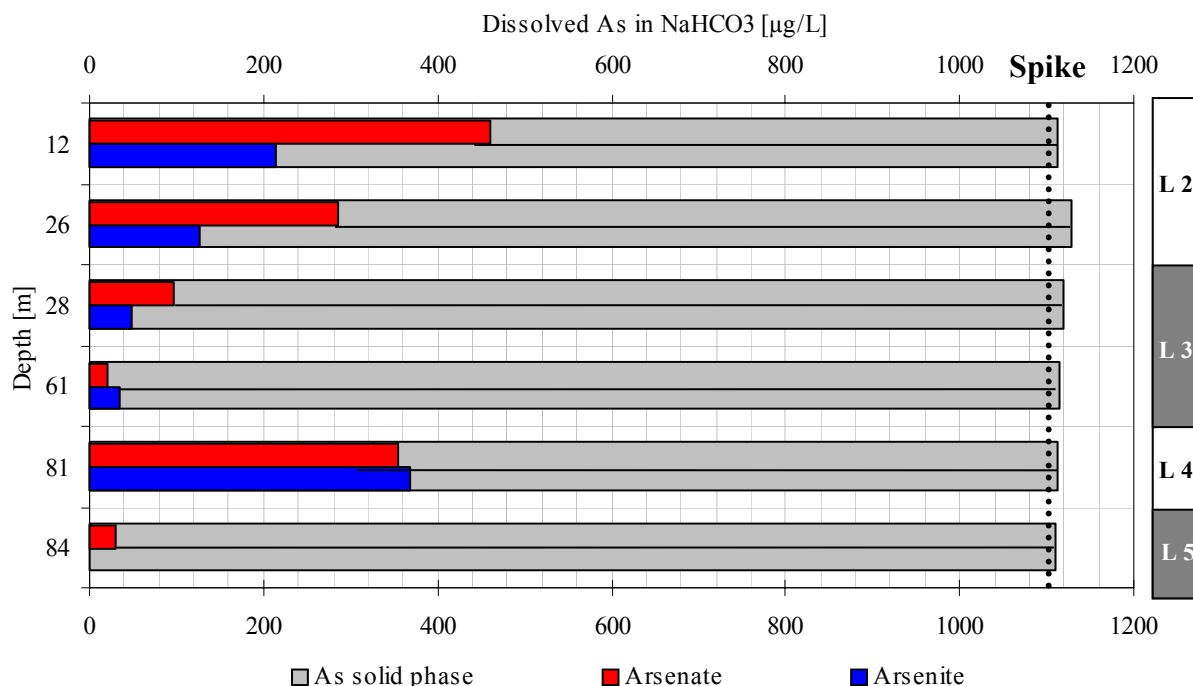
Figure 4.1.4.3 Dissolved and adsorbed As concentrations in NaHCO₃ after addition of Arsenite and Arsenate. The solid phase comprises As associated with the sediments, i.e. adsorbed concentration (from 1.11 mg/L As spike) and the leached As [µg/L] from the solid phase (Table 4.1.4.1).
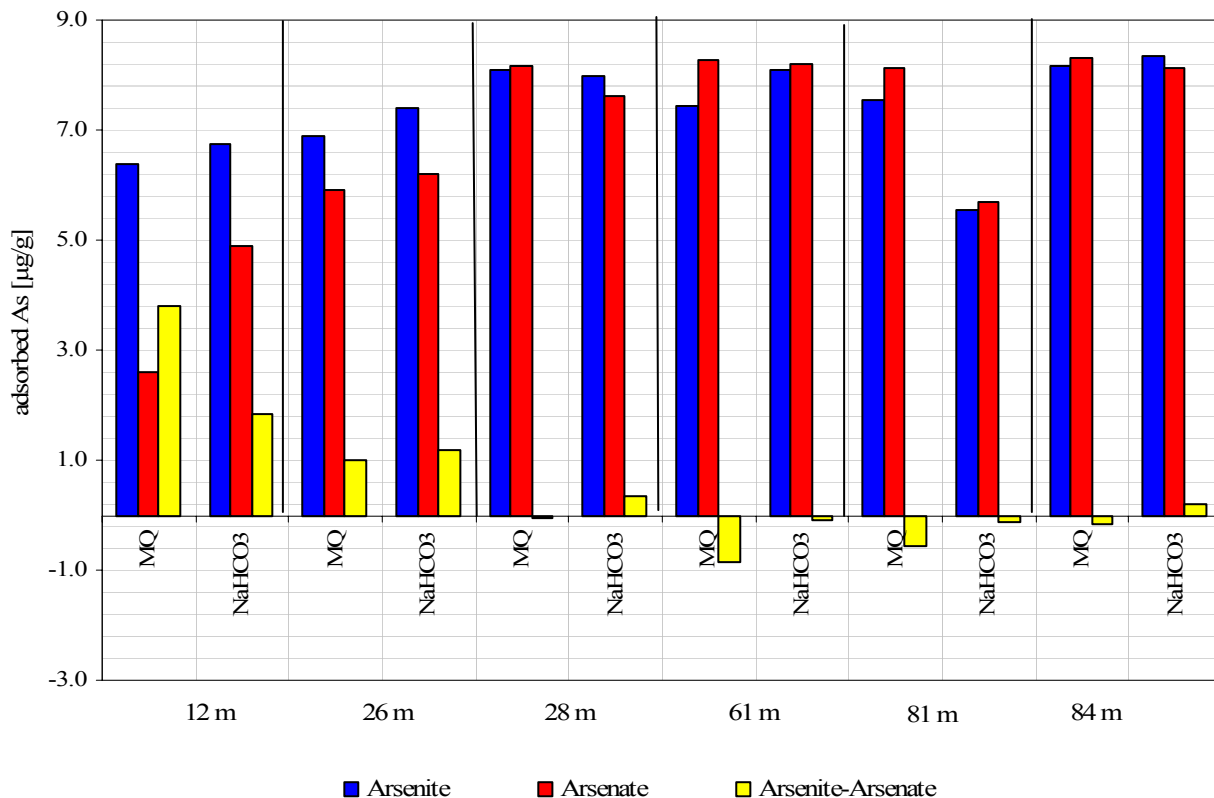
Figure 4.1.4.4 Comparison of adsorbed As concentration in MQ and NaHCO₃ after addition of arsenite and arsenate. The filled bars represent the difference between sorption arsenite and arsenate (arsenite-arsenate) to the sediment.

After the addition of arsenite and arsenate to the sediments in NaOH the sorption of As on the sediment varied from - 1 % in 26 m to 51 % in 61 m depth (Figure 4.1.4.5). Highest As sorption occurred in 61 and 84 m depth (aquicludes, L3 and L5). Almost no sorption was observed in 26 m depth (L2) where only 4 % (0.3 µg/g) As after addition of arsenite and -1 % (-0.01 µg/g) As after addition of arsenate were adsorbed. In the latter case the negative As value could derive from simultaneously occurring leaching processes in NaOH which had their maximum in 61 m depth (2.1 µg/g). Generally, As sorption seemed to be higher after adding arsenite to the solution with a maximum difference (arsenite – arsenate) of 24 % in 61 m depth.

Dissolved As in NaOH [µg/L]
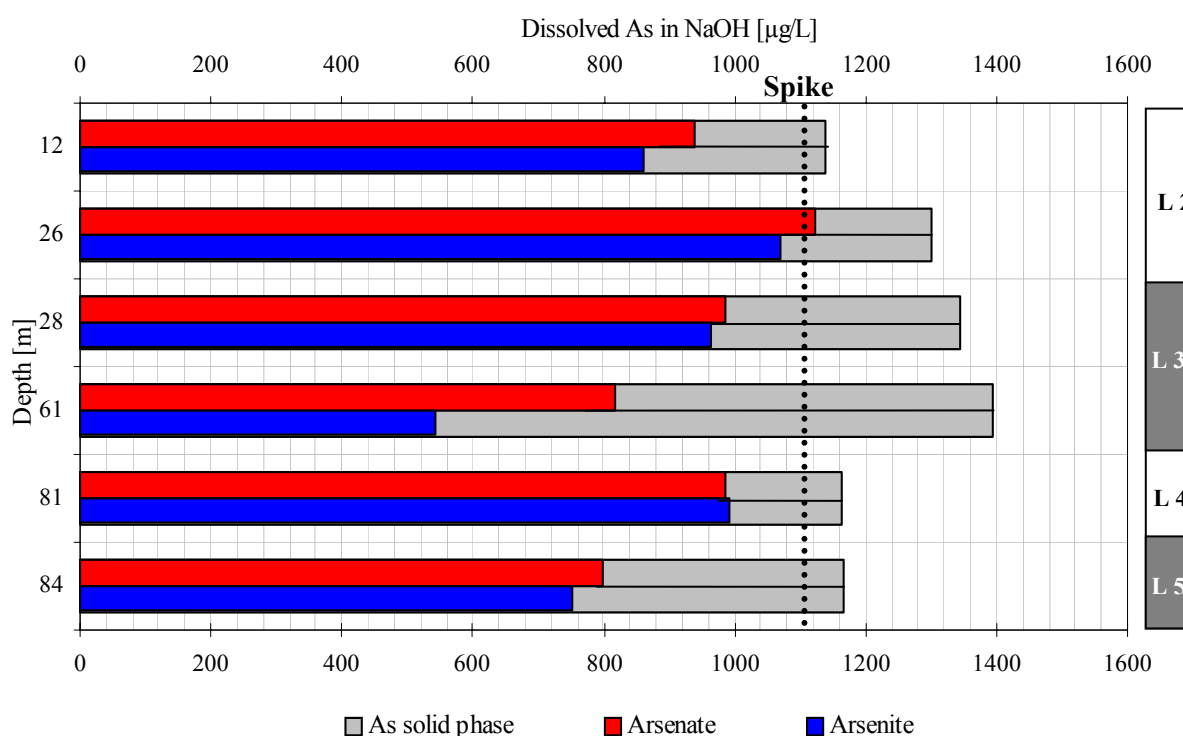
Figure 4.1.4.5 Dissolved and adsorbed As concentrations in NaOH after addition of Arsenite and Arsenate. The solid phase comprises As associated with the sediments, i.e. adsorbed concentration (from 1.11 mg/L As spike) and the leached As [µg/L] from the solid phase (Table 4.1.4.1).

In the aquicludes (L3 and L5) of the Bangladesh sediment highest sorption capacities were observed in all three solutions, MQ, NaOH, and NaHCO$_3$. Lower As sorption on the other hand was found in sediments from the aquifers (L2 and L4, sandy loam, and sand), except in MQ, where the sorption behaved similar in L3, L4, and L5.

After the addition of arsenic no conversion of arsenate into arsenite or other As-species was observed in NaHCO$_3$ and NaOH. In all solutions only arsenate (100 %) was detected after IC-ICP-MS analysis. The addition of arsenite on the other hand caused a change in speciation from the

initially spiked arsenite to arsenate for both solutions, $NaHCO_3$, and NaOH. Arsenate was the dominant arsenic species in all final solutions (74 % to 100 % arsenate; Table 4.1.4.2). In NaOH arsenite was oxidized completely to arsenate or even formed thioarsenates in 26, 61, and 84 m depth with 4.8, 1.8, and 11.0 % of total dissolved As. In $NaHCO_3$ only in 81 m (L4) all arsenite was converted to arsenate, whereas in the samples from lower depths still 14 to 26 % arsenite remained dissolved. No species analyses were conducted for MQ.

Table 4.1.4.2 Distribution of arsenic species in the dissolved phase after addition of 1.11 mg/L arsenite for the matrix solutions NaOH and $NaHCO_3$. Major arsenic species arsenite (arsenite, arsenate, and monothioarsenate) are listed in the table.

Sample No.	Depth [m]	NaHCO$_3$				NaOH			
		Arsenite [%]	Arsenate [%]	Monothio-arsenate [%]	As(tot) [µg/L]	Arsenite [%]	Arsenate [%]	Monothio-arsenate [%]	As(tot) [µg/L]
7	12	14.2	85.8	0.1	214	0.0	99.0	0.0	862
24	26	25.5	74.5	0.0	127	0.0	95.2	4.8	1070
27	28	16.3	83.7	0.0	49	0.0	99.1	0.9	963
32	61	16.3	83.7	0.0	35	0.0	98.2	1.8	543
RD	81	0.0	100.0	0.0	369	0.0	99.9	0.1	992
37	84	0.0	0.0	0.0	0	0.0	89.0	11.0	751

4.1.5. Sorption capacity test with Bangladesh sediments

Sorption capacity tests with increasing concentrations of arsenite and arsenate were investigated with sediments from the deeper aquifer in 81 m depth in AGW (2.5 mM $NaHCO_3$, $MgCl_2$ and $CaCO_3$) at pH 7.5 to 7.8 to estimate the total As concentration that can be adsorbed to the sediment. The results of the sorption experiment with 25, 50, 75, 100, 250, and 500 µg/L arsenite and arsenate showed that the sorption capacity of the oxidized sand (RD) was not reached after the addition of 500 µg/L arsenite and arsenate, respectively.

After 2 days equilibration time around 50 % to 70 % As of the initially spiked arsenite (25 to 500 µg/L) were adsorbed (5.4 µg/g in 500 µg/L As), more than 90 % after addition of arsenate (9.2 µg/g in 500 µg/L As; Table 4.1.5.1). Arsenic speciation showed that after 2 days more than 95 % arsenite were detected in the arsenite containing solution and more than 80 % arsenate in the arsenate solutions. Close to 100 % of the initially added arsenite and arsenate (9.8 µg/g of 10 µg/g in 500 µg/L As) were adsorbed to the sediments after 7 days equilibration time. Here the dominant species in all samples was arsenate (90 to 100 %). A linear sorption isotherm was observed between As in solution and the adsorbed As for the arsenate after 2 days and arsenate and arsenite after 7 days (Figure 4.1.5.1). The latter one can be defined by:

$$Q = K_d{}^*c_{eq} \qquad \text{(with } K_d = 0.0197, R^2 = 1\text{)} \qquad\qquad (2)$$

where Q is the quantity (µg/g) of arsenite or arsenate adsorbed to the sediment, K_d is the distribution coefficient of arsenite or arsenate, and c_{eq} is the equilibrium concentration (µg/L) of arsenite or arsenate. The linear relation describes the sorption of As to the sediment surface up to an dissolved As concentration of 500 µg/L and indicates that the surface concentrations were far from site saturation.

The adsorption of As after addition of arsenite on the second day was fitted with a polynomial sorption isotherm (second order). After 2 days the adsorption of arsenite was clearly below the adsorption of arsenate but an enhanced and almost complete sorption was observed after 7 days reaction time.
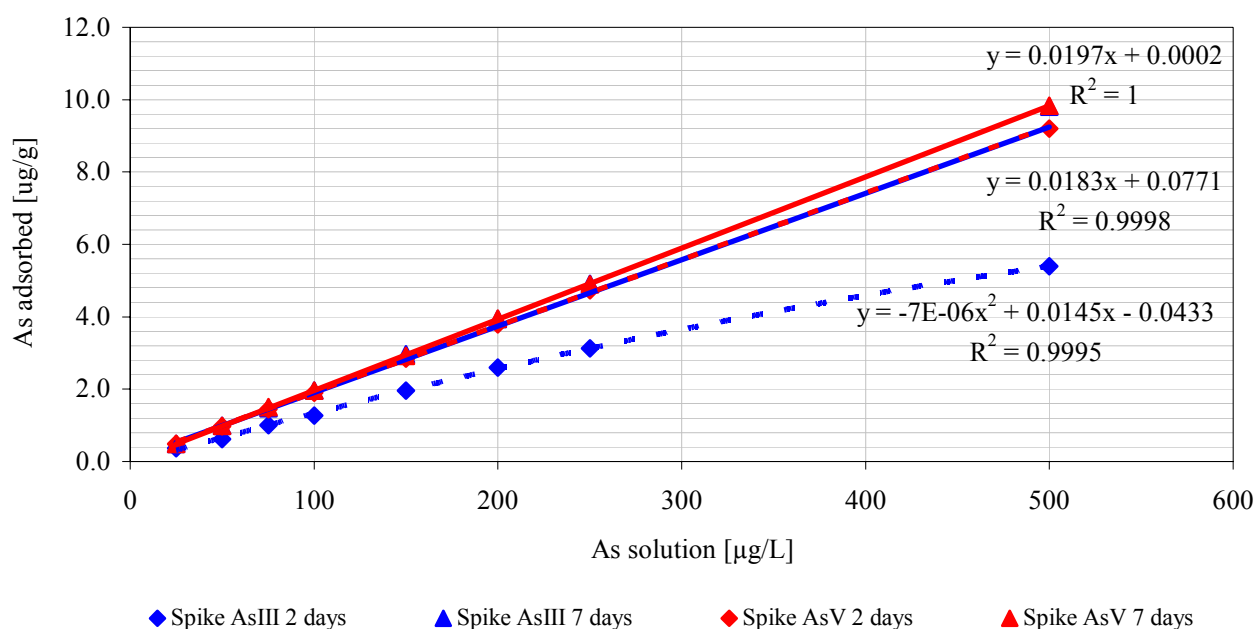
Figure 4.1.5.1 Linear regression of As sorption dependent on As concentration in solution on Bangladesh sediment (RD, 81 m depth).

Table 4.1.5.1 As-sorption dependent on As concentration in solution. In the table the total adsorbed As concentrations [µg/g] are listed together with those for dissolved arsenic species [%].

	Spike As [µg/l]	day 2			day 7		
		Arsenite [%]	Arsenate [%]	Total As adsorbed [µg/g]	Arsenite [%]	Arsenate [%]	Total As adsorbed [µg/g]
Spike Arsenite	25	100.0	0.0	0.37	0.0	100.0	0.49
	50	98.9	1.1	0.62	0.0	100.0	0.98
	75	97.8	2.2	1.01	0.0	100.0	1.47
	100	100.0	0.0	1.27	10.2	90.8	1.96
	150	98.4	1.6	1.97	4.8	95.7	2.96
	200	98.3	1.7	2.59	8.6	92.3	3.93
	250	98.3	1.7	3.13	3.6	96.8	4.91
	500	98.2	1.8	5.39	6.6	94.1	9.81
Spike Arsenate	25	0.0	100.0	0.49	27.2	75.5	0.49
	50	16.0	84.0	0.98	0.0	100.0	0.99
	75	18.0	82.0	1.44	0.0	0.0	1.50
	100	13.3	86.7	1.90	0.0	100.0	1.96
	150	13.4	86.6	2.85	5.4	95.1	2.92
	200	13.4	86.6	3.79	0.0	100.0	3.95
	250	10.7	89.3	4.74	0.0	100.0	4.90
	500	9.3	90.7	9.19	0.0	100.0	9.84

Sorption capacity tests conducted with higher concentrations arsenite, arsenate, and phosphate (0.5, 1, 2.5, 5, 10, and 20 mg/L) on Bangladesh sediments (13, 26, 28, 61, 81, and 84 m; Table 3.2.1) in MQ have shown a very high sorption after 2 days for all anions (Figure 4.1.5.2). There is no evidence of reaching the sorption limit of the sediments in the arsenite and phosphate containing solutions, where maximum As and P concentrations from 3 to 4.5 mg/g were adsorbed to the sediment in 13, 26, 61, and 81 m depth. Arsenate sorption appeared to be lower in the sediments and even the sorption capacity seemed to be reached after addition of 10 mg/L arsenate. Lowest sorption in all solutions was observed for the sediment in 28 m depth (top of L3).
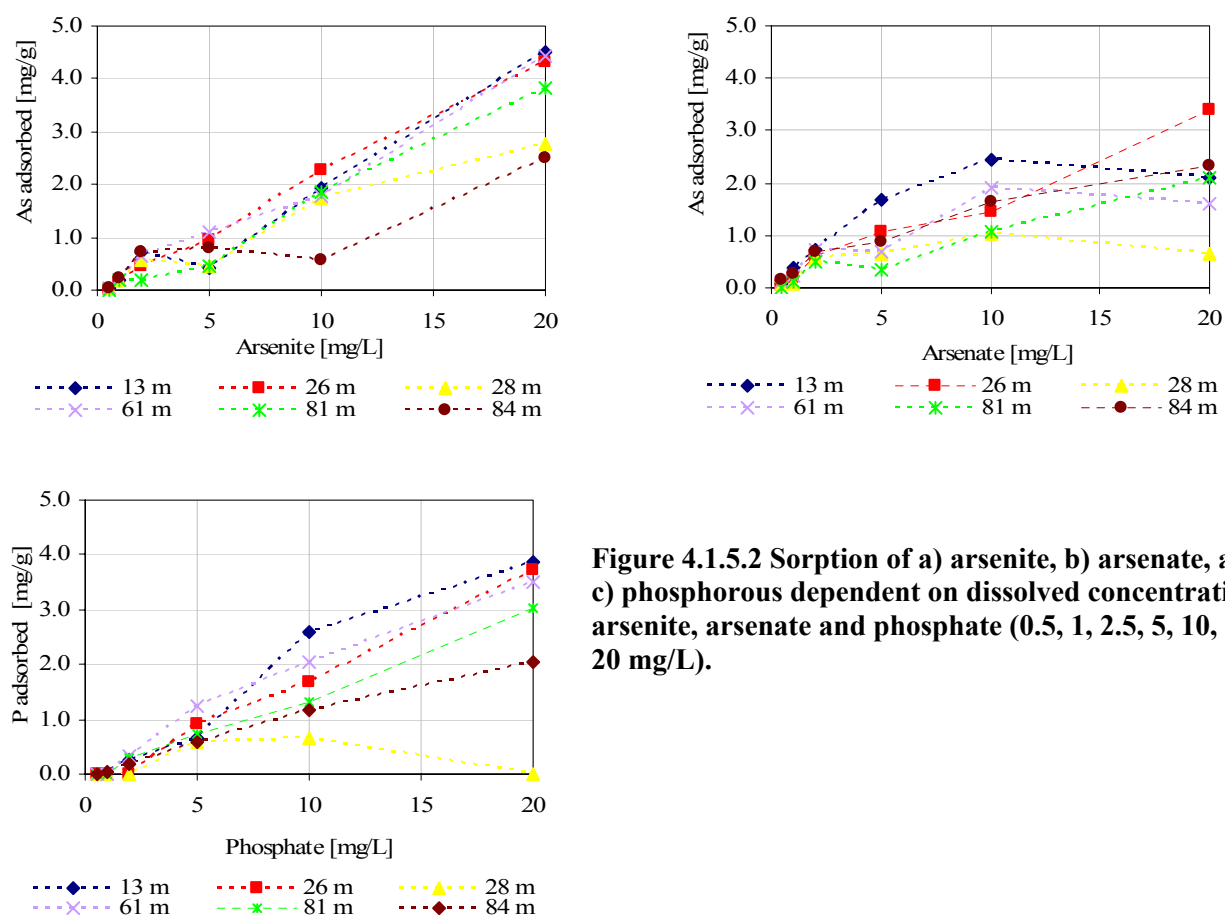
Figure 4.1.5.2 Sorption of a) arsenite, b) arsenate, and c) phosphorous dependent on dissolved concentration arsenite, arsenate and phosphate (0.5, 1, 2.5, 5, 10, and 20 mg/L).

4.1.6. Groundwater composition in the test field

The groundwater composition in the aquifer and the composition of the sediment strongly depend on each other. To compare the leachable fractions (As, Fe, and P) of the solid phase with the dissolved fractions in the groundwater, an overview from groundwater analyses at the test field investigated in the beginning of April 2007 (07/04/09) is given in the table below.

The samples were taken from 6 different depths in the shallow aquifer and from 81 m, where the groundwater derives from the deeper aquifer. The depth profile of the test field is shown in Figure 4.1.6.1 together with the stratigraphical units and the core drilling.

Table 4.1.6.1 Groundwater composition of the shallow and deeper aquifer at the test field.

	Shallow Aquifer						Deeper Aquifer
Depth [m]	**8**	**15**	**21**	**25**	**26**	**34**	**81**
As [µg/L]	15	128	102	224	147	222	60
P [mg/L]	0.3	1.2	0.4	1.6	1.3	5.4	2.0
Fe(II) [mg/L]	0.5 (71 %)	0.2 (50 %)	0.2 (33 %)	1.9 (95 %)	1.7 (85 %)	0.5 (10 %)	63.5 (95 %)
Fe(tot) [mg/L]	0.7	0.4	0.6	2.0	2.0	5.8	66.8
NH_4^+ [mg/L]	0.1	0.7	0.9	1.5	1.6	28.0	136.0
pH	7.0	7.1	7.3	7.1	7.2	7.2	6.3
Eh [mV]	253	206	158	111	122	90	211

Fe(II) in brackets: % of Fe(tot)

Arsenic concentrations increased with depth in the shallow aquifer and reached maximum values of 222 and 224 µg/L in 25 and 34 m depth. The lowest concentration was observed in 8 m depth with 15 µg/L. Between 8 and 15 m As sharply increased up to 128 µg/L. In the deeper aquifer the groundwater contains again less arsenic with 60 µg/L. Dissolved phosphorus concentrations also increased with depth, having the highest concentrations in 34 and 81 m (5.4 and 2 mg/L). The groundwater from the deeper aquifer and from 34 m depth (shallow aquifer) is enriched in iron and ammonium with remarkable concentrations of 67 µg/L Fe(tot) (with 95 % Fe(II)) and 136 µg/L NH_4^+ in the shallow aquifer. Further Fe(II) was dominant in most samples. The pH of the shallow aquifer can be considered as near neutral, while the pH in the deeper aquifer is slightly lower with 6.3. The highest redox potential (253 mV) was measured near the soil surface and dropped with increasing depth to a minimum in 34 m depth (90 mV). With 211 mV the redox potential in the deeper aquifer is again clearly above the redox potential of the shallow aquifer (deeper part).
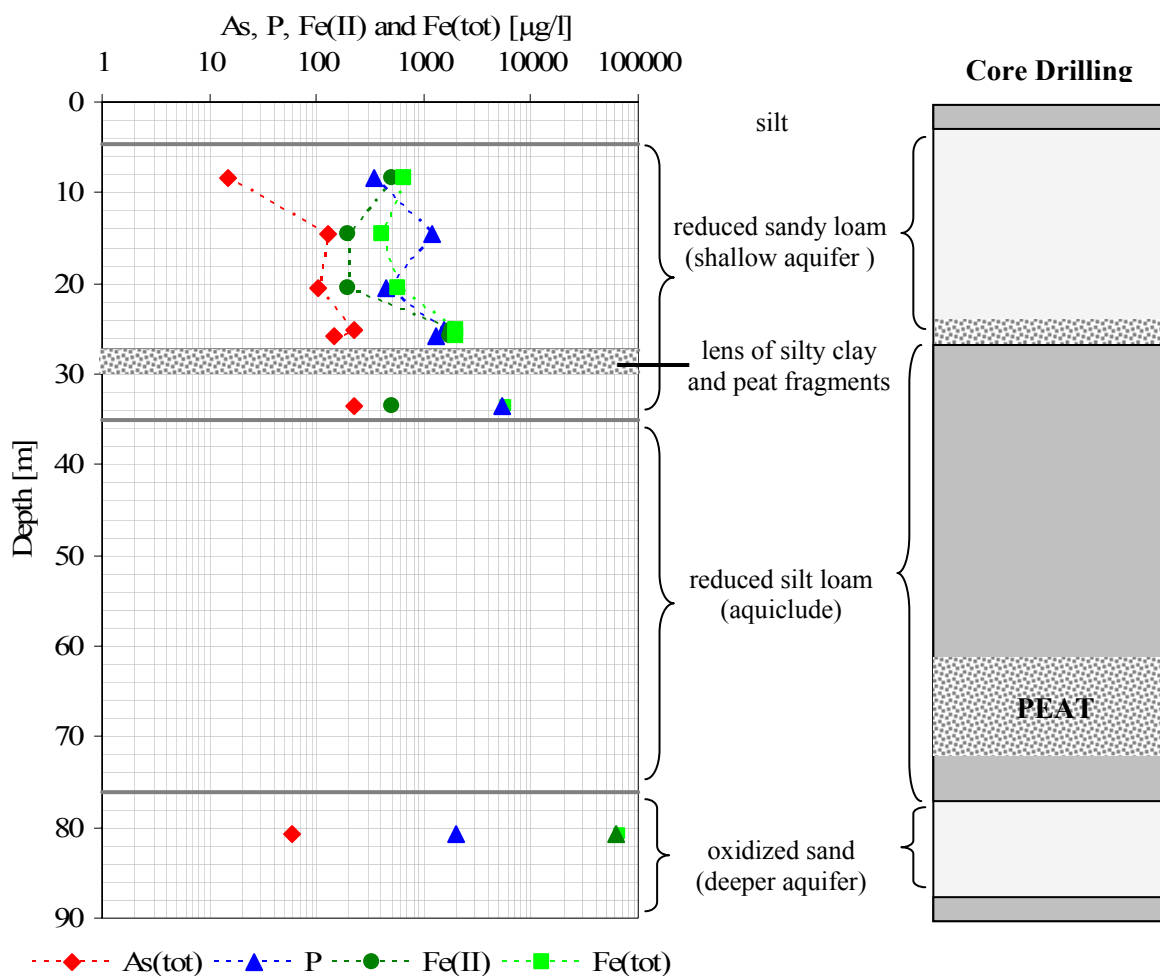
Figure 4.1.6.1 Depth profile of dissolved As, P, Fe(II) and Fe(tot) at the test field with main sediment layers. On the right, stratigraphical units of the core drilling in 50 m distance.

Below the lens of silty clay, which contains also fragments of peat, the groundwater showed elevated concentrations of phosphorous and iron. Arsenic levels are in the same range as just above this lens. Even though some differences in lithology were observed between the piezometers in the test field and the core drilling, that was located in a short distance ($\approx$ 30 m), the two aquifer units with the thick aquiclude in between match in both depth profiles. The lens of silty clay at the test field has not been observed during the core drilling but both profiles contained peat fragments in approximately the same depth.

4.2. Simulation As-mobilization in column experiments

Column experiments were conducted with sediments from the shallow and deeper aquifer (reduced sandy loam (No.15) and oxidized sand ("RD")) to observe the sorption behaviour of arsenic and to examine the effect of phosphate on arsenite and arsenate transport in a simulated subsurface environment (see also Table 3.2.1 and Figure 3.3.3.1). For competitive exchange the ions were added sequentially to the sediment to allow the adsorption of the first anion to the solid before the second ion was introduced and could compete for exchangeable sites.

The pH in the stock solutions and the effluent of the columns ranged between 8.0 and 8.3. The flow rates in the experiment ranged from 0.1 to 0.2 ml/min, resulting in pore water velocities of 1.4 to 2.8 $\cdot 10^{-3}$ m/s in the sediment. The pore volume (V_0) for $\approx$ 1 g of sediment was calculated to be around 0.9 ml.

Matrix influences for arsenate and phosphate were observed for IC-ICP-MS analyses in the AGW used (2.5 mM $NaHCO_3$ and 2.5 mM $MgCl_2$). The recovery of the matrix spike was only 60 % of the initial spike for arsenate. No matrix tests were performed for P speciation. Because of structural similarities and related chemical behaviour of arsenate and phosphate anions results from matrix speciation for arsenate were transferred to those of phosphate. Thus, arsenate and phosphate concentration from speciation analyses were corrected from 60 % to 100 % and then compared with the total concentrations determined by ICP-MS. The evaluation of experiment 2 (sorption behaviour arsenate-monothioarsenate) was only performed with results from ICP-MS analyses due to analytical problems with IC-ICP-MS measurements and high inaccuracy of the matrix recovery. Analyses only conducted with NaOH and $NaHCO_3$ have shown no matrix effects on As speciation, thus it seems that $MgCl_2$ interferes with speciation analysis.

4.2.1. Competitive anion exchange of As with phosphate

The first part of the experiment included the desorption of As (solution 1) with P (solution 2). Solutions containing either arsenite or arsenate ($\approx$ 200 µg/L As) were pumped through the columns, followed by a phosphate-containing solution (1 mg/L P; Table 4.10). In the second part, the solutions were applied in reverse order, i.e. first the phosphate-containing and then the arsenite/arsenate-containing solution. The concentrations of 200 µg/L (2.6 µM) As and 1 mg/L (32 µM) P were in the range of naturally occurring concentrations in Bangladesh's aquifers (see chapter 3.1.). Speciation analyses for one sample of each sub-experiment were performed to get informations about the conversion and formation of As species in contact with the sediment.

An example for the desorption of As through addition of P in the two sediments is given in Figure 4.2.1.1, which shows the effluent breakthrough curves of arsenic and phosphorous (total concentrations). Represented is the desorption of As by phosphate after equilibration of both sediment types (reduced and oxidized material) with arsenite. To make the single experiments comparable to each other, the volume and concentration in the effluent were normalized using V/V_0 (total volume/pore volume column = pore volumes) and c/c_0 (concentration effluent/concentration stock solution). The intersection point marks the quantity of pore volumes (V/V_0) where c/c_0 of As and P have the same value. This point may serve to indicate the grade of mobility and retention of the anions in the sediment.
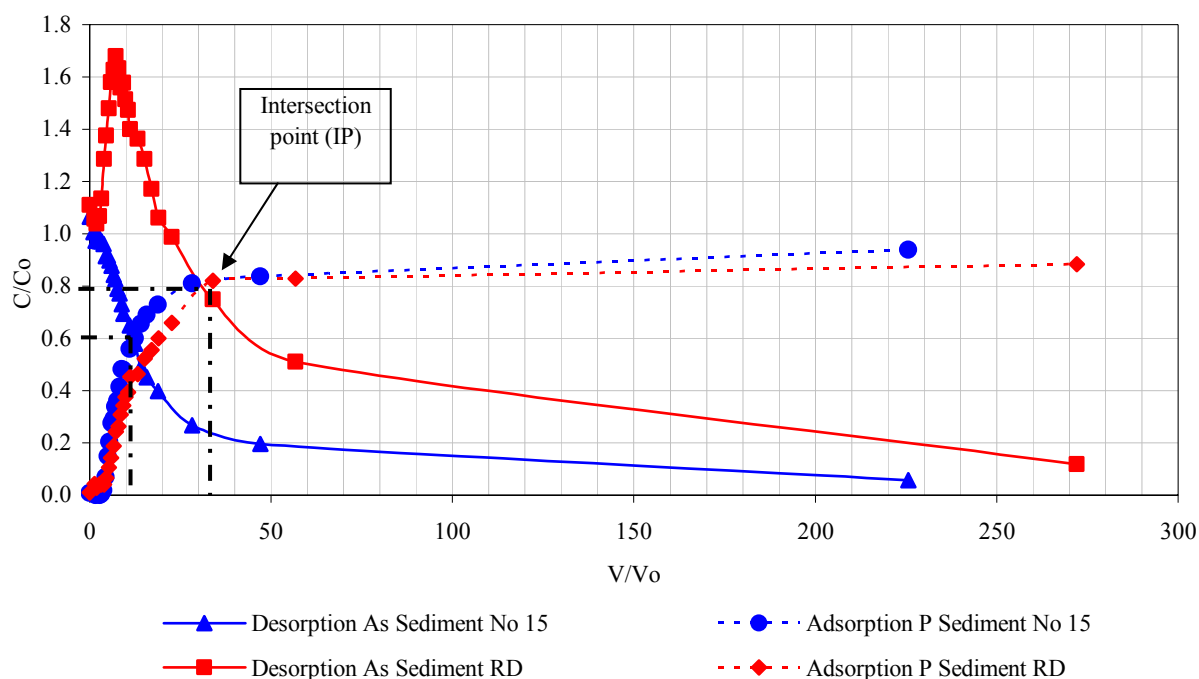
Figure 4.2.1.1 Effluent breakthrough curves for As and P in the reduced sediment (No. 15, 21 m) and oxidized material (RD, 81 m). First the column was equilibrated with an arsenite-containing solution, then phosphate as competing ion was added to the AGW and percolated through the column.

After pumping the P-containing solution through the columns, the As concentration drops immediately in the effluent of the reduced sediment (No. 15). P showed a faster increase in the reduced than in the oxidized sand (RD). In the reduced sediment the intersection point was already reached after 16 pore volumes at c/c_0 of 0.6, i.e. faster release of As out of the sediment and a faster saturation of the sediment with P. The oxidized sand on the other hand had its intersection point after 32 pore volumes at c/c_0 of 0.8. At this point still a high concentration of As is released out of the column because of an initial higher As adsorption on the sediment. The peak up to 1.7 c/c_0 after 8 pore volumes indicates the high sorption capacity of the sediment and the displacement of As by P. According to the sediment type the intersection point indicates a faster desorption of As in the reduced sediment. When looking at the intersection point of the eight sub-experiments (Table

4.2.1.1) it seems that after addition of P arsenic is retarded the most in the oxidized sand (experiment 2 and 4), thus more As is exchangeable. The competition of P with either arsenite or arsenate indicated the stronger interaction between P and arsenate. After 24 (experiment 7) and 56 (experiment 8) pore volumes still desorption of P (c/c_0 = 0.4 and 0.3) from the sediment occurred.

Table 4.2.1.1 Intersection Point of sub-experiments as an indication for sorption behaviour of As versus P in the sediment.

Sediment No.	Sub-experiment Desorption As	IP V/Vo	c/c₀	Sub-experiment Desorption P	IP V/Vo	c/c₀
15	1. $AsO_3^{3-} \rightarrow PO_4^{3-}$	12	0.6	*5. $PO_4^{3-} \rightarrow AsO_3^{3-}$*	7	0.4
RD	2. $AsO_3^{3-} \rightarrow PO_4^{3-}$	41	0.8	*6. $PO_4^{3-} \rightarrow AsO_3^{3-}$*	11	0.3
15	3. $AsO_4^{3-} \rightarrow PO_4^{3-}$	13	0.7	*7. $PO_4^{3-} \rightarrow AsO_4^{3-}$*	24	0.4
RD	4. $AsO_4^{3-} \rightarrow PO_4^{3-}$	42	0.8	*8. $PO_4^{3-} \rightarrow AsO_4^{3-}$*	56	0.3

Table 4.2.1.2 Summary of quantitative analyses of column experiments. Adsorbed, exchangeable, and non-exchangeable surface coverage of As and P added sequentially.

Sub-Expt.	Sediment No.	ion added first	competing ion	surface coverage As/P [µmol/g] adsorbed	exchangeable	non-exchangeable
1	15	AsO_3^{3-}	PO_4^{3-}	0.12	0.10	0.02
2	RD	AsO_3^{3-}	PO_4^{3-}	0.14	0.19	-0.05
3	15	AsO_4^{3-}	PO_4^{3-}	0.39	0.16	0.23
4	RD	AsO_4^{3-}	PO_4^{3-}	0.61	0.30	0.30
5	15	PO_4^{3-}	AsO_3^{3-}	0.75	0.39	0.36
6	RD	PO_4^{3-}	AsO_3^{3-}	1.09	0.59	0.50
7	15	PO_4^{3-}	AsO_4^{3-}	0.67	1.39	-0.73
8	RD	PO_4^{3-}	AsO_4^{3-}	0.97	2.62	-1.65

Equilibrium (c/c_0 = 1) or the complete desorption (c/c_0 = 0) of As and P was not reached in some of the experiments, which indicates in the first case that the maximum adsorption capacity was not reached and unoccupied sorption sites were still left after the input of As or P was stopped. In the latter case not the whole initially desorbed concentration was detected causing underestimation of the desorbed concentration. Negative values for non-exchangeable concentrations may appear as a result.

Quantitative analyses emphasized the higher sorption of arsenate (Table 4.2.1.2). In sub-experiments 3 and 4 0.61 µmol/g on sediment RD and 0.39 on the reduced sediment were adsorbed. Sorption of arsenite on both sediments was quite similar with 0.12 and 0.14 µmol/g. After P was added into the system arsenite seemed to be completely exchangeable, but only 40 - 50 % (experiment 3 and 4) of the initially adsorbed arsenate was recovered.

For the calculated adsorbed P concentration the problem raised that c/c_0 =1 was not reached and consequently the sorption capacity was underestimated (negative values in Table 4.2.1.2). Anyway, highest sorbed P concentrations were achieved in the oxidized sand with 1.09 µmol/g (experiment

6) and 0.97 µmol/g (experiment 8). The competition with either arsenite or arsenate showed that arsenate had a stronger effect on desorption of P, 1.39 and 2.62 µmol/g were exchangeable (experiment 7 and 8). After addition of arsenite, around 50 % P (0.36 and 0.5 µmol/g) were non-exchangeable in both sediments (experiment 5 and 7).

In Figure 4.2.1.2 the results from As-speciation are demonstrated based on experiment No. 2, desorption of As after equilibration with arsenite and addition of a P-containing solution to the oxidized sand (compare with Figure 4.2.1.1). Remarkable in this curve is the conversion of the initially spiked arsenite to arsenate. From the total desorbed As concentration 65 % were detected as arsenate and only 35 % as arsenite, thus dominantly As in the form of arsenate was adsorbed to the sediment. Arsenate desorption by phosphate after adding the arsenite containing solution was particularly observed in the oxidized sand (RD). Only a very small concentration of arsenate was quantified in the reduced sediment (experiment 1). In experiment 3 and 4 small quantities of arsenite (0 to 30 µg/L) were measured in the effluent after addition of arsenate. In experiment 5 and 6 arsenite was partially (up to 34 % in the effluent) converted to arsenate. No transformation of arsenate to arsenite appeared in experiments 7 and 8.
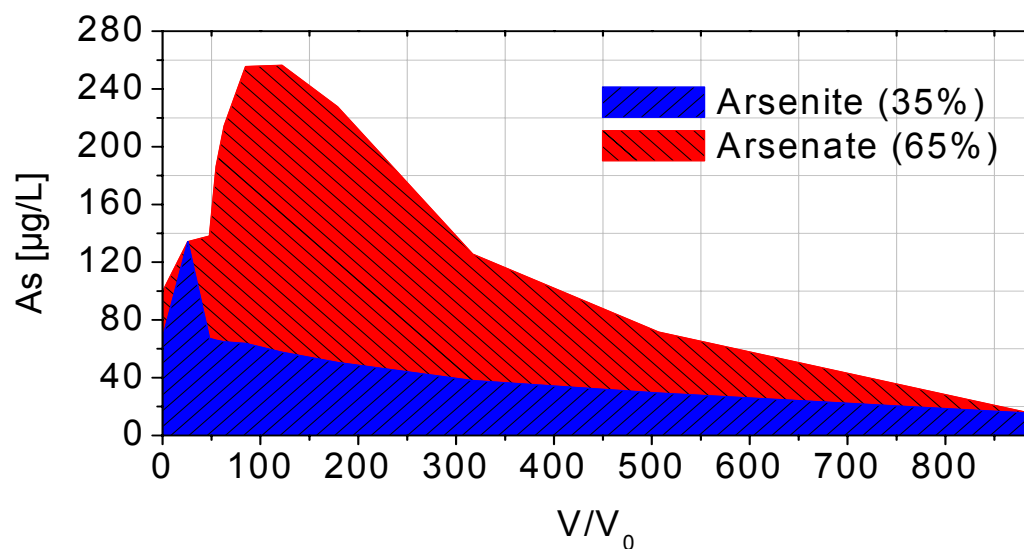
Figure 4.2.1.2 Desorption of arsenite and arsenate from sediment RD after equilibration with arsenite and application of P-containing solution to the column

4.2.2. Adsorption behaviour of arsenate and monothioarsenate

The sorption behaviour of arsenate (AsO_4^{3-}), monothioarsenate (AsO_3S^{3-}) or a mix of both is depicted in Figure 4.2.2.1, where the effluent breakthrough curves for each anion are shown. Total As concentrations in all experiments were about 200 µg/L (2.6 µg/L) in the AGW. The dashed curves mark the columns filled with the oxidized sand (RD). The slopes of all three curves are steeper for the reduced sediment (No. 15) than for the oxidized sand, i.e. the sorption capacity of the oxidized sand is higher than that of reduced sediment. In both sediments, the As concentrations in the effluent increased faster in the monothioarsenate-containing solution which indicates lower sorption capacity for monothioarsenate compared to arsenate. Arsenate seemed to be retarded the most, particularly in the oxidized sand.
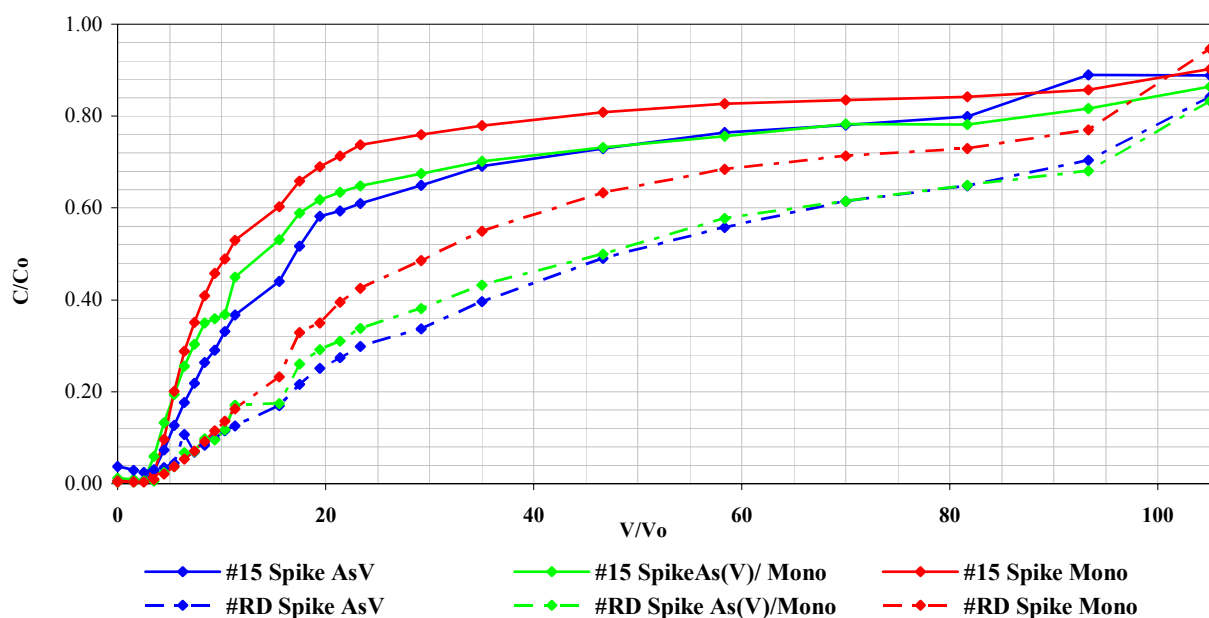
Figure 4.2.2.1 Effluent breakthrough curves of As after adding 200 µg/L arsenate, 200 µg/L monothio-arsenate, and a mix of both (each 100 µg/L).

Results from quantitative analyses of the effluent breakthrough curves are listed in Table 4.2.2.1. All solutions with a total of 94 ml were pumped with a flow rate of 0.18 ml/min through the columns. In all columns c/c_0 values were below 1, thus no equilibration with the sediment was reached and still sorption sites remained. As sorption is strongest in the oxidized sand where up to 11.7 µg/g As (solution arsenate) were adsorbed. Lowest values for As sorption were analysed for monothioarsenate, only 5.2 µg/g in the reduced sediment and 8.7 µg/g in the oxidized sand were adsorbed. The concentrations for the mixed solution containing arsenate and monothioarsenate were in between of the values obtained for pure arsenate and monothioarsenate solutions with 6.8 µg/g and 11.0 µg/g As adsorbed. The sorption of arsenate, monothioarsenate, and the mix

arsenate/monothioarsenate to both sediment types increased according to the following sequence: arsenate > arsenate/monothioarsenate > monothioarsenate (all in oxidized sediment) > arsenate > arsenate/monothioarsenate > monothioarsenate (all in reduced sediment).

Table 4.2.2.1 Quantitative analyses of As-sorption. Represented are results for arsenate (AsO_4^{3-}), monothioarsenate ($AsO_3S_3^-$), and a mix of both (AsO_4^{3-}/ $AsO_3S_3^-$).

sediment	Solution	C_o [μg/L]	Total As [μg]	As not adsored [μg]	As in Vo [μg]	As adsorbed		C/Co
						[μg/g]	[μmol/g]	
15	AsO_4^{3-}	239	22.5	15.2	0.2	**7.1**	**0.09**	0.89
	AsO_3S^{3-}	218	20.6	15.2	0.2	**5.2**	**0.07**	0.90
	AsO_4^{3-}/ AsO_3S^{3-}	230	21.7	14.7	0.2	**6.8**	**0.09**	0.86
RD	AsO_4^{3-}	239	22.5	10.7	0.2	**11.7**	**0.16**	0.84
	AsO_3S^{3-}	218	20.6	11.7	0.2	**8.7**	**0.12**	0.95
	AsO_4^{3-}/ AsO_3S^{3-}	230	21.7	10.5	0.2	**11.0**	**0.15**	0.83

In summary it can be said that for arsenite, arsenate, monothioarsenate and phosphate highest sorption capacities were observed on the oxidized sand from the shallow aquifer in 81 m depth. In addition, species analyses have shown the conversion of arsenite to arsenate and its sorption on the oxidized sand which leads to higher sorption rates of arsenite on this material compared to the reduced sandy loam from the shallow aquifer, where no noticeable conversion from arsenite to arsenate occurred. Arsenic sorption was highest for arsenate. Competitive anion exchange dominated between arsenate and phosphate, where most of the sorbed As and P concentrations were exchangeable by the competitive anion.

4.2.3. Formation of thioarsenates

A third column experiment was conducted to monitor the formation of thioarsenates by the sequential addition of As and S^{2-} to the sediment. An arsenic-containing solution ($\approx$ 200 μg/L) was pumped through the column followed by S^{2-} (1 mg/L) and vice versa. Arsenic speciation of the effluent could not show the conversion of either arsenite or arsenate into As-S species (monothioarsenate). Arsenate was reduced to arsenite in all experiments, particularly after S^{2-} was first introduced to the sediment. No arsenate was detected in those samples.

4.3. Laboratory experiments for arsenic mobilization depending on carbonate concentration

The influence of carbonate and pH on As-sorption and release was investigated on 3 mineral phases, As_2O_3 and As_2S_3 as As-bearing minerals and Fe_2S_3, in an anaerobic, reducing environment. The experiments were performed in $NaHCO_3$ and $NaOH$. The ionic strength of each solution ranged from 0.01 M and 0.04 M to 0.1 M. The reaction time in all experiments was 40 h.

4.3.1. Sorption arsenite and arsenate on pyrite (FeS$_2$)

Sorption of arsenite and arsenate was studied on FeS_2 (Figure 4.3.1). After the reaction time of 40 h the pH in 0.01 M $NaOH$ had values of 11.3, for 0.04 M 11.9, and for 0.1 M 12.3 in both samples (spike arsenite and arsenate). In $NaHCO_3$ the pH ranged from 8.6 to 8.8. Only the measured pH in 0.01 M $NaHCO_3$ (arsenite) was slightly lower with 8.4. The initial spikes had concentrations of 1 mg/L each for arsenite and arsenate.
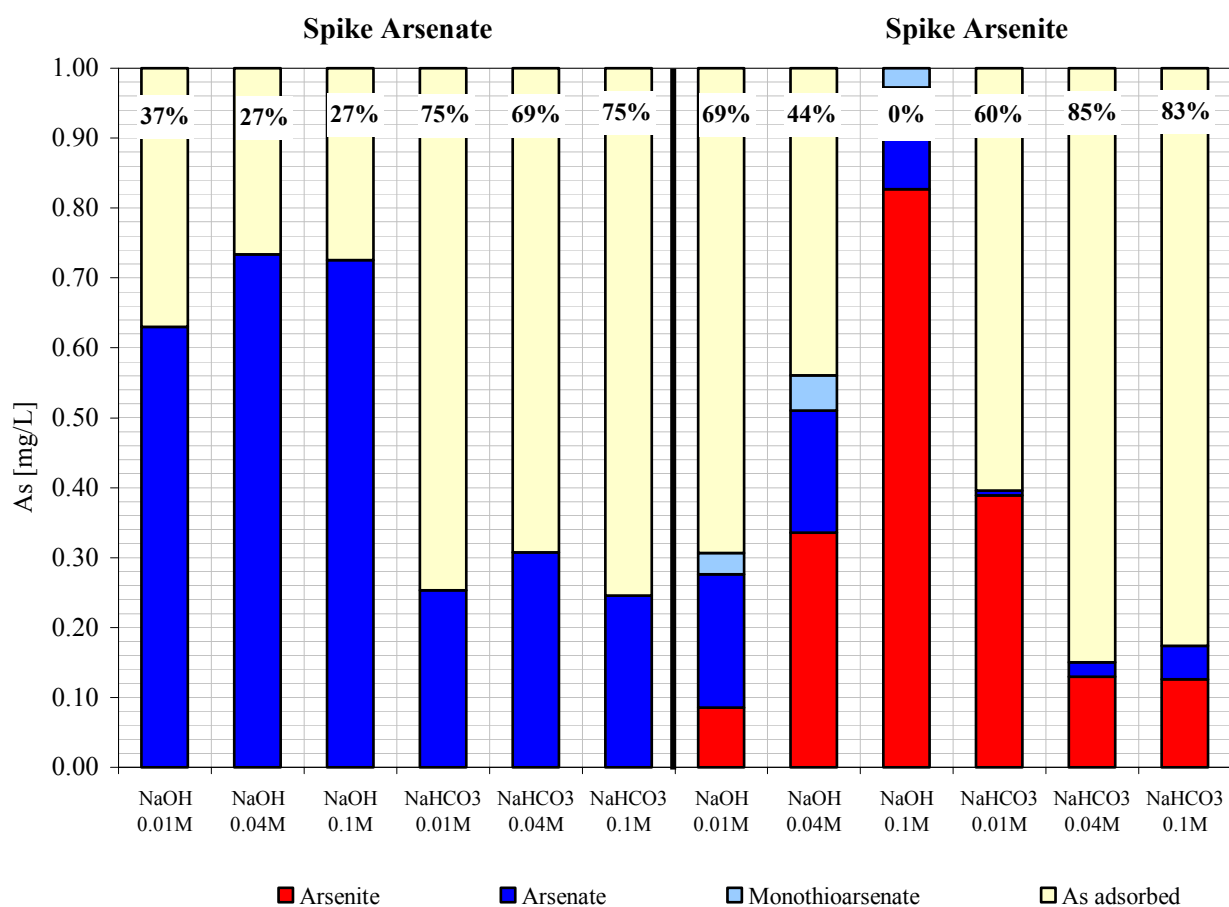
Figure 4.3.1 Sorption of arsenite and arsenate on FeS$_2$. The percentage values represent dissolved As concentrations after addition of either 1 mg/L arsenite or 1 mg/L arsenate.

Sorption is low in NaOH with high pH. Only after addition of arsenite sorption was higher (69 %) in 0.01 M NaOH at the pH of 11.3. After addition of arsenite no As-sorption was observed in 0.1 M NaOH, whereas after addition of arsenate 27 % of the initial spike was adsorbed, the same value as for 0.04 M NaOH. Apparently the concentration of NaOH affected more the sorption of arsenite than that of arsenate on FeS_2, because dissolved As concentrations increased remarkably with increasing concentrations after arsenite was added to the solution but not after addition of arsenate, where As sorption showed only little dependence on NaOH concentration.

In $NaHCO_3$ no strong influence of the concentration on As-sorption was observed (69 % and 75 % after addition arsenate). Sorption of arsenite was highest in 0.04 M and 0.1 M $NaHCO_3$ with 85 and 83 % of the initial arsenite concentration followed by 60 % in 0.01 M $NaHCO_3$ which was even lower than in 0.01 M NaOH, where 69 % were adsorbed. Compared to arsenate arsenite sorption appeared lower in the solutions, except in 0.1 M NaOH and 0.01 M $NaHCO_3$.

Arsenic speciation showed the partial conversion of arsenite to arsenate in all solutions. The detected concentrations of arsenate in NaOH ranged from 150 to 190 µg/L, in $NaHCO_3$ from 10 to 50 µg/L. Moreover, the formation of monothioarsenates was observed in NaOH with concentrations of 3 and 5 mg/L, indicating geochemical interactions between FeS_2 and the arsenite-containing solution.

4.3.2. Dissolution arsenic trioxide (As_2O_3) and orpiment (As_2S_3)

The dissolution of As_2O_3 caused a drop in pH in each of the solutions (Table 4.3.2.1). In 0.01, 0.04, and 0.1 M NaOH high concentrations of 627, 618, and 613 mg/g dissolved arsenic were measured, 231, 228, and 220 mg/g only in 0.01, 0.04, and 0.1 M $NaHCO_3$ (Figure 4.3.2.1). In all solutions only arsenite, no arsenate, was detected. Further in both solutions the dissolution seemed to be unaffected by the ionic strength.

Table 4.3.2.1 pH before and after dissolution As_2O_3

	pH (initial)	pH (after 40h)
NaOH 0.01 M	11.5	11.0
NaOH 0.04 M	12.1	11.9
NaOH 0.1 M	12.6	12.3
$NaHCO_3$ 0.01 M	8.9	8.6
$NaHCO_3$ 0.04 M	9.0	8.8
$NaHCO_3$ 0.1 M	9.0	8.8
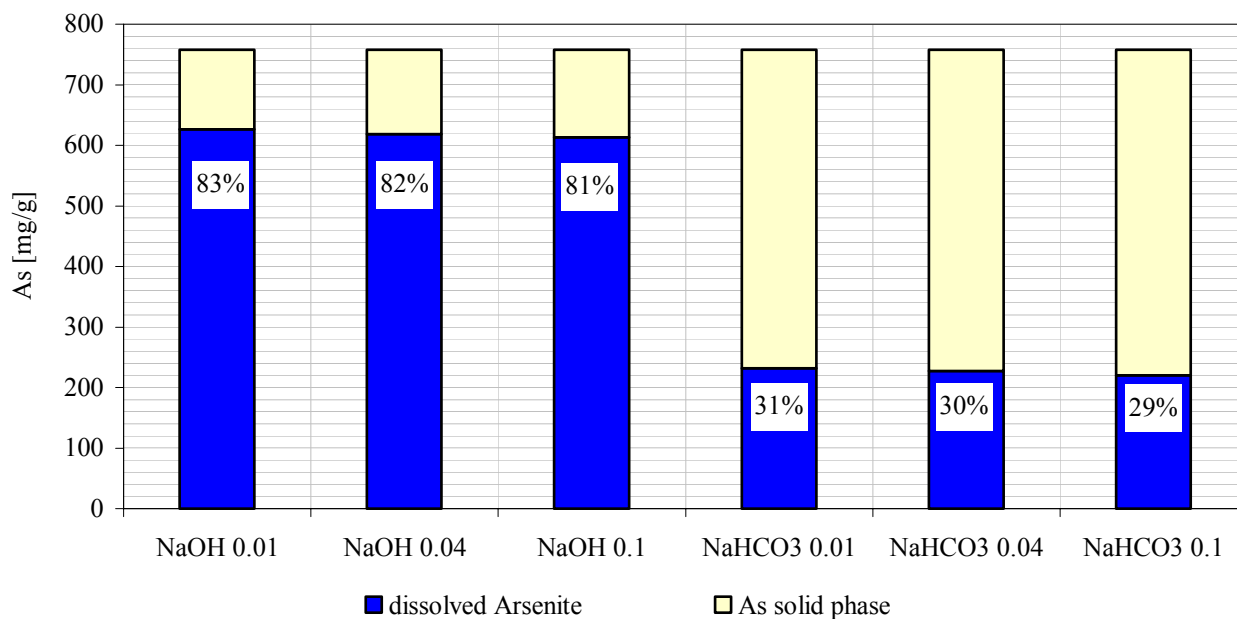
Figure 4.3.2.1 As$_2$O$_3$ dissolution in NaOH and NaHCO$_3$. The percentage value represents the concentration of arsenic (Arsenite) that was soluble within different solutions. The maximum arsenic concentration soluble from As$_2$O$_3$ was modelled to be 758 mg/g using PhreeqC.

In Figure 4.3.2.2 the results from As$_2$S$_3$ dissolution in 0.01, 0.04 and 0.1 M NaOH and NaHCO$_3$ are represented. As$_2$S$_3$ dissolution led to the decrease in pH (Table 4.3.2.2). Maximum solubility was modelled to be 758 µg/g using PhreeqC. Based on this value, 95, 94, and 96 % (around 580 µg/g As) of As$_2$S$_3$ dissolved in 0.01, 0.04, and 0.1 M NaOH. The solubility of As$_2$S$_3$ increased with increasing concentrations of NaHCO$_3$ from 6 %, 15 % to 26 % (36, 90, and 157 mg/g As).

Table 4.3.2.2 pH before and after dissolution As$_2$S$_3$

	pH (initial)	pH (after 40h)
NaOH 0.01 M	11.3	10.3
NaOH 0.04 M	12.0	11.7
NaOH 0.1 M	12.5	12.3
NaHCO$_3$ 0.01 M	8.9	8.5
NaHCO$_3$ 0.04 M	9.0	8.9
NaHCO$_3$ 0.1 M	8.9	8.8
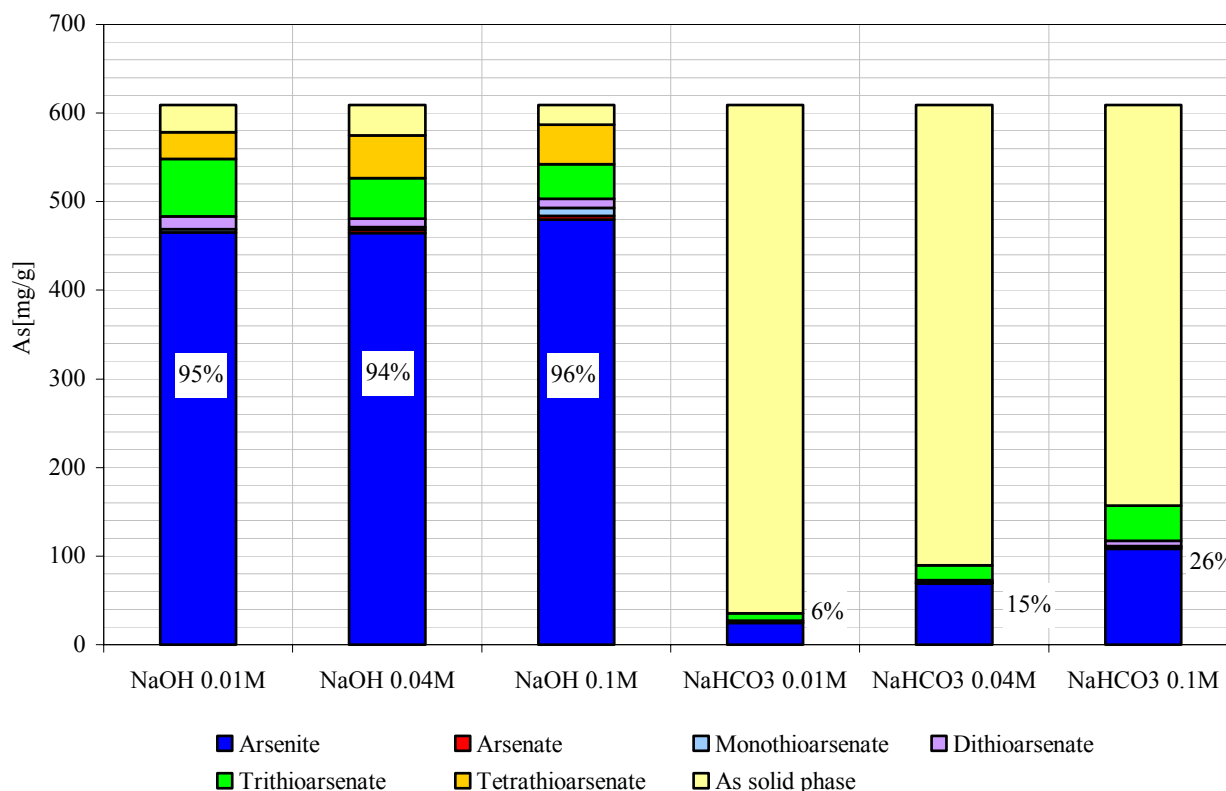
Figure 4.3.2.2 As$_2$S$_3$ dissolution in NaOH and NaHCO$_3$. Total As soluble from As$_2$S$_3$ was modelled with 609 mg/g using PhreeqC.

The percentages of thioarsenates determined from total dissolved arsenic concentrations are listed in Table 4.3.2.3. Arsenite was the dominant species in NaOH and NaHCO$_3$. In NaOH trithioarsenate increased with decreasing concentrations up to 11.3 % in 0.01 M NaOH (pH 10.3), while tetrathioarsenate increased with increasing pH in NaOH.

In NaHCO$_3$ trithioarsenate was the most abundant As species after arsenite with up to 25 % in 0.1 M NaHCO$_3$. In NaHCO$_3$ and NaOH dithioarsenate and monothioarsenate were only detected in minor concentrations. No tetrathioarsenate was quantified in NaHCO$_3$.

Table 4.3.2.3 Percentage values of dissolved As species from As$_2$S$_3$ dissolution in NaOH and NaHCO$_3$.

	pH	Arsenite (%)	Arsenate (%)	Monothio-arsenate (%)	Dithio-arsenate (%)	Trithio-arsenate (%)	Tetrathio-arsenate (%)	total As dissolved [mg/g]
NaOH 0.01M	10.3	*80.4*	*0.0*	*0.6*	*2.5*	*11.3*	*5.2*	*579*
NaOH 0.04M	11.7	*80.9*	*0.6*	*0.6*	*1.6*	*8.0*	*8.4*	*575*
NaOH 0.1M	12.3	*81.7*	*0.7*	*1.5*	*1.8*	*6.7*	*7.6*	*587*
NaHCO$_3$ 0.01M	8.5	*69.2*	*1.0*	*0.4*	*4.5*	*25.0*	*0.0*	*36*
NaHCO$_3$ 0.04M	8.9	*77.2*	*0.9*	*0.4*	*2.7*	*18.8*	*0.0*	*90*
NaHCO$_3$ 0.1M	8.8	*69.1*	*1.1*	*0.7*	*3.8*	*25.3*	*0.0*	*157*

Compared to As$_2$O$_3$, As$_2$S$_3$ showed a better dissolution in 0.01, 0.04, and 0.1 M NaOH (more than 10 %). As$_2$O$_3$ showed no ionic strength dependence in NaHCO$_3$ and had constant dissolved As concentrations of around 30 % in all three solutions, while in As$_2$S$_3$ total dissolved As concentrations increased from 6 %, 15 % to 26 % depending on the concentration of NaHCO$_3$.

4.3.3. Dissolution As$_2$S$_3$ in MQ and 0.04 M NaHCO$_3$ at different pH

After first results from As$_2$S$_3$ dissolution in chapter 4.3.2., which have shown the likely influence of NaHCO$_3$ on As-release, the effect of 0.04 M NaHCO$_3$ on As$_2$S$_3$ dissolution was studied more detailed over a pH ranging from 3 to12. For comparison the same experiment was additionally conducted in MQ. In this kinetic experiment samples were analysed for dissolved As concentrations over a time period of 50 days (Table 3.6.1).

The pH measurements after each sampling showed the effect of As$_2$S$_3$ dissolution on the pH in MQ and NaHCO$_3$ (Figure 4.3.3.1). Most notably, the pH dropped in MQ, where pH values from 7 to 11 were affected, e.g. pH 10, 10.5, 11 reached values below 8. Consequently, in MQ no As concentrations for As$_2$S$_3$ dissolution could be measured for a pH between 8 to 11 after 8 days. In NaHCO$_3$ no decrease in pH was observed. Looking at pH 5 to 7 even a slight increase was observed. The shift of pH in MQ made also the comparability of As$_2$S$_3$ dissolution in the two solutions, MQ and NaHCO$_3$, difficult.
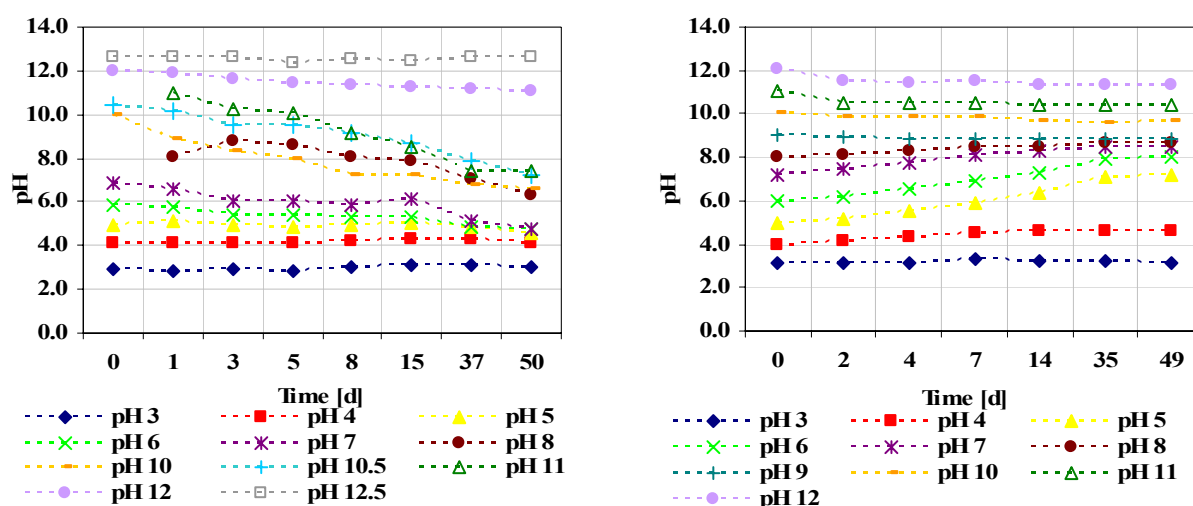
Figure 4.3.3.1 Development of pH values after As$_2$S$_3$-dissolution in MQ (left) and NaHCO$_3$ (right) over 50 days. The values given in the legend represent initial pH values.

Concentrations of As species from As_2S_3 dissolution in MQ and $NaHCO_3$ depending on time and pH are represented in Figure 4.3.3.2 and Figure 4.3.3.3. The distribution of As-species in MQ and $NaHCO_3$ are described taking samples of comparable pH later. The values of dissolved As concentrations dependent on time and pH in MQ and $NaHCO_3$ are listed in Appendix A.3 and A.4. The dissolution in MQ over 50 days showed a maximum in dissolved concentrations for pH 12 and 12.5 (three highest bars in the graph below) with 450 to 577 µg/g after the first 5 days. Until day 5 the dissolved As concentration increased at pH 12 from 100 to 460 µg/g. After day 5 suddenly the concentrations at pH 11.4 to 12.4 dropped to around 300 µg/g. This concentration corresponded to approximately half of the maximum soluble As concentration (609 µg/g) expected from As_2S_3 dissolution based on modelling with PhreeqC. At lower pH (pH < 10) As_2S_3 was only dissolved up to 70 µg/g (after 3 and 5 days at pH 9.5).
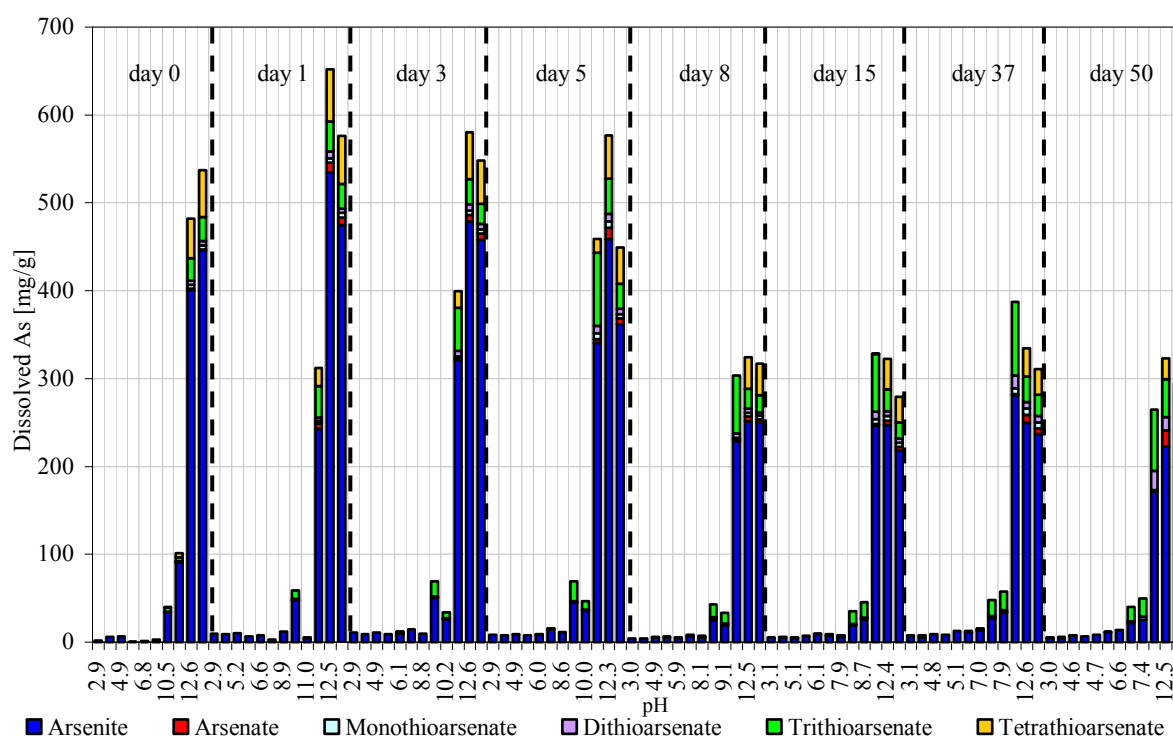
Figure 4.3.3.2 Overview As_2S_3 dissolution in MQ over a time period of 50 days.
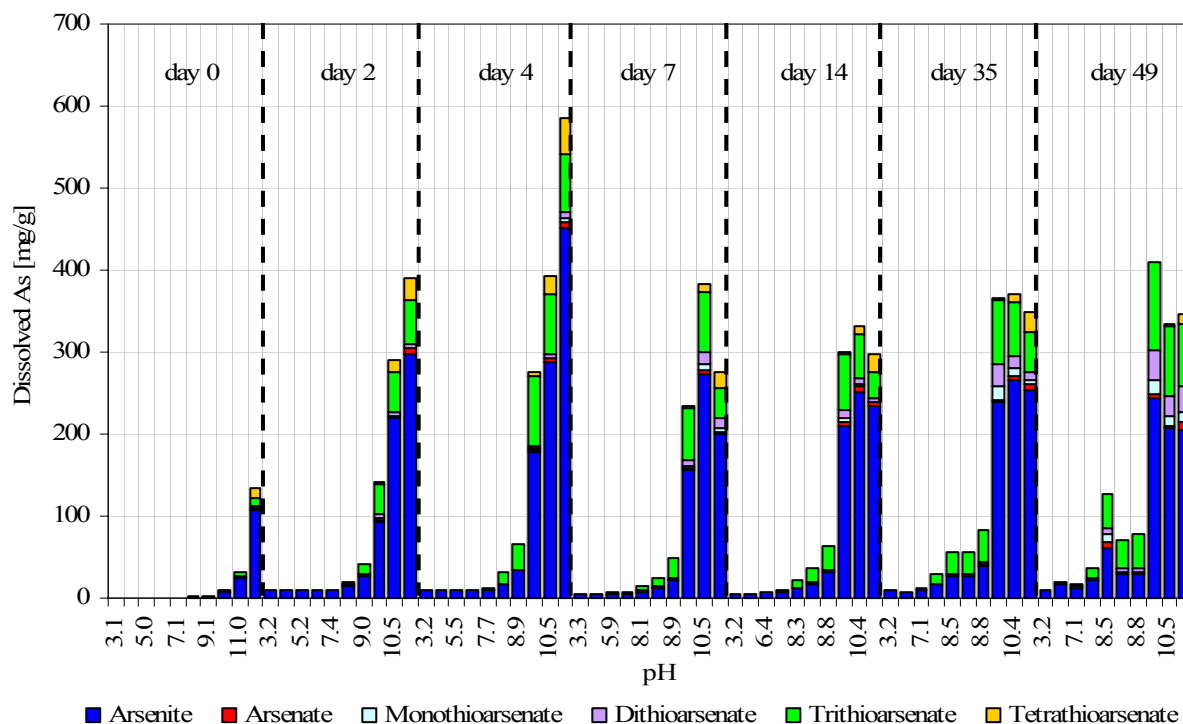
Figure 4.3.3.3 Overview As₂S₃ dissolution in NaHCO₃ over a time period of 49 days.

In NaHCO$_3$ low dissolved As concentrations were observed after the first sampling. Except for pH 12 (134 µg/g As) all values were below 40 µg/g (Appendix A.5). Further the dissolved concentrations increased with time at different pH (3, 7, 9, 10.5, and 11.5) as depicted in Figure 4.3.3.4. At pH 3 and 7 the solubility of As$_2$S$_3$ is low (3 to 10 µg/g As) and no time-dependence could be observed. As$_2$S$_3$ dissolution at pH 9 increased from 40 to 83 µg/g (day 2 to 35). A jump in dissolution was observed at pH higher than 10, where a maximum of around 350 to 370 µg/g As was dissolved after 35 days. It seemed that dissolution at pH 10 is most time-dependent because As$_2$S$_3$ dissolution increased from 114 to 365 µg/g dissolved As within 33 days what makes an increase of around 250 µg/g.
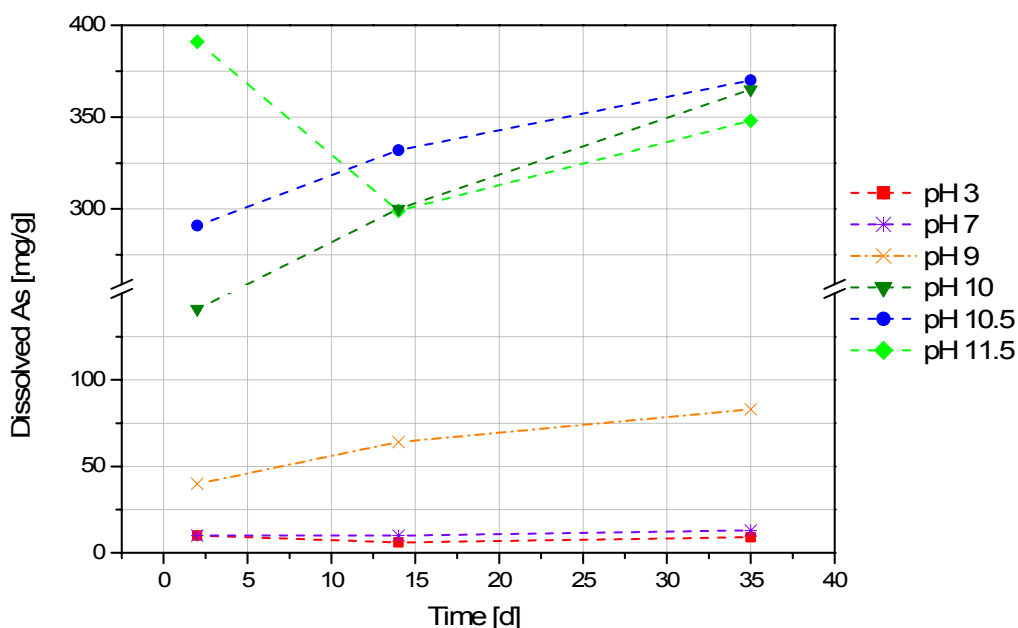
Figure 4.3.3.4 Dissolution As$_2$S$_3$ dependent on pH and time in NaHCO$_3$

The difference in solubility in MQ and NaHCO$_3$ at day 0 may result from a longer equilibration time in MQ before filtering the samples. In NaHCO$_3$ the samples for speciation were taken immediately while those in MQ after around 1 h. Reasons were problems in pH adjustment.

In the figure below (Figure 4.3.3.5), As$_2$S$_3$ dissolution compared between MQ and NaHCO$_3$ with increasing pH is shown dependent on time.
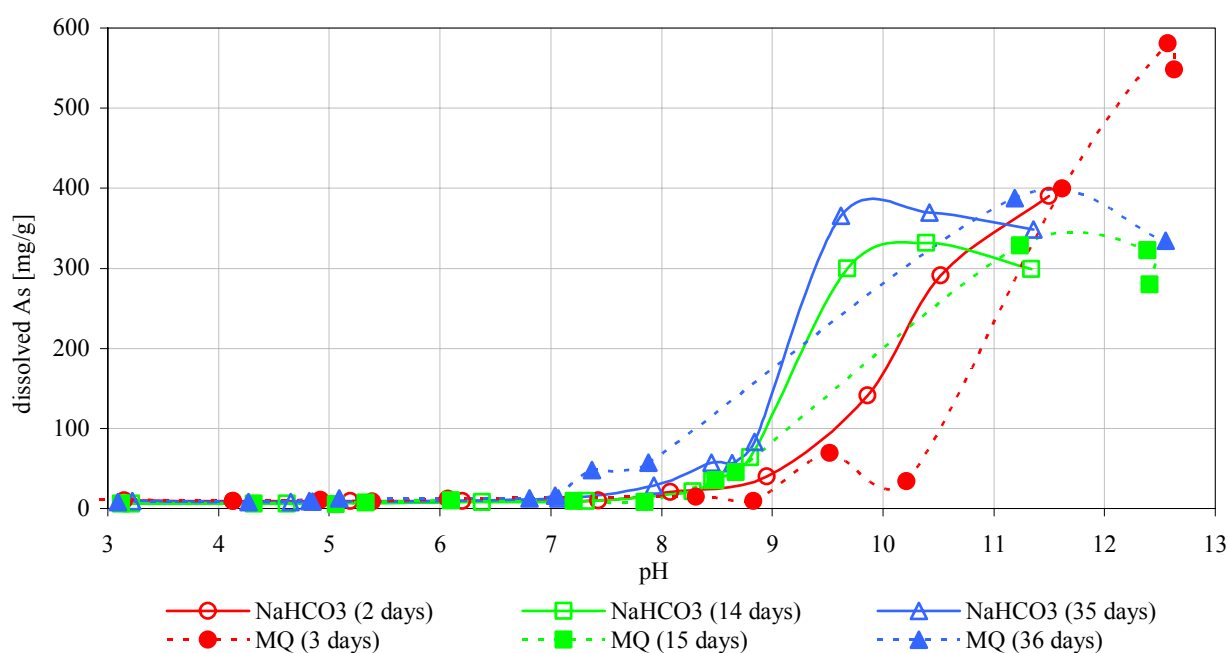
Figure 4.3.3.5 Comparison of As$_2$S$_3$ dissolution in MQ and NaHCO$_3$ with increasing time.

After a short equilibration time (2/3 days) As_2S_3 dissolution seemed higher in $NaHCO_3$ than in MQ up to pH 11. After 14/15 days the difference at pH near neutral to 9 was negligible and after 35/36 days the dissolution in MQ at pH near neutral even was higher. At pH 7.9 the dissolution was favoured in MQ with approximately 30 µg/g more dissolved arsenic. Due to the already mentioned problems in the comparability of the pH in both solutions with the time, the range of missing pH values, particularly in MQ, was interpolated and can cause inaccuracies. Therefore the As concentration at higher pH values (pH > 9) after 14/15 and 35/36 days were not comparable and taken into account.

In Figure 4.3.3.6 the distribution of As-species at pH ≈ 8 and ≈ 11 is emphasised for both solutions after 2/3, 14/15, and 35/36 days (also compare with Figure 4.3.3.2 and Figure 4.3.3.3). In all solutions arsenite is the dominant species, followed by trithioarsenate. Dithioarsenate and tetrathioarsenate occurred in minor quantities at pH over 9. At pH higher than 10 arsenate and tetrathioarsenate were observed. No tetrathioarsenate was detected after 15 and 36 days in MQ. Remarkable was the increase of trithioarsenate from 29 to 47 % with increasing time at pH 8.5 to 9 while arsenite decreased from 69 to 48 %, thus both species were present in equal portions of total dissolved As in solution after 15 days reaction time (Figure 4.3.3.7).
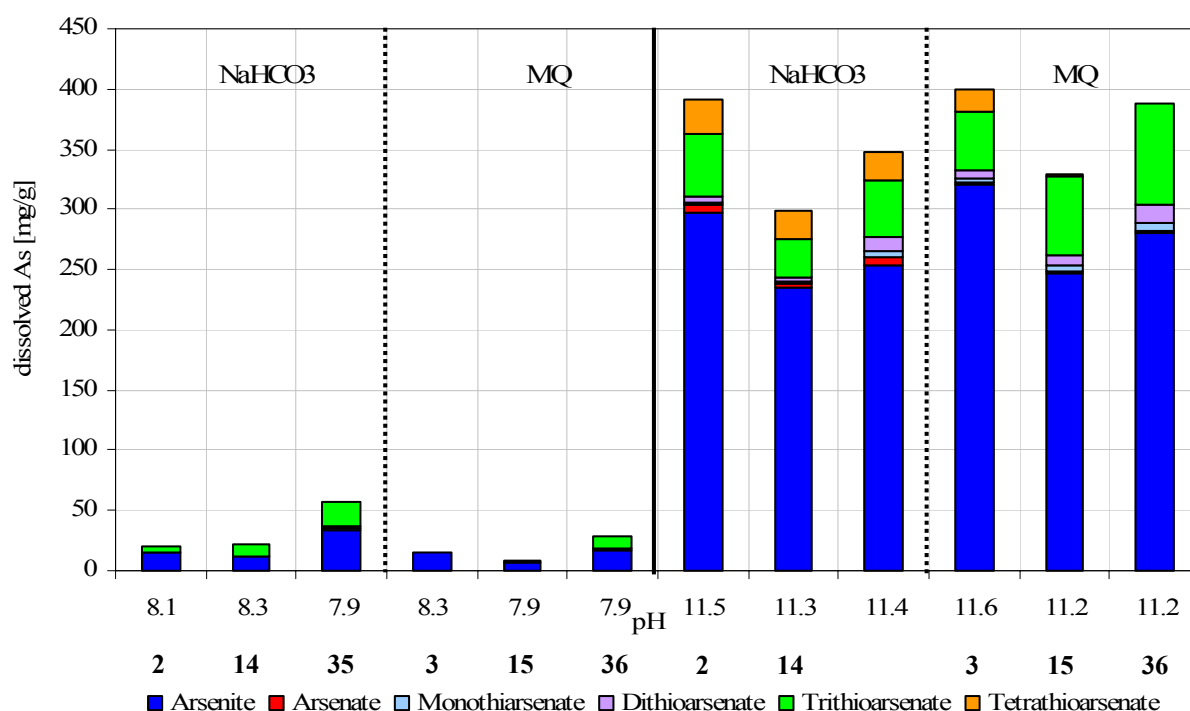
Figure 4.3.3.6 Distribution of As-species in NaHCO₃ and MQ at comparable pH after 2, 14, and 35 days (NaHCO₃) and 3, 15, and 36 days (MQ).
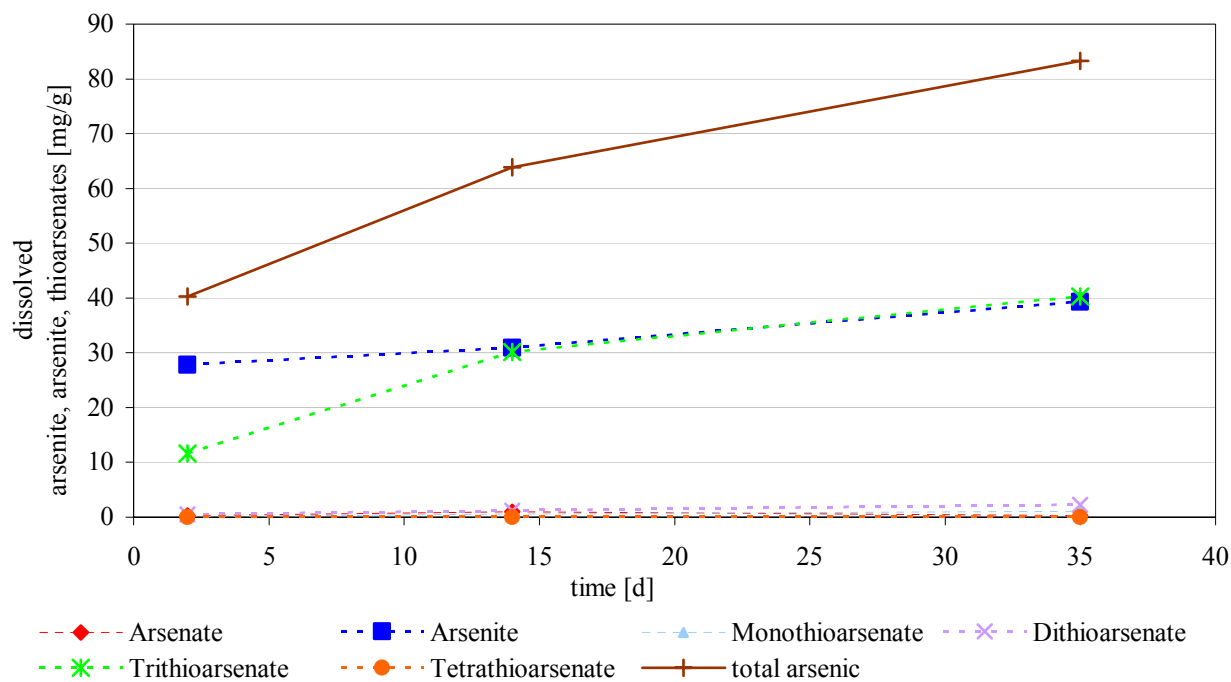
Figure 4.3.3.7 Arsenic speciation in NaHCO3 at pH 9 with increasing time.

Modelling (PhreeqC) As_2S_3 dissolution has shown considerable differences between the received results in both solutions, MQ and $NaHCO_3$ (Figure 4.3.3.8). The initial pH for the modelling ranged between 2 and 13 in steps of 1 pH unit. The represented pH values already consider the pH-shift due to As_2S_3 dissolution. The pH-shift, particularly in MQ, led to the lack of pH values in the range of 8.3 to 11.4 in MQ. The modeled values showed higher concentrations of dissolved As, starting at pH 6.4 in MQ and $NaHCO_3$. Further, in $NaHCO_3$ dissolved Arsenic increased steeply up to pH 8.3 and a complete dissolution occurred already at a pH of 9.8 in $NaHCO_3$. The maximum dissolved As concentration from modelling was 609 mg/g. Maximum values within the experiment were measured with only 300 to 400 µg/g As, except for the dissolution in MQ after 3 days (Figure 4.3.3.2). Thus, the results from the experiments and the modelling do not match very well.
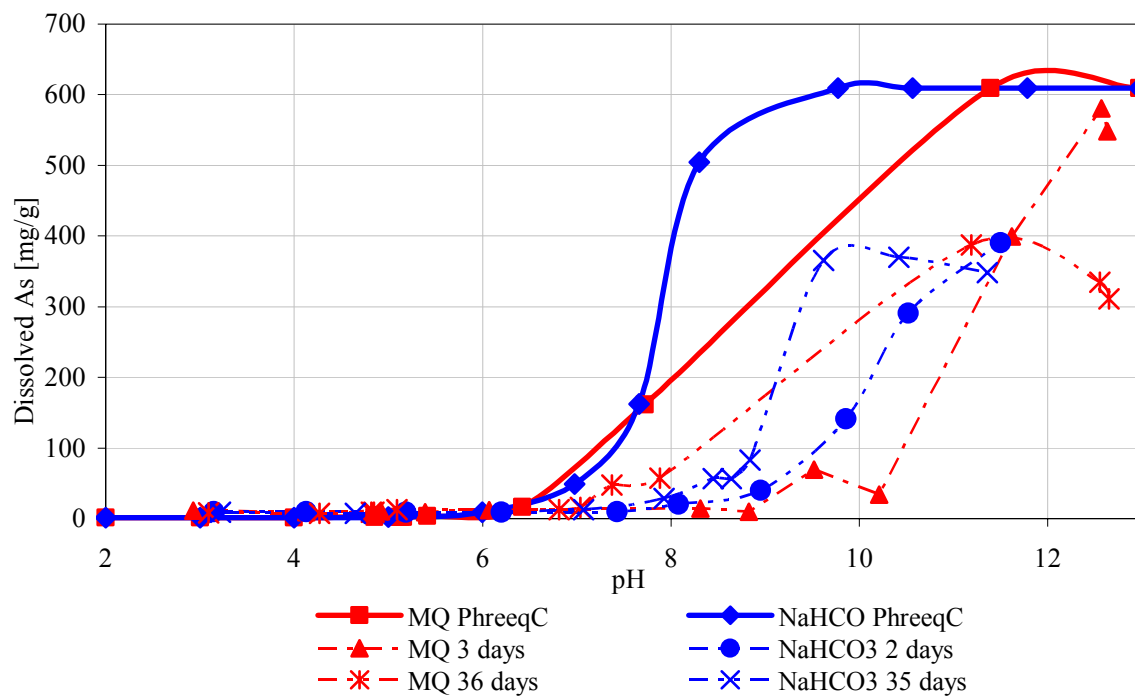
Figure 4.3.3.8 Dissolved As concentrations with respect to PHREEQC modelling, in MQ (after 3 and 36 days) and in NaHCO₃ (after 2 and 35 days)

5. Discussion

5.1 Associations between sediment properties in the depth profile

The study site is located close to the main river channel of Meghna, and thus receiving sediments once a year during the Monsoon flood (Figure 3.1.1). The average reported values for As in the sediments are 1.2 to 2.6 µg/g for the Ganges 1.4 to 5.9 µg/g for the Brahmaputra, and 1.3 to 5.6 µg/g for the Meghna Rivers (MCARTHUR et al., 2004). Utilizing lithological investigations, mineral determination with XRD, and sediment characterization, the depth profile shown in Figure 4.1.1.1 can be characterized as follows.

Below the man made earth bank of the hospital, a one m thick silty layer (L1) overlies a 23 m deep sandy aquifer (L2, shallow aquifer). The shallow aquifer is underlain by an aquiclude with silty texture, 52 m thick (L3, silt loam) enclosing the sand aquifer in 79 to 83 m depth (deepest aquifer) together with the deepest aquiclude (L5, silt). The sediment from the shallow aquifer is grey in color over the entire depth of this layer. The sediment from the deeper aquifer varies in its composition and consists of brown sand in the upper part and grey sandy loam at the bottom of this layer (Figure 5.1.1). It can be assumed that the brown color indicates the occurrence of iron(hydr)oxides, which might be formed during oxidative weathering of the sediments prior to the deposition of the overlying sediments (MCARTHUR et al., 2004). Due to reducing conditions iron(hydr)oxide is reduced, explaining the grey color of the sediments in the shallow aquifer.

Figure 5.1.1 Reduced sediment from the shallow aquifer on the left
and oxidized sand from the deeper aquifer on the right.

The sedimentation of the fluviatile materials of the upper layers (L1-L3) can be attributed to the Holocene (HARVEY et al., 2002; MCARTHUR et al., 2004), while the deposition time of the upper oxidized aquifer (L4) is uncertain. Its characteristic brown colour (due to the content of iron(hydr)oxides) and the sandy texture suggest that it is more likely Pleistocene sediment, which was exposed to oxidative weathering (biotite (traces in L4, oxidized sand) and other Fe-bearing minerals) during the lowering of the sea-level that occurred between 125 and 18 ka (DPHE, 1999; MCARTHUR et al., 2004). Furthermore, it might be a product of a capillary fringe or water table fluctuation (BREIT et al., 2001). A thick peat layer was found in 61 to 73 m depth within the aquiclude (L3), which contained the highest contents of total organic carbon with a maximum value of 4.9 wt% in 61 m depth (silty clay) (Figure 4.1.2.2). These layers were also observed in other studies (ANAWAR et al., 2003; MCARTHUR et al., 2004). In both aquifers TOC contents were low and reached 0.08 to 0.40 wt%. The biological degradation of organic matter in the aquicludes (e.g. peat in 61 m depth) generates organic acids, which can dissociate and contribute to the acidity in these sediments (Figure 4.1.2.2) (BRADY and WELL, 2005). GRAFE et al.(2001) investigated the competitive effect of humic and fulvic acids on the adsorption of arsenite and arsenate on goethite and found that a decrease of As sorption on goethite took place at different pH, suggesting that a variety of functional groups on fulvic and humic acids are responsible for competition with arsenic (GRAFE et al., 2001). The aquifer sediments exhibit pH values near neutral (pH 6.5 to 7). The difference in pH measured in MQ and $CaCl_2$ (MQ - $CaCl_2$) was higher in the fine-grained clayey sediments than in the sandy aquifer material. The higher pH may be due to the higher exchange capacity of the fine-grained clayey sediments, which are enriched in clay, chlorite, mica and OM. The aquifer sediments are free of calcite, which could be due to dissolution and leaching of calcite under the given hydraulic and geochemical conditions. Dissolution and leaching of calcite would be consistent with the enriched carbonate (HCO_3^-) concentrations found in these groundwaters ($\approx$ 30 mg/L). The buffer capacity of the HCO_3^- dominated waters seems to be sufficient to stabilize the sediment pH to a neutral level. As shown in other studies Bangladesh's groundwaters are near neutral in pH and often saturated or close to saturation with calcite or dolomite (KINNIBURGH and SMEDLEY, 2001). Another assumption for the lack of calcite in the aquifer sediments could be the deposition of calcite poor sediments deriving from the Brahmaputra River (KINNIBURGH and SMEDLEY, 2001; MCARTHUR et al., 2004). Calcite contents in the aquicludes exceed 1 wt% (Figure 4.1.2.2). The impermeable characteristics of these layers prevent contact and reaction with the groundwater and thus, its dissolution. Calcite can act as a sorbent for arsenic through adsorption of As at the mineral surface or co-precipitation, resulting in mineral associated arsenic concentrations of 1 to 8 µg/g (ALEXANDRATOS et al., 2007). However, the abundance of calcite in the sediments of

the recent study is low and therefore a major contribution to total arsenic contents in the sediments is assumed to be low. Clay minerals are dominant in the aquiclude layers, which mainly consist of smectite, kaolinite, chlorite, and mica as determined with XRD. Smectite, kaolinite, chlorite, and mica can act as active sorption sites for arsenic. This is consistent with the observed higher arsenic sorption capacity determined for aquiclude sediments in comparison to the coarse grained, sandy, quartz, and feldspar dominated aquifer materials (Table 4.1.1.1). Generally arsenic concentrations associated with quartz and feldspar are relatively low with 0.1 to 2.1 µg/g As (SMEDLEY and KINNIBURGH, 2002).

Extracted As and Fe concentrations (HCl and NaOH) were higher in the grey fine-grained overbank sediments of the aquicludes (clay and silt) than in the coarser aquifer sediments (dominated by sand) (Figure 4.1.3.1). The differences in the amount of initially sorbed As and Fe, in addition to the differences in the sorption capacity of the sediments may be explained by the composition of the sediments. For the reducing grey sediments in the aquiclude it can be concluded that high As concentrations are derived from present clay minerals (particularly smectite and kaolinite), mica (muscovite), chlorite, organic matter (e.g. peat), and maybe residuals of iron(hydr)oxides (BREIT et al., 2001; GOLDBERG, 2002; KINNIBURGH and SMEDLEY, 2001; MANNING and GOLDBERG, 1997). In the recent study the strong relation of clay and arsenic was confirmed by sorption and extraction experiments, where in the clayey aquiclude material (49 % clay in 61 m depth) the highest content of As was extracted in the HCl leaching and arsenic was sorbed most efficient (see also Figure 4.1.4.1 and Figure 4.1.4.4). Consequently there is a strong association between As and the fine grained aquiclude minerals, which contribute to high As sorption with their large external surface area (smectite, 80 to 150 m^2/g; kaolinite, 5 to 30 m^2/g; mica, 70 to 175 m^2/g in BRADY and WELL (2005)) (ANAWAR et al., 2003). But compared to Fe- and Al(hydr)oxides As sorption on clay minerals and OM is less due to their constant negative charge on the mineral surface. Arsenic sorption on clay minerals occurs on functional groups ($\equiv$Al-OH and $\equiv$Al-OH$_2^+$) at exposed crystal edge sites that have pH – dependent charge (JAIN et al., 1999; LIN and PULS, 2000). VIOLANTE and PIGNA (2002) estimated a maximum surface coverage of 152 mmol/kg arsenate on goethite, while arsenate sorption was comparatively low on smectite and kaolinite with 18.9 and 8.1 mmol/kg. Chlorite contributes more to As sorption because of its higher adsorption capacities for arsenite and arsenate than other clay minerals (LIN and PULS, 2000).

The high iron contents extracted from the aquiclude sediments (Figure 4.1.3.1) could be derived from solid state Fe-minerals (e.g. magnetite), the occurrence of siderite ($FeCO_3$, minor in L5), iron former incorporated in carbonates and phosphates, sorbed Fe on clay particles and organic matter,

or iron from iron(hydr)oxide dissolution. (HARVEY et al., 2002; KINNIBURGH and SMEDLEY, 2001; SWARTZ et al., 2004). In relatively immobile pools of anoxic waters iron is bound in silicates and pyretic phases (HARVEY et al., 2002). In the recent study iron(hydr)oxides were not detected with XRD. This is likely because iron(hydr)oxides are weakly detectable due to the missing crystalline structure and the minor abundance compared to other minerals, which reduces the detection limit. Leaching with hot HCl has shown low As concentrations associated with the low mineral contents in the aquifer material and the lack of possible sorption sites for As (Figure 4.1.3.3). The visually observed brown coatings on the minerals (mainly quartz) and the high amounts of extracted Fe suggest the occurrence of iron(hydr)oxides in the deeper aquifer (Table and Figure 4.1.3.1). Iron(hydr)oxide has a very high specific surface area ($\approx$ 100 to 300 m^2/g in BRADY and WELL, (2005)) which makes it a very strong sorbent for arsenic in the sediment, even in small quantities (ANAWAR et al., 2003). There is no evidence for the presence of iron(hydr)oxide in the shallow aquifer, but if iron(hydr)oxide reduction is incomplete iron(hydr)oxides might also contribute to As sorption along with clay, chlorite and mica (ANAWAR et al., 2003; MCARTHUR et al., 2004). Clay, chlorite, and mica represent only a minor fraction in the aquifer material, but might also play a role in As sorption as long as the content of iron(hydr)oxide is low, particularly in the shallow aquifer. Arsenic sorption and leaching experiments have shown that arsenic was less extracted and sorbed by the coarser aquifer material (dominated by quartz and feldspar) compared to the fine-grained sediments of the aquiclude material (Figure 4.1.4.1), indicating the lower sorption capacity of the sediment, caused by the lack of sorbents.

The simulation of the effect of AGW on sediment leaching (As, Fe, Mn, and P) has shown that only small quantities of manganese and iron were extractable, indicating that arsenic release by the groundwater is negligible (Figure 4.1.3.5). Leaching of arsenic with 0.04 M $NaHCO_3$ (influence HCO_3^-) only released very small quantities of arsenic in solution (Table 4.1.4.1), thus bicarbonate does not seem to contribute to As mobilization from the Bangladesh sediments as proposed in previous studies (ANAWAR et al., 2004; APPELO et al., 2002).

Leachings with NaOH (pH 11.1 to 12.4) solution extracted arsenic from the sediment samples very efficiently (Figure 4.1.4.1). Extracted As concentrations (0.2 to 2.1 μg/g) were close to the concentrations leached in hot HCl (0.3 to 3.8 μg/g) and emphasized that the sediments of the aquicludes contain higher As concentrations while the sandy aquifer material is low in extractable arsenic. Differences may occur because both types of leaching target various sediment compounds. For example, NaOH targets amorphous iron(hydr)oxides and organic matter, while hot HCl extracts As that is adsorbed and co-precipitated to solids and the fraction associated with poorly

crystallized and amorphous iron(hydr)oxide, Mn oxides, carbonates, and acid volatile sulphides (HARVEY et al., 2002; HORNEMAN et al., 2004; HUDSON-EDWARDS et al., 2004; VAN GEEN et al., 2004). The lower As concentrations leached with NaOH from the aquiclude sediments can be explained by the sediment compounds (e.g. clays, chlorite, and mica) which are not affected by NaOH but hot HCl. There is no explanation as to why As concentrations in NaOH solutions were higher in 26 and 81 m (aquifers). NaOH should not be a stronger extractant than hot HCl. Extractable As concentrations from Bangladesh sediments were determined in several studies, using hot HCl, other extraction methods (e.g. oxalate, cold and hot nitric acid, hydrofluoric acid), or spectroscopic methods (e.g. XRF) (AHMED et al., 2004; HARVEY et al., 2002; KINNIBURGH and SMEDLEY, 2001; SWARTZ et al., 2004; VAN GEEN et al., 2004). In most depth profiles arsenic concentration varied between 1 and 10 µg/g dependent on depth, sediment type and mineral composition. For example, VAN GEEN et al.(2004) extracted 0.6 to 1.8 µg/g from the sediments with hot HCl (comparable range) and HARVEY et al.(2002) extracted higher As concentrations in clayey soils (up to 7 µg/g) than in sandy soils (2 µg/g As) materials with hot nitric acid. Usually the fine grained clayey sediments contain higher contents arsenic than the coarser sandy material (see also KINNIBURGH and SMEDLY, 2001).

Associations: As-Fe

Dissolved As was low in groundwater from 8 m depth (< 20 µg/L), at the top of the shallow aquifer beneath a layer of brownish sand. It can be presumed that this groundwater is most likely oxic (Eh 250 mV) which limits arsenic pollution from iron(hydr)oxide reduction (Figure 4.16.1). Dug wells below 10 m depth are usually low in arsenic (RAVENSCROFT et al., 2005).

Goundwaters in both aquifers contained dissolved Fe from iron(hydr)oxide reduction, which would imply that they are anoxic. Eh-measurements have shown that the shallow aquifer is more reduced (Eh ≈ 100 mV) than the deeper aquifer (Eh ≈ 200). In the deeper aquifer maximum values of more than 60 mg/L Fe (mainly Fe(II)) occurred with lower As concentrations in the groundwater (50 to 60 µg/L) compared to the shallow aquifer with ≈ 200 µg/L As (Figure 4.1.6.1). Thus, high dissolved Fe concentrations in the deeper aquifer are associated with the brown colour of the sediment, which implicate the incomplete dissolution of iron(hydr)oxides and the release of Fe and As in the groundwater (MCARTHUR et al., 2004). The reduction of iron(hydr)oxide might be due to the biodegradation of the overlying, organic-rich Holocene sediment (peat in L3) (Figure 4.1.6.1) which releases short-chain carboxylic acids and methylated amines that will drive iron(hydr)oxide reduction (BERGMAN et al., 1999). Resorption of As to residual iron(hydr)oxides serves as a sink for As in the groundwater; this could explain lower As concentrations in the deeper aquifer.

Resorption of As may occur when the groundwater moves away from the areas where reduction is complete, to areas where it is not complete (DPHE, 1999). This process would also decouple As and Fe concentrations in the groundwater and explain the seldom good correlation between these two constituents (MCARTHUR et al., 2004; RAVENSCROFT et al., 2001; VAN GEEN et al., 2004). However, leachable As from the sediment was relatively low at 0.3 µg/g and not remarkably higher than the extracted arsenic in the reduced sediment from the shallow aquifer. This was expected due to the higher content of iron(hydr)oxides. A possible explanation for the lower arsenic concentrations in the deeper aquifer may be that the deeper aquifer has been well-flushed (oxidized weathering) and As has been mobilized, while the Holocene shallow aquifer (< 40 m and < 7 Ka age) has not been flushed (DPHE, 1999; MCARTHUR et al., 2004; RAVENSCROFT et al., 2001; SMEDLEY and KINNIBURGH, 2002).

The presence of peat in a layer of silty clay within the shallow aquifer (Figure 4.1.6.1) could also explain the higher Fe and As concentrations ($\approx$ 200 µg/L) detected in the groundwater above and below this thin layer. How far high As concentrations in the shallow aquifer are influenced by the presence of peat or OM, from external sources (e.g. human waste from the surface), cannot be concluded from this data. It seems obvious that the degradation of peat plays a dominant role in iron(hydr)oxide reduction in the deeper aquifer.

Peat is common beneath the Old Meghna Estuarine Floodplain in Comilla, and would explain the high number of polluted wells that tap their water from depths between 20 to 60 m where they most likely were screened close to existent peaty layers (AHMED et al., 2004; RAVENSCROFT et al., 2001).

Associations: As-Mn

Arsenic and manganese correlated in the solid phase what results from sorption of As on both, Fe(hydr)oxides and Mn oxides (Table 4.1.3.1 and Figure 4.1.3.2). When the iron and manganese concentrations were compared, the manganese concentrations were remarkably lower in the sediments than those of Fe by an average of 117 µg/g in the aquifers and 260 µg/g in the aquicludes (Figure 4.1.3.1). The reduction of Mn oxides is thermodynamically more favourable than it is the reduction of iron(hydr)oxide. It has been suggested that As, that is released due to the reduction of Mn oxides is resorbed to iron(hydr)oxides, rather than be released into the groundwater (MCARTHUR et al., 2004).

Moreover, Mn oxides are considered to be an important oxidizing reagent in the sediment over a wide range of pH, resulting in the oxidation of arsenite to arsenate, which would subsequently enhance As sorption by the sediment (CHEN et al., 2006; DESCHAMPS et al., 2003; MANNING, 2005; MANNING and GOLDBERG, 1997; SCOTT and MORGAN, 1995). Scott and Morgan further pointed

out that Mn oxides were more important in the oxidation of arsenite to arsenate, than for As adsorption.

Sorption experiments in the recent study have shown that the partial oxidation of arsenite to arsenate resulted in a mixture of arsenite/arsenate adsorbed to the mineral surface, what might be explained by microbial oxidation of arsenite or the contact with oxidative soil compounds such as MnO_2 (MANNING, 2005; MANNING and GOLDBERG, 1997; SCOTT and MORGAN, 1995), because the influence of atmospheric oxygen on arsenite oxidation is low. Arsenite standards exposed to homogeneous oxic solutions remain stable over a period of several months. The Bangladesh sediments contained between 52 to 476 µg/g extractable Mn, but there is no information about the oxidation state and compounds. The reaction of arsenite with MnO_2 was studied more detailed by SCOTT and MORGAN (1995). They discovered that at a pH ranging from 4 to 8.2 arsenite is depleted from the solution by forming an inner-sphere complex with MnO_2, where arsenite displaces surface-bound OH^- and H_2O via ligand substitution and bind directly to the oxidized metal ion (Figure 5.1.2). The following step includes the electron transfer from arsenite to the metal ion, the breaking of Mn-O bonds, and the addition of oxygen from water to form arsenate. Finally, the reduced metal ion (Mn (IV) $\rightarrow$ Mn (II)) and arsenate are released into solution. The depletion of arsenite and the release of arsenate occur quickly and were almost complete within 90 minutes. Arsenite oxidation by Mn oxides takes place over a wide pH range while iron oxides are capable of arsenite oxidation only under acid conditions. Because of the unknown content of MnO_2 in the Bangladesh sediments the extent to which this mechanism contributes to the oxidation of arsenite to arsenate remains undefined. But the interaction of arsenite with the sediment surface might explain the observed oxidation of arsenite to arsenate and consequently the enhanced adsorption and desorption of arsenate to and from the oxidized sand.

Adsorption of Arsenite

A ──────▶ B

Equivalent

E C

Electron Transfer

Mn²⁺

Release of Mn(II)

Release of Arsenate

D
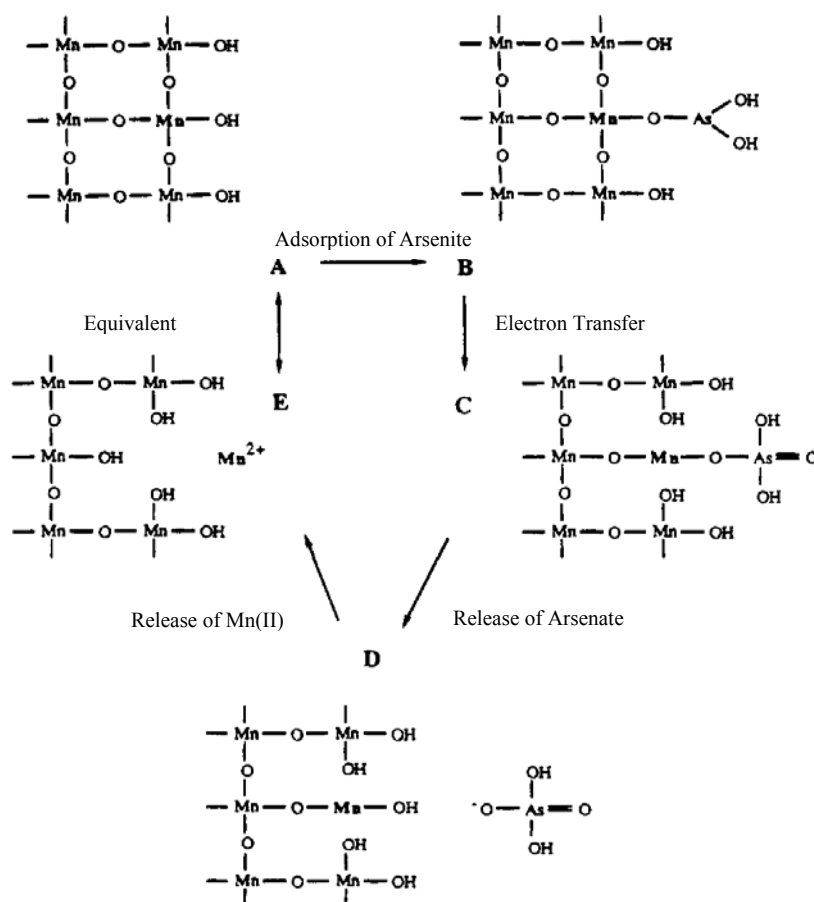
Figure 5.1.2 (A) Schematic representation of the cross section of the surface layer of a Mn (IV) oxide. (B) the resulting surface structure following arsenite adsorption, (C) electron transfer, (D) arsenate release, and (E) Mn²⁺ release (SCOTT and MORGAN, 1995).

Associations: As-P

High phosphorus concentrations were leached by aqua regia from samples near the surface (8 m depth). The elevated phosphorous concentration may indicate the extensive application of phosphate fertilizers in the surrounding area (Figure 4.1.3.4). Dissolved As and P concentrations in this depth are considered to be relatively low at < 20 µg/L As and < 500 µg/L P (Figure 4.1.6.1). Low concentration of both elements in the groundwater, but elevated concentrations of As and P in the solid phase may result from the presence of sorbents, such as clay minerals and iron(hydr)oxides, and the subsequent adsorption of both anions (MCARTHUR et al., 2001).

Moreover, ammonium concentrations in the deeper aquifer were extremely high (up to 200 mg/L) and reached around 30 mg/L in the shallow aquifer (Table 4.1.6.1) This is an indicator of the degradation of OM, which is derived from the overlying thick peat layer in L3 (Figure 4.1.6.1) (ANAWAR et al., 2003; HARVEY et al., 2002; MCARTHUR et al., 2004; RAVENSCROFT et al., 2001). The silty texture at the bottom of the aquiclude allows a greater hydraulic connectivity with the underlying aquifer and consequently makes the ingress of OM in the aquifer possible (MCARTHUR

et al., 2004). The occurrence of peat and high concentrations of ammonium also explains the high dissolved iron (dissolution iron(hydr)oxides) and phosphorous concentrations in the shallow (in 61 m > 5 mg/L P) and deeper aquifer (≈ 2 mg/L). A strong correlation between ammonium and phosphorus in well-waters was postulated by MCARTHUR et al.(2004). Phosphorous most likely derived from the microbial fermentation of buried peat deposits in the overlying clayey layers, while the derivation of P from fertilizer phosphate would not explain these high concentrations in 61 and 81 m. However, there are some explanations for the enrichment of the sediments with phosphate though it remains "every bit as much of a challenge as explaining the high arsenic concentrations" (KINNIBURGH and SMEDLEY, 2001).

5.2. Determination of the sorption capacity of different lithological units

The sorption behaviour of arsenite and arsenate on the sediment was studied in MQ, $NaHCO_3$, and NaOH (Figures 4.1.4.2 – 4.1.4.5) which showed a strong variation between the different sediments. The observed variation could be possibly due to sediment and solution composition and the resulting pH in the sediment-solution mixtures.

Different studies investigated the sorption behaviour of arsenite and arsenate on different mineral phases and examined the influence of pH (MANNING and GOLDBERG, 1997). Arsenate has its maximum sorption in the pH range of 3 to 7 on clay minerals (kaolinite, smectite, and illite) and amorphous iron oxides while arsenite sorption has its maximum at pH 7 to 8 on the same mineral phases (GOLDBERG, 2002). However, these findings do not automatically imply that more arsenite is adsorbed to the sediments than arsenate at pH 8, because arsenate adsorption was observed to be still higher on clay minerals even though it was considerable lower than at pH 6 (GOLDBERG, 2002; LIN and PULS, 2000). Further it has been reported that arsenite sorbs more strongly to sediment compounds under high pH than arsenate what explains that arsenate was less bound than arsenite to the sediments in NaOH (pH 11.1 to 12.4, Figure 4.1.4.5) (GOLDBERG, 2002; JAIN et al., 1999).

In all solutions highest As sorption was observed in the aquicludes (L3 and L5), due to their high contents of clay, chlorite, mica, and OM which are potential sorption sites for arsenite and arsenate (GOLDBERG, 2002; LIN and PULS, 2000; SMEDLEY and KINNIBURGH, 2002). Arsenite and arsenate adsorption in the aquiclude sediments has comparable rates, what might be due to the high content of phyllosilicates, showing an enhanced sorption of arsenite but still have a high affinity for arsenate at pH 8. The sediment-solution mixture with the clayey material from 61 m depth (L3) in MQ showed that a low pH (5.4), favours arsenate sorption compared to arsenite sorption on the sediment as described in former studies (GOLDBERG, 2002).

Arsenic sorption on the aquifer materials is quite different, particularly in the shallow aquifer where arsenite sorption exceeds that of arsenate (Figure 4.1.4.4). It seems that these differences are

explicable with the pH dependent sorption capability of arsenite and arsenate at pH > 8 with the higher sorption rates for arsenite under these conditions. The oxidized sand showed a slightly better adsorption for arsenate. With MQ, a high sorption of As was achieved for the oxidized sand in the deeper aquifer, possibly due to sorption of As on iron(hydr)oxides. By contrast, it seemed that arsenite sorption in $NaHCO_3$ was higher in the shallow aquifer than in the deeper one. In NaOH As sorption to the aquifer material is supposed to be lower compared to the strong sorption potential of the phyllosilicates in the aquiclude material. In 26 m depth additional As was even desorbed from the sediment in the arsenate-spiked solution (Figure 4.1.4.5). The low sorption rates in NaOH result from the capability of NaOH to remove arsenic from the sediment, particularly As which is adsorbed to iron(hydr)oxides and organic matter (see section 4.1.4). The lower sorption rates of the aquifer material compared to the aquiclude sediments are consistent with the low As fractions extractable from these sediment, indicating the lower content of sorption sites compared to the aquiclude material.

The limited sorption of arsenite and arsenate in $NaHCO_3$ compared to MQ in the deeper aquifer might be explained by the strong competition between bicarbonate and arsenic for exchangeable sites in the oxidized sediment as described in APPELO et al. (2002). Additional arsenic speciation analyses have shown a conversion of the added arsenite into arsenate in all $NaHCO_3$ and NaOH solutions, even the experiments were conducted under anoxic conditions. Possibly anoxic oxidation was induced through the presence of Mn oxides (e.g. MnO_2) (CHEN et al., 2006; SCOTT and MORGAN, 1995). But also clay minerals (kaolinit, illit) enhance the abiotic oxidation of arsenite to arsenate by heterogeneous reactions with the components on these mineral surfaces (MANNING and GOLDBERG, 1997). Furthermore, monothioarsenates were observed in the arsenite containing NaOH solution, particularly in 26 and 84 m depth, indicating that sulphur was extracted from the sediment and further formed monothioarsenate with the dissolved arsenite (Table 4.1.4.2).

The sorption capacity tests conducted with higher concentrations of arsenite, arsenate, and phosphate (0.5 to 20 mg/L), as well as with sediments from different stratigraphical units (L2, L3, L4 and L5) in MQ have shown that the saturation of free bonds at the mineral surfaces for arsenite and phosphate was not reached, while arsenate sorption reached its maximum sorption potential (Figure 4.1.5.2). Further higher sorption rates for arsenite and phosphate were observed for the sediments from the shallow aquifer. The obtained results are not consistent with the sorption behaviour of the sediment described above (As sorption in MQ, NaOH and $NaHCO_3$), where arsenite sorption exceeded arsenate sorption remarkably in the shallow aquifer and the sorption on the aquiclude material was noticeably higher than on the shallow aquifer material.

Due to the different conditions in the sediment-solution mixtures of the various batch experiments, e.g. different solutions composition (MQ, NaOH and NaHCO$_3$), different solid : liquid ratios (different loadings), and oxic/anoxic conditions, a direct comparison of the results is weak. Moreover the occurrence of iron(hydr)oxides, manganese-oxides, and minor mineral phases was below detection limit and could not be determined by XRD in this study. Thus it is uncertain to make a general conclusion about the sorption behaviour of arsenite and arsenate.

The results from the sorption capacity test with concentrations in the range of 0.5 and 20 mg/L for arsenite, arsenate, and phosphate demonstrated that the Bangladesh aquifer materials have a high sorption capacity considering the settings in the batch experiments. Under natural conditions in the groundwater these capacities might be lower, because of the influence of other factors, e.g. pH, redox potential, ionic strength, soil solution composition, on controlling As mobility.

5.3. Simulation sorption behaviour of specific anions in column experiments

Competitive sorption between arsenite/arsenate and phosphate

The competitive adsorption of arsenic (arsenite and arsenate) with phosphate was investigated on two different sediment types, the reduced sandy loam from the shallow aquifer and the oxidized sand from the deeper aquifer, at a pH of 7.8 to 8.5. The predominant arsenic species under these conditions are the zero charged H_3AsO_3 as well as the negatively charged $HAsO_4^{2-}$ and $H_2AsO_4^{-}$. Phosphate dominates as $H_2AsO_4^{-}$ (Figure 2.5.1 and 2.5.2).

The adsorption affinity of the reduced sediment for As and P was less than the adsorption affinity of the oxidized sand (Figure 4.2.1.1 and Table 4.2.1.2). Both sediments are poor in mica, chlorite OM (0.22 and 0.33 wt%) and almost free of clay. About 4.5 mg/g Fe were extracted from both sediments, but the reduced material contained a higher content of Fe (II) (dominant Fe-species at measured pH 7 and Eh ≈ 100 mV), and thus does not contribute to the sorption capacity as compared the iron(hydr)oxide visible in the oxidized material. The distribution of the soil minerals as determined with XRD, e.g. mica, clay, and OM, is similar between both sediments and thus might not be a reason for the observed differences in sorption capacity, but definitely the differences can be explained by the higher content of iron(hydr)oxides in the oxidized sand (deeper aquifer).

When comparing the sorption behaviour of the arsenic species, arsenite and arsenate, with phosphate, the results indicated that arsenite was less sorbed to both aquifer sediments than arsenate and phosphate (Figure 4.2.1.1 and Table 4.2.1.2). Although it is not obvious if the adsorption of phosphate compared to arsenate is favoured or not because the maximum sorption capacity of the anions was not reached in most experiments and further the initial concentrations of phosphate (32 µM), arsenite, and arsenate (2.6 µM) used in these experiments were different. Arsenite was almost completely exchangeable after addition of phosphate, while around 50 % phosphate was non-exchangeable in the presence of competing arsenite, indicating that phosphate is competing stronger for exchangeable sites on the solids than arsenite and that arsenite is easily replaced by phosphate. These findings have been already mentioned in other studies (MANNING and GOLDBERG, 1997; RADU et al., 2005; VIOLANTE and PIGNA, 2002; ZHAO and STANFORTH, 2001). The desorption of adsorbed As by phosphate from the arsenite treated oxidized sand revealed that the initial arsenite was dominantly adsorbed in form of arsenate (65 %) (Figure 4.2.1.2). Unfortunately, the total adsorbed concentration in this experiment is underestimated. Because of the limited adsorption of arsenite to the oxidized sediment it can be assumed that the gradual oxidation of arsenite to arsenate results in an increase of As sorption, but remained undetected.

The competition of arsenate and phosphate showed that more phosphate previously adsorbed was desorbed by arsenate than arsenate was desorbed by phosphate (40 to 50 % arsenate non-exchangeable). Apparently, the sorption of arsenate to the soil surface is stronger than that of phosphate and the access of phosphate to certain exchangeable sites is inhibited (MANNING and GOLDBERG, 1996). .

Differences between the sorption capacity of arsenite and arsenate might be explained with the mineral composition of the sediments, their available sorption sites and pH-dependence, and the different attractiveness for arsenite and arsenate (SUN and DONER, 1996). Generally, the adsorption of arsenite is assumed to be weaker than the sorption of arsenate on Fe and Al oxides (GOLDBERG, 2002). Spectroscopic observations of the adsorption mechanisms showed that both anions, arsenite and arsenate, form stable inner-sphere bidentate surface complexes on the goethite surface (GOLDBERG and JOHNSTON, 2001; MANNING, 2005). SUN and DONER (1996) postulated that some surface sites on goethite are more attractive for arsenite, while others were preferred by arsenate. Furthermore, the sorption of arsenate on clay minerals is assumed to be higher than the sorption of arsenite (GOLDBERG, 2002), while sorption experiments with arsenite and arsenate on goethite (point zero charge ≈ 7.8) have shown comparable values at pH 8 (DESCHAMPS et al., 2003; VIOLANTE and PIGNA, 2002).

Considering these findings the differences in arsenite and arsenate sorption were due to the enhanced sorption of arsenate on the soil minerals (e.g. clays) compared to arsenite. It can be assumed that arsenate formed more stable (inner-sphere-bidentate) complexes with the surface sites of these sediment compounds than arsenite, resulting in non-exchangeable arsenate fractions.

A more precise description of the adsorption behaviour of arsenite and arsenate would require a better knowledge of the sediment composition and the occurring bonding mechanism on the mineral surfaces.

Many authors investigated the similar sorption behaviour of arsenate and phosphate by sediment compounds; therefore it can be assumed that differences in the sorption behaviour between arsenite and phosphate are comparable with those of arsenite and arsenate (as described above). Both anions, arsenate, and phosphate, have similar deprotonation constants in solution, which should have similar effects on the surface charge of the solid (LIU et al., 2001; MANNING and GOLDBERG, 1996; VIOLANTE and PIGNA, 2002). Consequently, both ligands form similar types of surface-complexes (e.g. inner-sphere complexes) and compete strongly for a similar set of exchangeable sites (HIEMSTRA and VAN RIEMSDIJK, 1999). Some sites might be uniquely available for adsorption of either arsenate or phosphate (MANNING and GOLDBERG, 1996).

VIOLANTE et al. (2002) confirmed that the competition of arsenate and phosphate strongly depends on the sediment with its sorbents and the pH. They concluded that the sorption of arsenate is favoured on iron(hydr)oxides (e.g. goethite), Mn and Ti oxides, and phyllosilcates particularly rich in Fe (e.g. nontronite and ferruginous smectites). By contrast, the sorption of phosphate is more effective on minerals rich in Al (e.g. gibbsite and kaolinite). In contrast, MANNING and GOLDBERG (1996) proposed the similar affinity of arsenate and phosphate for goethite and gibbsite surfaces at neutral pH. LUMSDON et al. (1984) explained the stronger adsorption of arsenate with the larger size of the arsenate anion and that it interacts more strongly with OH groups remaining on the surface compared to phosphate. VIOLANTE and PIGNA (2002) supported these findings and confirmed that particularly Fe and Mn oxides may form stronger surface complexes with arsenate than with phosphate. Thus, the formation of stronger surface complexes of arsenate on certain sediment compounds would explain that less arsenate is exchangeable by phosphate than phosphate by arsenate.

In Figure 5.3.1 the formation of an inner-sphere complex between arsenate/phosphate and iron(hydr)oxide is depicted. In the first step a monodentate complex is formed, which shares one ligand with the iron(hydr)oxide surface. During the second step another – OH group of the iron(hydr)oxide is penetrated to form a more stable bidentate, binuclear bridging complex with two common ligands. The main surface species on goethite at pH 8 was indicated to be the bidentate surface complex $Fe_2O_2AsO_2/Fe_2O_2PO_2$. At low pH one finds the protonated bidentate species $Fe_2O_2AsOOH/Fe_2O_2AsOOH$, while at high pH the monodentate species $FeOAsO_3/FeOPO_3$ are dominant (HIEMSTRA and VAN RIEMSDIJK, 1999).
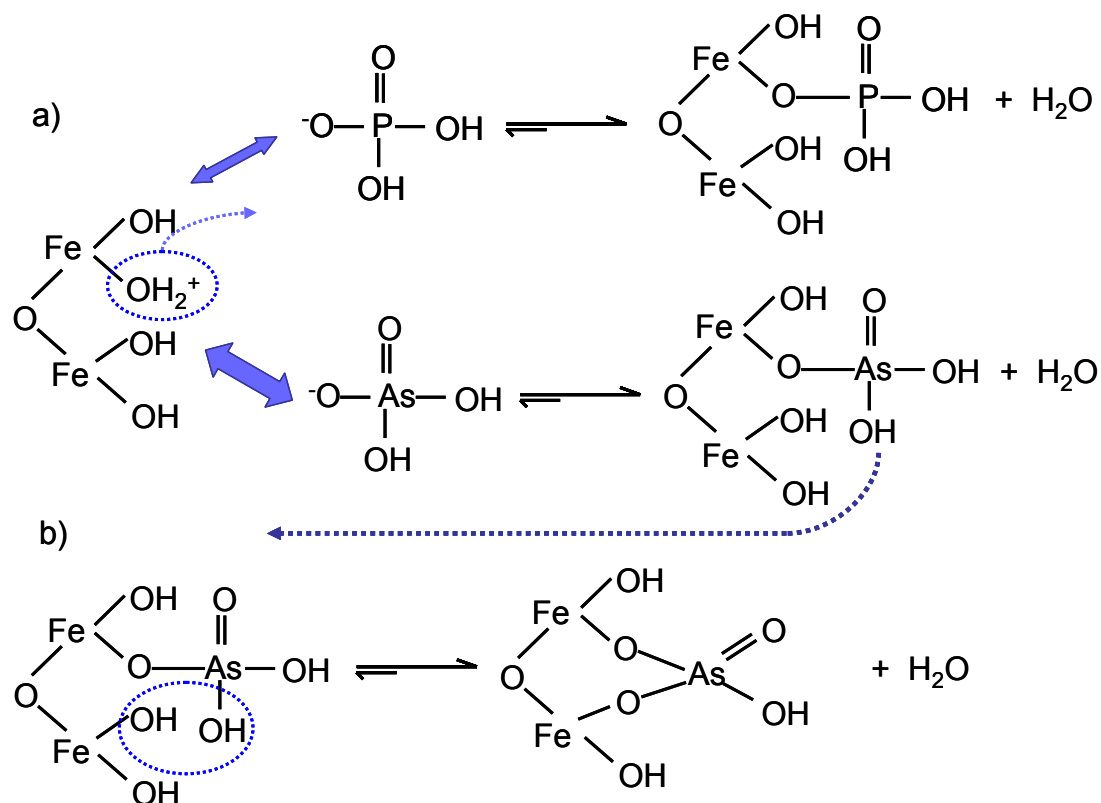
Figure 5.3.1 Formation of an inner-sphere complexes. (a) Phosphate and arsenate replace an – OH₂ or an – OH group in the surface structure of iron(hydr)oxide (monodentate surface complex). In a second step (b) the anions penetrate the mineral surface by forming a stable binuclear bridge (bidentate, binuclear bridging complex). Thereby arsenate is supposed to form stronger surface complexes (after BRADY and WELL 2005).

However, the competition between arsenate and phosphate is effective in both directions, the displacement of either arsenate by phosphate or phosphate by arsenate from exchangeable sites. Assuming, that arsenic was first adsorbed to the sediment followed by the exposure of high phosphate concentrations (e.g. anthropogenic origin) the competitive exchange between arsenic and phosphate can effectively contribute to As release into groundwater (as already suggested by RADU et al.(2005), GAO and MUCCI (2001) and ACHARRYA et al.(2000)), even if As is not completely exchanged, as demonstrated in the experiments. This process of course also depends on the initial sorbed As concentrations, AsO_4^{3-}/PO_4^{3-} molar ratio, mineral compounds, other competing anions, resident time, pH etc. (HIEMSTRA and VAN RIEMSDIJK, 1999; VIOLANTE and PIGNA, 2002). These results are in contrast to the findings of MANNING and GOLDBERG (1997), who found that 5 mg/L phosphorus would only replace approximately 2 µg/L arsenic into solution.

The observed oxidation of arsenite to arsenate in the oxidized sand (Figure 4.2.1.2, explained in section "As-Mn") can result in a stronger adsorption of arsenate to the sediment, which can consequently cause the decrease in mobility of As in the aquifers (MANNING and GOLDBERG, 1997). The oxidation of arsenite to arsenate also is important in its application in arsenic removal from drinking water. The presence of Mn oxide coated sands in filtration systems as well as the application of other oxidants, such as H_2O_2 chlorine dioxide and calcium hypochlorite, advance the oxidation process of arsenite. Fixed sand bed filters, containing adsorbents such as FeOOH or zero-valent iron fillings, can effectively remove arsenate from the drinking water (BISSEN and FRIMMEL, 2003b).

Differences in sorption behaviour arsenate and monothioarsenate

The studied adsorption behaviour of arsenate and monothioarsenates clearly demonstrated the higher mobility of monothioarsenate in the reduced and oxidized sediments, while arsenate was mainly retarded (Table 4.2.2.1 and Figure 4.2.2.1). The observed sorption behaviour disagrees with the theoretical assumptions made in STAUDER et al. (2005), that thioarsenates are less mobile compared to arsenite and arsenate, due to the formation of strong anionic arsenic complexes with a higher sorption affinity for soil minerals, e.g. pyrite and goethite. The assumptions made by STAUDER et al. (2005) can be referred to tri – and tetrathioarsenate, because of their different protonation states compared to arsenate (pK values, trithioarsenate pK 3 = 10.8, tetrathioarsenate pK 3 = 5.2). Arsenate, monothioarsenate and dithioarsenate have comparable pK values (monothioarsenate pK 1 = 3.3, pK 2 = 7.2, pK 3 = 11; dithioarsenate pK 1 = 2.4, pK 2 = 7.1, pK3 = 10.9), thus the strength of the anionic complexes is similar and would not explain the better sorption of either arsenate or mono -/dithioarsenate. It is likely that a weaker bonding mechanism, as also observed for arsenite, caused the enhanced mobility of monothioarsenate compared to arsenate. The mobility of monothioarsenate would subsequently also increase arsenic mobility in sulphidic waters, where thioarsenates species play a more important role.

5.4. Influence of carbonate on arsenic sorption and release from different mineral phases

Sorption arsenite and arsenate on pyrite (FeS₂)

The adsorption of arsenite and arsenate on pyrite revealed that arsenate sorption seemed to be almost independent on NaOH and NaHCO₃ concentrations (Figure 4.3.1). Previous investigations in the recent study have already shown that NaOH prevented arsenic sorption to the mineral surfaces what would explain that only 27 to 37 % arsenate was adsorbed in NaOH (pH 11.3 to 12.3). In contrast 69 to 75 % were adsorbed in NaHCO₃ (pH 8.6 to 8.8). Apparently arsenate adsorption remained unaffected by the NaHCO₃ concentration (ionic strength) of the solution. An assumption to explain the limited sorption of arsenate compared to arsenite would be that arsenate first has to be reduced to arsenite, before it is adsorbed to the mineral surface (e.g. through forming As(III)-surface complexes).

The observed adsorption of arsenite in NaOH was quite different from that of arsenate. The decrease of arsenite sorption with increasing NaOH (0.01 to 0.1 M) concentrations was remarkable in these solutions (69, 44 and 0 % As adsorbed). In addition, the formation of arsenate and monothioarsenate (minor) was observed. In 0.01, 0.04 M NaOH and 0.04, 0.1 M NaHCO₃ more arsenite was adsorbed compared to the sorption rates of arsenate. Again there was almost no influence observed for the ionic strength-dependence of NaHCO₃ on As sorption. The better sorption of arsenite might result from the direct sorption to the mineral surface. The presence of arsenate in the solution can result from the oxidation of arsenite to arsenate in the presence of sulphur intermediates (FLOROIU et al., 2004) or the stepwise ligand exchange of SH – by OH – groups and the consequently transformation of monothioarsenate into arsenate (PLANER-FRIEDRICH et al., 2007). That 100 % of the initial As concentration was recovered in 0.1 M NaOH in form of different As species further suggests the partial dissolution of FeS₂ in NaOH at high pH and the release of sulphide (H₂S/HS⁻) into solution. Following, sulphur may react with arsenite in the solution and form monothioarsenate, which subsequently undergoes the transformation via ligand exchange into arsenate (STAUDER et al., 2005). This process would also explain the lower concentrations monothioarsenate compared to arsenate in the arsenite containing NaOH solutions.

There are not many studies describing the adsorption of arsenate and arsenite on pyrite. A previous work of BOSTICK and FENDORF (2002) investigated the sorption of arsenite on two sulphide minerals (trollite (FeS) and FeS₂) at different pH. Using spectral analyses they proposed that arsenite sorption results in the formation of stable FeAsS-like surface precipitates, where arsenite is

reduced and the surface-bound Fe(II) and (di-)sulphide oxidized to Fe(III)(hydr)oxide ($Fe(OH)_3$) and polysulphides, such as iron tetrasulphide (FeS_4). The reaction of arsenite with FeS_2 and the formation of longer chain polysulphides can be described as follows:

$$7\ FeS_2 + 2\ As(OH)_3 \leftrightarrow 3\ FeS_4 + 2\ FeAsS + 2\ Fe(OH)_3 \qquad (3)$$
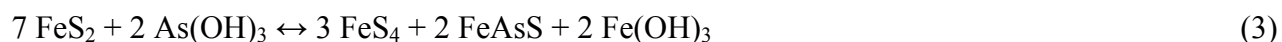
Simultaneously to this reaction, small concentrations of iron and sulphate are released into solution (BOSTICK and FENDORF, 2003). Species analyses were not investigated by BOSTICK and FENDORF (2002) to observe the formation of other As species than arsenite in solution.

BOSTICK and FENDORF (2002) also investigated that arsenite had its minimal sorption at low pH, while at high pH arsenite was almost completely adsorbed. The results of the recent study showed the opposite sorption behaviour for arsenic on FeS_2, with a minimal sorption at high pH in NaOH (except arsenite in 0.01 M NaOH) and highest sorption in $NaHCO_3$ at pH around 8. It was not possible to explain the great difference of arsenite sorption on FeS_2 in NaOH within the concentration range from 0.01 to 0.1 M (pH 11.3 to 12.3). The inconsistence of the recent findings with the previous study of BOSTICK and FENDORF (2003) and the finding that occurring processes of As sorption on FeS_2 remained unclear recommends further investigations on arsenic sorption on FeS_2 under different pH and in different solutions.

For both arsenic species, arsenite and arsenate, high sorption rates were observed in $NaHCO_3$ at pH 8 to 9, suggesting that FeS_2 may contribute to As retention in anoxic environments through adsorption of As on the mineral surface and the likely formation of As(III)-surface complexes and FeAsS precipitates.

Dissolution of orpiment (As_2S_3)

As_2S_3 dissolution in the pH range of 6 to 11 in MQ resulted in a drop of the pH (1 to 3 units), This drop in pH can be attributed to the dissolution process and the production of H^+ (Figure 4.3.3.1).

$$As_2S_3 + 6H_2O = 2H_3AsO_3 + 3HS^- + 3H^+ \qquad (4)$$

The $NaHCO_3$ solution (CO_3^{2-} and HCO_3^-) acts as a buffer solution and resists the change in hydronium ions, whereas the MQ solution is very vulnerable to slight shifts in H^+ concentration.

In both solutions dissolved arsenic was low at pH 3 to 7 (see also Figures 4.3.3.2 – 4.3.3.4). At pH 9, an increase in As_2S_3 dissolution was observed in $NaHCO_3$, which became more important with

the further increase in pH (pH > 10). The increase in the pH indicated an increase in the solubility of As_2S_3 under alkaline conditions. These observations are in agreement with previous reports (FLOROIU et al., 2004; STAUDER et al., 2005; WEBSTER, 1990; WILKIN et al., 2003). Further As_2S_3 dissolution was found to be dependent on time (pH > 9) as demonstrated in Figure 4.3.3.4, where a maximum increase of 250 mg/g dissolved As was observed at pH 10 (day 2 to 35).

The enhanced As_2S_3 solubility under alkaline conditions might be explained by the weakening of the interstitial bonds of the chain-layered structure (S-As-S-As-S) through surface complexation of arsenic with hydroxide ions under alkaline conditions, and with the resulting charge on the surfaces. This process promotes the dissolution of arsenic species from As_2S_3 and is proportional to the activity of the hydroxylated surface species (FLOROIU et al., 2004). Solubility constants for the dissolution of amorphous As_2S_3 and the formation of As species are documented by WILKIN and WALLSCHLÄGER (2003), even though they determined the formation of thioarsenite species, while with our recent equipment thioarsenates were determined as species formed due to As_2S_3 dissolution.

Arsenite was the predominant dissolved arsenic species in both solutions, MQ and $NaHCO_3$. Trithioarsenate was the second most abundant As species, which was detected in the solutions with a pH that ranged from 7 to 12. Particularly in $NaHCO_3$ at pH 9 an increase of trithioarsenate (29 % to 47 %) was observed with increasing time during the 15 days reaction time, while the contents of dissolved arsenite decreased (69 % to 48 %) (Figure 4.3.3.7). Thus the formation of trithioarsenate is time dependent, increased with increasing total dissolved As and resulted from the transformation of arsenite into trithioarsenate. Tetrathioarsenate was only observed at high pH values (pH > 10) because of its small stability range of 10 to 13 (PLANER-FRIEDRICH et al., 2007). In contrast to tetrathioarsenate monothioarsenate is stable over a wide pH-range, as well under acidic conditions (pH 2.5) as also under alkaline conditions (pH 9) (PLANER-FRIEDRICH et al., 2007). But the formation of mono- and dithioarsenate was just observed in small quantities at high pH values (pH > 9).

The distribution of thioarsenates species varied and was observed to be dependent on hydrochemical parameters, including pH, dissolved sulphide concentrations and S/As ratios (1:1, 1:2, 1:3 and 1:4), and redox potential in the solutions. WILKIN et al. (2003) postulated that thioarsenates become dominant when sulphide concentrations are greater than about 0.1 to 1 mM. Apparently, the formation of trithioarsenate over a wide range pH is favoured due to high S/As ratios in solution.

The presence of arsenate at high pH might be attributed to the formation of sulphur intermediates, which can promote arsenite oxidation to arsenate (FLOROIU et al., 2004). Another reaction describes a stepwise ligand exchange of SH – by OH – groups and the consequently transformation of thioarsenates into arsenate (PLANER-FRIEDRICH et al., 2007). There was a disagreement between the experimental total dissolved As concentration and the modeled value calculated with PhreeqC, particularly at high pH (Figure 4.3.3.8). Approximately half of the expected dissolved As concentration was detected in NaHCO$_3$ over the entire time period and in MQ after the eight day. One explanation for the observed low dissolved arsenic concentration might be the formation of zero-valent arsenic from the reaction of arsenite with sulphide as proposed by STAUDER et al. (2005), suggesting that thioarsenates are formed by a disproportion reaction. Equal parts of arsenite are thereby oxidized to monothioarsenate with arsenic in the As(V) oxidation state and reduced to elemental As(0). The reduction of As(V) to elemental As(0) caused the loss of 50 % As, because As(0) remains undetected during As speciation with IC-ICP-MS (STAUDER et al., 2005). The study by WALLSCHLÄGER and STADEY (2007) rejected the hypothesis of disproportion, because they observed quantitative recovery of the starting arsenite concentration in form of soluble As species. Furthermore, the formation of other positive charged complexes or colloidal structures would cause an underestimation of total dissolved arsenic, because they are not detectable with the recent method.

Influence of bicarbonate on arsenic release from arsenic trioxide (As$_2$O$_3$) and orpiment (As$_2$S$_3$)

The influence of bicarbonate ions on arsenic mobilization was studied on As$_2$O$_3$ and As$_2$S$_3$ dissolution under anoxic conditions. Moreover, arsenic speciation provided information about the formation of inorganic As species as arsenite, arsenate and thioarsenates.

The dissolution of As$_2$O$_3$ in 0.01, 0.04, and 0.1 M NaHCO$_3$ seemed to be independent on HCO$_3^-$ concentration, because all solutions contained around 220 to 230 mg/g dissolved arsenite (Figure 4.3.2.1). Experiments on As$_2$O$_3$ dissolution investigated by NEUBERGER and HELZ (2005), have also shown only slight differences in arsenite solubility with increasing HCO$_3^-$ concentration (0.35 and 0.72 M NaHCO$_3$), but a distinctly greater solubility than was observed in the solutions containing no HCO$_3^-$. They explained the enhanced solubility of As$_2$O$_3$ in NaHCO$_3$ with the formation of a single As(III)-carbonate complex (NEUBERGER and HELZ, 2005).

In contrast, As$_2$S$_3$ dissolution showed an increase in dissolved As with increasing HCO$_3^-$ concentrations, indicating that bicarbonate contributes to arsenic mobilization from As$_2$S$_3$ (Figure 4.3.2.2 and Figure 5.4.1). The comparison of As$_2$S$_3$ dissolution in MQ and 0.04 M NaHCO$_3$ as depicted in Figure 4.3.3.5, showed that in both solutions As$_2$S$_3$ dissolution is time dependent. After

a short equilibration time (2/3 days) more arsenic was released in $NaHCO_3$ up to pH 11, what might result from the promotion of As_2S_3 dissolution by HCO_3^- and the associated complex formation. Also an increase of the ionic strength can influence the dissolution behaviour of As_2S_3. A higher As_2S_3 dissolution was observed in MQ at pH 7 to 9 after 36 days.

Several studies proposed that the formation of As(III)-carbonate complexes leads to the enhanced arsenic release from mineral phases (HAN et al., 2007; KIM et al., 2000; NEUBERGER and HELZ, 2005; TOSSELL, 2005). KIM et al.(2000) suggested the formation of 3 stable arseno-complexes to be responsible for effective arsenic leaching from arsenic sulphide minerals, such as orpiment (As_2S_3). NEUBERGER and HELZ (2005) confirmed this hypothesis by measuring the solubility of As_2O_3 in concentrated carbonate solutions but attributed the enhanced arsenic solubility to the formation of only a single As(III)-carbonate complex, that has modest stability in water ($As(OH)_2CO_3^-$). They concluded that the complexes proposed by KIM et al.(2000) would be too unstable relative to $As(OH)_3^0$ (TOSSELL, 2005). They further confirmed that the effect of the carbonate complex on As solubility is low and only observable at high concentrations of HCO_3^- (> 0.4 M), hence carbonate concentrations found in Bangladesh's groundwaters are too low for the formation of As(III) carbonate-complexes. Speciation analyses from As_2O_3 and As_2S_3 dissolution in $NaHCO_3$ in the recent study only showed the formation of the As species, arsenite, arsenate, and thioarsenates, as depicted for As_2S_3 dissolution in 0.01 and 0.1 M $NaHCO_3$ in Figure 5.4.1, thus another mechanism might promote As_2S_3 dissolution in $NaHCO_3$. ACHARYYA (2005) and APPELO (2002) found that the formation of carbonate-complexes on the surface of Fe- and Mn-(hydr)oxides decreased the binding capacity of the surface sites resulting in the substitution of adsorbed As by bicarbonate (ACHARYYA, 2005; APPELO et al., 2002). There is the possibility that a similar mechanism works on the surface sites of As_2S_3, weakening the interstitial bonds of the structure through surface complexes and thereby promoting As_2S_3 dissolution, and thus the release of arsenic in the solution. The effect of bicarbonate in a concentration range of 0.01 to 0.1 M seemed thereby to be stronger on As-S bonds in As_2S_3 than on As-O bonds in As_2O_3 (compare also with Figures 4.3.2.1 and 4.3.2.2).
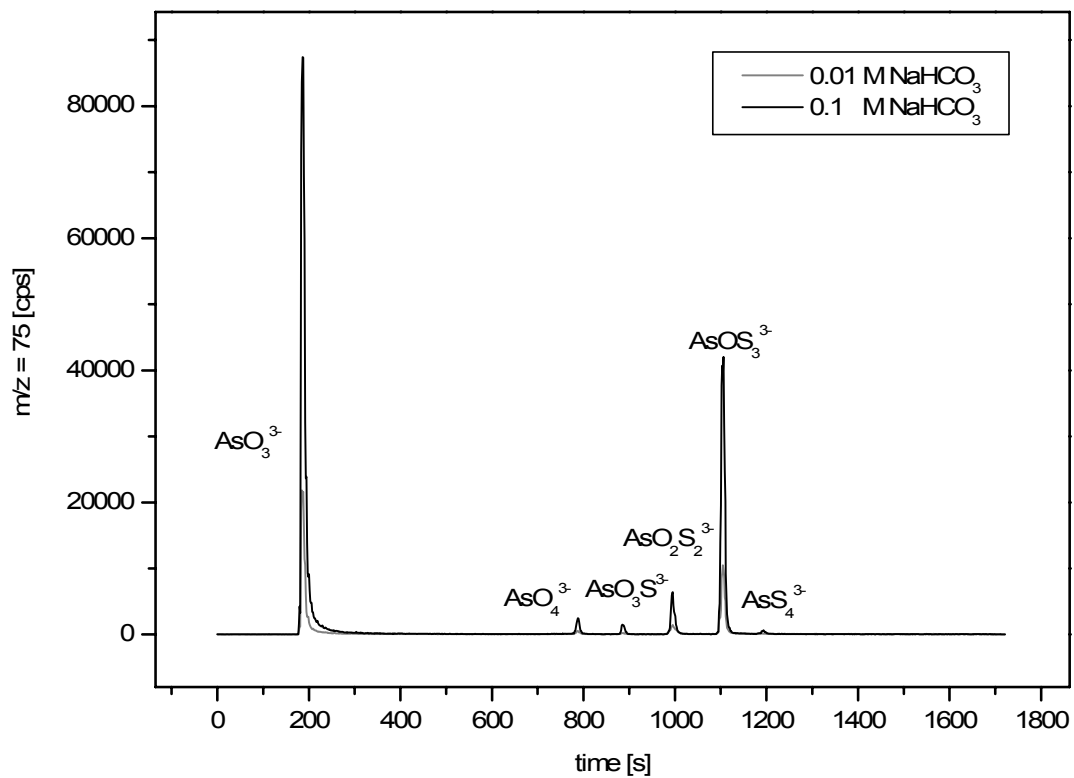
Figure 5.4.1 Chromatogram of As₂S₃ dissolution in 0.01 and 0.1 M NaHCO₃

6. Problems encountered and recommendations

Inhomogeneities of the sediment used for different leaching and sorption experiments can cause variations in the results, as noticeable in the StDev for HCl-extractable As and P concentrations in Table 4.1.3.1. To improve the homogeneity of the sediment, it must be uniformly crushed, particularly the clogged, claylike, and hard sediment compounds (as in this study); additionally, portioning must occur randomly (e.g. by sample splitter). For most batch experiments, no replicates were prepared and measured, due to the high quantity of samples. Consequently, in some cases, doubts arose as to the accuracy of the values (e.g. dissolved As after spike arsenate in MQ appeared too high in 12 m depth, Figure 4.1.4.2). To avoid this problem, it is better to at least determine duplicates. Furthermore, the reaction conditions (equilibration time, liquid : solid ratio, concentration range) within the different sorption experiments were not consistent, preventing a final comparison of the results. Sorption experiments investigated with the "first column setup" have shown that the quantity of the used sediment was magnitudes too high for the observed sorption capacity of the sediment. Again, the properties of the sediments according to their sorption behaviour had to be studied in advance to avoid this problem. A problem during the "small column" experiments was the difficulty in maintaining a stable flow rate (variations of 0.1 to 0.2 ml/min), due to practical constraints. As already reported by KIM et al. (2005), kinetic factors as well as thermodynamic parameters can effect the adsorption of anions, such as arsenate and phosphate, to the sediment surface as well as the competition between them. A longer residence time would cause a longer anion-mineral phase contact time, allowing more arsenate/phosphate to be adsorbed (KIM et al., 2000). With 1.4 to $2.8 \cdot 10^{-3}$ m/s the flow rate most likely exceeded the naturally occurring pore water velocities in the aquifers. Furthermore, most of the experiments were stopped before reaching equilibration between sediment and As/P-containing solution, resulting in the underestimation of adsorbed and exchanged concentrations. Sorption and desorption proceeded quickly in the beginning (where sufficient samples were taken), but turned out to be a slow and long-lasting process. The effect of As_2S_3 dissolution on pH-shift in MQ caused great problems in the pH adjustment of the samples. Finally, the drop in pH made the comparability with the $NaHCO_3$ solutions impossible (lack of pH values in the range of 8 to 11).

According to the obtained results, I would propose the following ideas for further research:

Depth profile – mineralogy:

- The calculation of correlations between As, Fe, and P (sediment) with As, Fe, and P (groundwater) to obtain more information about interactions between sediment surface and groundwater in the depth profile.

- Involving additional hydrogeochemical parameters of the groundwater, such as dissolved organic matter (DOM) and arsenic species (arsenite/arsenate), in the recent findings, which might provide a better understanding for the ongoing geochemical processes.

- More detailed mineralogical identification by combining XRD, X-ray fluorescence analyses (XRF), and scanning electron microscopy with energy dispersive X-ray analysis (SEM-EDX), especially separate XRD analyses for the finer sediment fractions to determine also minor mineral phases.

- Investigations on solid phases to determine oxidation state and sorption structure of arsenic species bound to mineral surfaces with X-Ray Absorption Spectroscopy (XAS), e.g. also investigations and sorption experiments for chlorite and mica as major minerals in our sediment samples, and identification of iron coatings, and their interactions with arsenic; compared analyses of liquid phase to identify complexes in solution and for clarification of their structure and coordination.

- Radiocarbon dating. Measuring carbon isotopes of groundwater and peat fragments nearby to get an idea as to the age of the stratigraphical units (e.g. to explain the occurrence of oxidized aquifer material in "shallow" depths).

Batch experiments:

- Study the competition of As with competing anions, such as carbonate and phosphate, in a wider range of AsO_4^{3-}/PO_4^{3-} and AsO_4^{3-}/HCO_3^{-} molar ratios.

- Determine the influence of varying concentrations of bicarbonate on As sorption and release (e.g. on Bangladesh sediments, As_2S_3, As_2O_3), starting with low concentrations (≈ 2 mM) (to enable comparisons with naturally occurring concentrations, e.g. ≈ 2.5 mM in Bangladesh's aquifer) up to approximately 0.7 M (e.g. the effect of HCO_3^{-} on As_2O_3 solubility was only observed at high concentrations by NEUBERGER and HELZ (2005)).

- Observations as to whether the influence of $NaHCO_3$ on As sorption and release derives from HCO_3^{-} or if the ionic strength of the solution also plays a role, e.g. observe As

sorption/release in another solution (e.g. NaCl) with the same ionic strength, but which does not interact – or only marginally interacts – with arsenic.

▪ Avoiding the shift in pH by pH regulation via autotitrator and the use of a pH buffer (e.g. $KH_2PO_4 + Na_2HPO_4$), respectively.

▪ More detailed studies on arsenite and arsenate sorption on FeS_2 and the influence of pH on As sorption, as the results represented in this study were inconsistent with previous findings.

▪ Using equal solid : liquid ratios within one set of experiments for comparison of the results.

▪ Investigation of As sorption on chlorite and OM (an aspect which has not been investigated very deeply so far).

Column experiments:

▪ First determination of sorption isotherms for specific anions on the sediment before conducting other, more complex sorption experiments, such as column experiments.

▪ A better simulation of natural groundwater conditions in column experiments, e.g. through avoiding preferential flow and turbulences in the column, achieving comparable bulk densities and permeabilities of the sediment as they occur in the aquifers and increasing residence time of the solution in the column (lowering flow rate or use of more sediment).

▪ Continuous sampling and analyses until the attainment of equilibration, so as to avoid uncertainties.

▪ After the sequential addition of the anions to the solution, the adsorption behaviour could be also observed after adding both competing anions (AsO_4^{3-}, PO_4^{3-}) together (also using different molar ratios) to see which anion is adsorbed preferably to the mineral surface when both anions are present.

▪ Additional simulation of the effect of pH (pH 6 to 9).

▪ Further observations on mobility of thioarsenates using specific (synthesized) minerals (e.g. different clay minerals and goethite) and the investigation of occurring bonding mechanisms (e.g. XAS, as already investigated for arsenite and arsenate on different mineral surfaces and varying pH).

7. References

Acharyya S. K. (2005) Arsenic levels in groundwater from quaternary alluvium in the Ganga Plain and the Bengal Basin, Indian subcontinent: Insights into influence of stratigraphy. *Gondwana Research* **8**(1), 55-66.

Acharyya S. K., Lahiri S., Raymahashay B. C., and Bhowmik A. (2000) Arsenic toxicity of groundwater in parts of the Bengal basin in India and Bangladesh: the role of Quaternary stratigraphy and Holocene sea-level fluctuation. *Environmental Geology* **39**(10), 1127-1137.

Acharyya S. K. and Shah B. A. (2004) Genesis of pandemic arsenic pollution affecting Bengal Basin. *National Academy Science Letters-India* **27**(5-6), 215-219.

Ahmed K. M., Bhattacharya P., Hasan M. A., Akhter S. H., Alam S. M. M., Bhuyian M. A. H., Imam M. B., Khan A. A., and Sracek O. (2004) Arsenic enrichment in groundwater of the alluvial aquifers in Bangladesh: an overview. *Applied Geochemistry* **19**(2), 181-200.

Akai J., Izumi K., Fukuhara H., Masuda H., Nakano S., Yoshimura T., Ohfuji H., Anawar H. M., and Akai K. (2004) Mineralogical and geomicrobiological investigations on groundwater arsenic enrichment in Bangladesh. *Applied Geochemistry* **19**(2), 215-230.

Akter K. and Naidu R. (2006) Arsenic speciation in the environment (ed. B. Salbu and E. Steinnes). CSIRO Publishing.

Alam M. (1989) Geology and Depositional History of Cenozoic Sediments of the Bengal Basin of Bangladesh. *Palaeogeography Palaeoclimatology Palaeoecology* **69**(1-2), 125-139.

Alam M., Alam M. M., Curray J. R., Chowdhury A. L. R., and Gani M. R. (2003) An overview of the sedimentary geology of the Bengal Basin in relation to the regional tectonic framework and basin-fill history. *Sedimentary Geology* **155**(3-4), 179-208.

Alexandratos V. G., Elzinga E. J., and Reeder R. J. (2007) Arsenate uptake by calcite: Macroscopic and spectroscopic characterization of adsorption and incorporation mechanisms. *Geochimica Et Cosmochimica Acta* **71**(17), 4172-4187.

Anawar H. M., Akai J., Komaki K., Terao H., Yoshioka T., Ishizuka T., Safiullah S., and Kato K. (2003) Geochemical occurrence of arsenic in groundwater of Bangladesh: sources and mobilization processes. *Journal of Geochemical Exploration* **77**(2-3), 109-131.

Anawar H. M., Akai J., and Sakugawa H. (2004) Mobilization of arsenic from subsurface sediments by effect of bicarbonate ions in groundwater. *Chemosphere* **54**(6), 753-762.

Anderson M. A., Ferguson J. F., and Gavis J. (1976) Arsenate adsorption on amorphous aluminum hydroxide. *Journal of Colloid and Interface Science* **54**(3), 391-399.

Appelo C. A. J., Van der Weiden M. J. J., Tournassat C., and Charlet L. (2002) Surface complexation of ferrous iron and carbonate on ferrihydrite and the mobilization of arsenic. *Environmental Science and Technology* **36**(14), 3096-3103.

Bergman I., Lundberg P., and Nilsson M. (1999) Microbial carbon mineralisation in an acid surface peat: effects of environmental factors in laboratory incubations. *Soil Biology & Biochemistry* **31**(13), 1867-1877.

Bissen M. and Frimmel F. H. (2003a) Arsenic - a Review. Part I: Occurrence, Toxicity, Speciation, Mobility. *Acta hydrochimica et hydrobiologica* **31**(1), 9-18.

Bissen M. and Frimmel F. H. (2003b) Arsenic - a Review. Part II: Oxidation of Arsenic and its Removal in Water Treatment. *Acta hydrochimica et hydrobiologica* **31**(2), 97-107.

Bostick B. C. and Fendorf S. (2003) Arsenite sorption on troilite (FeS) and pyrite (FeS2). *Geochimica et Cosmochimica Acta* **67**(5), 909-921.

Brady N. C. and Well R. R. (2005) *The nature and properties of soils*. Delhi, Pearson Education.

Breit G. N., Whitney J., Foster A., Welch A. H., Yount J., Sanzolone R., Islam M. K., Islam M. S., Islam M. M., Sutton S., and Newville M. (2001) Preliminary Evaluation of Arsenic Cycling in the Sediments of Bangladesh. *USGS Report*, 4.

Chen Z., Kim K. W., Zhu Y. G., McLaren R., Liu F., and He J. Z. (2006) Adsorption (As-III,As-V) and oxidation (As-III) of arsenic by pedogenic Fe-Mn nodules. *Geoderma* **136**(3-4), 566-572.

Deschamps E., Ciminelli V. S. T., Weidler P. G., and Ramos A. Y. (2003) Arsenic sorption onto soils enriched in Mn and Fe minerals. *Clays and Clay Minerals* **51**(2), 197-204.

DPHE. (1999) Groundwater studies for arsenic contamination in Bangladesh. Final Report. Rapid Investigation Phase. Department of Puplic Health Engineering, Government of Bangladesh. Mott MacDonald.

Floroiu R. M., Davis A. P., and Torrents A. (2004) Kinetics and mechanism of As2S3(am) dissolution under N-2. *Environmental Science and Technology* **38**(4), 1031-1037.

Gao Y. and Mucci A. (2001) Acid base reactions, phosphate and arsenate complexation, and their competitive adsorption at the surface of goethite in 0.7 M NaCl solution. *Geochimica Et Cosmochimica Acta* **65**(14), 2361-2378.

Gault A. G., Jana J., Chakraborty S., Mukherjee P., Sarkar M., Nath B., Polya D. A., and Chatterjee D. (2005) Preservation strategies for inorganic arsenic species in high iron, low-Eh groundwater from West Bengal, India. *Analytical and Bioanalytical Chemistry* **381**(2), 347-353.

Gaus I., Kinniburgh D. G., Talbot J. C., and Webster R. (2003) Geostatistical analysis of arsenic concentration in groundwater in Bangladesh using disjunctive kriging. *Environmental Geology* **44**(8), 939-948.

Goldberg S. (2002) Competitive adsorption of arsenate and arsenite on oxides and clay minerals. *Soil Science Society of America Journal* **66**(2), 413-421.

Goldberg S. and Johnston C. T. (2001) Mechanisms of Arsenic Adsorption on Amorphous Oxides Evaluated Using Macroscopic Measurements, Vibrational Spectroscopy, and Surface Complexation Modeling. *Journal of Colloid and Interface Science* **234**(1), 204-216.

Grafe M., Eick M. J., and Grossl P. R. (2001) Adsorption of Arsenate (V) and Arsenite (III) on Goethite in the Presence and Absence of Dissolved Organic Carbon. *Soil Sci Soc Am J* **65**(6), 1680-1687.

Han M. J., Hao J. M., Christodoulatos C., Korfiatis G. P., Wan L. J., and Meng X. G. (2007) Direct evidence of arsenic(III)-carbonate complexes obtained using electrochemical scanning tunneling microscopy. *Analytical Chemistry* **79**(10), 3615-3622.

Harvey C., Swartz C., Badruzzaman A., Keon-Blute N., Yu W., Ali M., Jay J., Beckie R., Niedan V., Brabander D., Oates P., Ashfaque K., Islam S., Hemond H., and Ahmed M. (2002) Arsenic Mobility and Groundwater Extraction in Bangladesh. *Science* **298**(5598), 1602.

Hiemstra T. and Van Riemsdijk W. H. (1999) Surface structural ion adsorption modeling of competitive binding of oxyanions by metal (hydr)oxides. *Journal of Colloid and Interface Science* **210**(1), 182-193.

Horneman A., Van Geen A., Kent D. V., Mathe P. E., Zheng Y., Dhar R. K., O'Connell S., Hoque M. A., Aziz Z., Shamsudduha M., Seddique A. A., and Ahmed K. M. (2004) Decoupling of As and Fe release to Bangladesh groundwater under reducing conditions. Part 1: Evidence from sediment profiles. *Geochimica Et Cosmochimica Acta* **68**(17), 3459-3473.

Hudson-Edwards K. A., Houghton S. L., and Osborn A. (2004) Extraction and analysis of arsenic in soils and sediments. *Trac-Trends in Analytical Chemistry* **23**(10-11), 745-752.

Jain A., Raven K. P., and Loeppert R. H. (1999) Arsenite and arsenate adsorption on ferrihydrite: Surface charge reduction and net OH- release stoichiometry. *Environmental Science & Technology* **33**(8), 1179-1184.

Kim M.-J., Nriagu J., and Haack S. (2000) Carbonate ions and arsenic dissolution by groundwater. *Environmental Science and Technology* **34**(15), 3094-3100.

Kinniburgh D. G. and Smedley P. L. (2001) Arsenic contamination of groundwater in Bangladesh. British Geological Survey & Department of Public Health Engineering.

Kopp G. (2005) MLS Application E708 – according to DIN EN 13346, Vol. E 708, pp. 1. MLS GmbH.

Lin Z. and Puls R. W. (2000) Adsorption, desorption and oxidation of arsenic affected by clay minerals and aging process. *Environmental Geology* **39**(7), 753-759.

Liu F., De Cristofaro A., and Violante A. (2001) Effect of pH, phosphate and oxalate on the adsorption/desorption of arsenate on/from goethite. *Soil Science* **166**(3), 197-208.

Luxton T. P., Tadanier C. J., and Eick M. J. (2006) Mobilization of arsenite by competitive interaction with silicic acid. *Soil Science Society of America Journal* **70**(1), 204-214.

Manning B. (2005) Arsenic Speciation in As(III)- and As(V)-Treated Soil Using XANES Spectroscopy. *Microchimica Acta* **151**(3), 181-188.

Manning B. A. and Goldberg S. (1996) Modeling competitive adsorption of arsenate with phosphate and molybdate on oxide minerals. *Soil Science Society of America Journal* **60**(1), 121-131.

Manning B. A. and Goldberg S. (1997) Adsorption and stability of arsenic(III) at the clay mineral-water interface. *Environmental Science & Technology* **31**(7), 2005-2011.

McArthur J. M., Banerjee D. M., Hudson-Edwards K. A., Mishra R., Purohit R., Ravenscroft P., Cronin A., Howarth R. J., Chatterjee A., Talukder T., Lowry D., Houghton S., and Chadha D. K. (2004) Natural organic matter in sedimentary basins and its relation to arsenic in anoxic ground water: the example of West Bengal and its worldwide implications. *Applied Geochemistry* **19**(8), 1255-1293.

McArthur J. M., Ravenscroft P., Safiulla S., and Thirlwall M. F. (2001) Arsenic in groundwater: Testing pollution mechanisms for sedimentary aquifers in Bangladesh. *Water Resources Research* **37**(1), 109-117.

Meng X. G., Bang S., and Korfiatis G. P. (2000) Effects of silicate, sulfate, and carbonate on arsenic removal by ferric chloride. *Water Research* **34**(4), 1255-1261.

Mueller G. and Gastner M. (1971) The "Karbonat-Bombe", a simple device for the determination of the carbonate content in sediments, soils, and other materials. *Neues Jahrb. Mineral. Monatsh.* **10**, 466-469.

Neuberger C. S. and Helz G. R. (2005) Arsenic(III) carbonate complexing. *Applied Geochemistry* **20**(6), 1218-1225.

Nickson R., McArthur J., Burgess W., Ahmed K. M., Ravenscroft P., and Rahman M. (1998) Arsenic poisoning of Bangladesh groundwater. *Nature* **395**(6700), 338-338.

Nickson R. T., McArthur J. M., Ravenscroft P., Burgess W. G., and Ahmed K. M. (2000) Mechanism of arsenic release to groundwater, Bangladesh and West Bengal. *Applied Geochemistry* **15**(4), 403-413.

Planer-Friedrich B., London J., McCleskey R. B., Nordstrom D. K., and Wallschlager D. (2007) Importance of thioarsenates for arsenic redox processes along geothermal drainages, Yellowstone National Park. *Geochimica Et Cosmochimica Acta* **71**(15), A795-A795.

Radu T., Subacz J. L., Phillippi J. M., and Barnett M. O. (2005) Effects of dissolved carbonate on arsenic adsorption and mobility. *Environmental Science & Technology* **39**(20), 7875-7882.

Ravenscroft P., Burgess W. G., Ahmed K. M., Burren M., and Perrin J. (2005) Arsenic in groundwater of the Bengal Basin, Bangladesh: Distribution, field relations, and hydrogeological setting. *Hydrogeology Journal* **13**(5-6), 727-751.

Ravenscroft P., McArthur J., and Hoque B. (2001) Geochemical and Palaeohydrological Controls on Pollution of Groundwater by Arsenic. In *Arsenic exposure and health effects* (ed. W. R. Chappell, C. O. Abernathy, and R. L. Calderon), pp. 53-78. Elsevier Science Ltd.

Scheffer F. and Schachtschabel P. (2002) *Lehrbuch der Bodenkunde*. Berlin, Spektrum Akademischer Verlag.

Scott M. J. and Morgan J. J. (1995) Reactions at Oxide Surfaces .1. Oxidation of as(Iii) by Synthetic Birnessite. *Environmental Science & Technology* **29**(8), 1898-1905.

Smedley P. L. and Kinniburgh D. G. (2002) A review of the source, behaviour and distribution of arsenic in natural waters. *Applied Geochemistry* **17**, 517-568.

Stauder S., Raue B., and Sacher F. (2005) Thioarsenates in sulfidic waters. *Environmental Science and Technology* **39**(16), 5933-5939.

Staudinger G., Hangl M., and Pechtl P. (1986) Quick Optical Measurement of Particle Distribution in a Sedimentation Apparatus. *Particle and Particle Systems Characterization* **3**(4), 158-162.

Sun X. H. and Doner H. E. (1996) An investigation of arsenate and arsenite bonding structures on goethite by FTIR. *Soil Science* **161**(12), 865-872.

Swartz C., Blute N., Badruzzman B., Ali A., Brabander D., Jay J., Besancon J., Islam S., Hemond H., and Harvey C. (2004) Mobility of arsenic in a Bangladesh aquifer: Inferences from geochemical profiles, leaching data, and mineralogical characterization. *Geochimica et Cosmochimica Acta* **68**(22), 4539-4557.

Tossell J. A. (2005) Calculation of the interaction of bicarbonate ion with arsenites in aqueous solution and with the surfaces of Al hydroxide minerals. In *Advances in Arsenic Research*, Vol. 915, pp. 118-130.

van Geen A., Rose J., Thoral S., Garnier J., Zheng Y., and Bottero J. (2004) Decoupling of As and Fe release to Bangladesh groundwater under reducing conditions. Part II: Evidence from sediment incubations. *Geochimica et Cosmochimica Acta* **68**(17), 3475-3486.

Violante A. and Pigna M. (2002) Competitive Sorption of Arsenate and Phosphate on Different Clay Minerals and Soils. *Soil Sci Soc Am J* **66**(6), 1788-1796.

Wallschläger D. and Stadey C. J. (2007) Determination of (Oxy)thioarsenates in Sulfidic Waters. *Analytical Chemistry* **79**, 3873-3880.

Webster J. (1990) The solubility of As_2S_3 and speciation of As in dilute and sulphide-bearing fluids at 25 and 90° *Geochimica et Cosmochimica Acta* **54**(4), 1009-1017.

Wilkin R., Wallschläger D., and Ford R. (2003) Speciation of arsenic in sulfidic waters. *Geochemical Transactions* **4**(1), 1-7.

Zhao H. S. and Stanforth R. (2001) Competitive adsorption of phosphate and arsenate on goethite. *Environmental Science & Technology* **35**(24), 4753-4757.

Zheng Y., Stute M., van Geen A., Gavrieli I., Dhar R., Simpson H. J., Schlosser P., and Ahmed K. M. (2004) Redox control of arsenic mobilization in Bangladesh groundwater. *Applied Geochemistry* **19**(2), 201-214.

<u>DIN</u>

DIN Deutsches Institut für Normung e.V. (2004) *Plastics- Methods for determining the density of noncellular plastics Part 1: Immersion method, liquid pyknometer method and titration method (ISO 11831:2004)*; German version EN ISO 11831:2004, DIN Deutsches Institut für Normung e. V., Berlin, 14 p.

Appendix A Tables

Appendix A.1 Grain size distribution according USDA
(BRADY and WELL (2005))

	particle size [mm]
Clay	< 0.002
Silt	0.002-0.05
fine silt	0.002 - 0.02
coarse silt	0.02-0.05
Sand	0.05-2
very fine sand and fine sand	0.05-0.25
medium sand	0.25-0.5
coarse and very coarse sand	0.5-2

Appendix A.2 Depth profile with litholog

from [m]	to [m]	average [m]	Description Sediment
0.0	3.0	1.5	Hospital filling
3.0	3.7	3.3	sandy silt
3.7	4.6	4.1	
4.6	5.2	4.9	brown-grey fine sand
5.2	6.1	5.6	
6.1	6.7	6.4	grey clayey, silty fine sand
6.7	7.6	7.2	
7.6	8.2	7.9	grey fine sand – silt
8.2	9.1	8.7	
9.1	9.7	9.4	grey fine sand - silt with red hematite crystals
9.7	10.7	10.2	
10.7	11.3	11.0	grey fine sand
11.3	12.2	11.7	
12.2	12.8	12.5	grey fine sand, silty
12.8	13.7	13.2	
13.7	14.3	14.0	grey fine sand
14.3	15.2	14.8	
15.2	15.8	15.5	grey fine sand
15.8	16.7	16.3	
16.7	17.3	17.0	grey fine sand
17.3	18.3	17.8	
18.3	18.9	18.6	grey fine sand
18.9	19.5	19.2	grey fine sand
19.5	20.1	19.8	grey fine sand
20.1	20.7	20.4	grey fine sand
20.7	21.3	21.0	grey fine sand
21.3	21.9	21.6	grey fine sand
21.9	22.5	22.2	grey fine sand
22.5	23.1	22.8	grey fine sand
23.1	23.7	23.4	grey fine sand
23.7	24.3	24.0	grey fine sand
24.3	25.0	24.6	liner 21 empty
25.0	25.6	25.3	grey fine sand
25.6	26.2	25.9	liner 23 empty
26.2	26.8	26.5	grey fine sand, peat fragments
26.8	27.4	27.1	grey fine sand / clay
27.4	28.0	27.7	clay
28.0	28.6	28.3	clay
28.6	33.5	31.0	clay
33.5	34.1	33.8	fine sand / silt
34.1	34.7	34.4	clay

|			
34.7	36.5	35.6	clay
36.5	39.6	38.0	clay
39.6	42.6	41.1	clay
42.6	43.2	42.9	clay
43.2	43.8	43.5	clay / silt
43.8	45.6	44.7	clay, partly more silt
45.6	48.7	47.2	silty clay
48.7	51.7	50.2	clay
51.7	54.8	53.3	clay
54.8	57.8	56.3	clay
57.8	60.9	59.3	clay
60.9	61.5	61.2	clay, peat fragments up to cm size (liner broken)
61.5	63.9	62.7	clay
63.9	64.5	64.2	liner 33 empty
64.5	65.1	64.8	clay (liner broken)
65.1	66.9	66.0	clay with peat fragments
66.9	70.0	68.5	clay with peat fragments
70.0	73.0	71.5	clay with peat fragments, at the end no more peat fragments
73.0	75.5	74.2	clay, no peat
75.5	76.1	75.8	silty clay
76.1	79.1	77.6	silty clay
79.1	82.2	80.6	first few , from 265 ft on more brown medium to coarse sand pieces, maybe start even earlier, but mud pit was overflowing, backflow into hole might have suggested higher clay content than actually there
82.2	82.8	82.5	top clay, then brown, at bottom grey fine to medium sand
82.8	83.4	83.1	grey fine to medium sand
83.7	84.3	84.0	clay, very heavy

Appendix A.3 Development of pH and dissolved total As concentrations [mg/g] in MQ over 50 days equilibration time. Bolded values indicate pH values.

Day	pH 3	pH 4	pH 5	pH 6	pH 7	pH 8	pH 10	pH 10.5	pH 11	pH 12	pH 12.5	pH 12.5
0	**2.9**	**4.1**	**4.9**	**5.9**	**6.8**		**9.9**	**10.5**		**12.0**	**12.6**	**12.6**
	1.8	5.9	6.4	0.6	1.1		3.0	40.0		101.2	482.2	537.1
1	**2.9**	**4.1**	**5.2**	**5.8**	**6.6**	**8.0**	**8.9**	**10.1**	**11.0**	**11.9**	**12.5**	**12.7**
	9.7	9.2	10.2	6.7	8.1	3.2	12.2	58.9	5.2	312.0	651.9	576.4
3	**2.9**	**4.1**	**4.9**	**5.4**	**6.1**	**8.3**	**8.8**	**9.5**	**10.2**	**11.6**	**12.6**	**12.6**
	11.1	9.1	10.9	8.9	11.9	14.7	9.6	69.3	34.0	399.4	580.4	548.4
5	**2.9**	**4.1**	**4.9**	**5.4**	**6.0**	**8.0**	**8.6**	**9.5**	**10.0**	**11.4**	**12.3**	**12.4**
	8.3	7.9	8.8	8.2	9.0	15.6	11.6	69.2	46.9	459.1	577.0	449.3
8	**3.0**	**4.2**	**4.9**	**5.3**	**5.9**	**7.2**	**8.1**	**9.1**	**9.1**	**11.4**	**12.5**	**12.6**
	4.4	4.4	6.0	6.9	5.3	8.5	7.5	43.1	33.5	303.3	324.0	316.6
15	**3.1**	**4.3**	**5.1**	**5.3**	**6.1**	**7.2**	**7.9**	**8.5**	**8.7**	**11.2**	**12.4**	**12.4**
	5.7	6.1	5.4	7.1	9.7	9.2	7.9	35.4	45.6	328.3	322.1	279.4
37	**3.1**	**4.3**	**4.8**	**4.9**	**5.1**	**6.8**	**7.0**	**7.4**	**7.9**	**11.2**	**12.6**	**12.7**
	8.0	7.7	9.2	8.8	12.9	13.0	15.9	47.8	57.4	387.6	334.3	310.9
50	**3.0**	**4.2**	**4.6**	**4.7**	**4.7**	**6.3**	**6.6**	**7.2**	**7.4**	**11.1**	**12.5**	**12.6**
	5.4	6.1	7.7	6.9	8.7	12.2	14.6	40.8	50.8	274.0	337.8	309.7

Appendix A.4 Development of pH and dissolved total As concentrations [mg/g] in NaHCO$_3$ over 49 days equilibration time. Bolded values indicate pH values.

day	pH 3	pH 4	pH 5	pH 6	pH 7	pH 8	pH 9	pH 10	pH 11	pH 12
0	**3.1**	**4.0**	**5.0**	**6.0**	**7.1**	**8.0**	**9.1**	**10.0**	**11.0**	**12.1**
	1.0	1.2	1.2	0.9	0.6	3.1	3.4	9.0	32.1	133.8
2	**3.2**	**4.1**	**5.2**	**6.2**	**7.4**	**8.1**	**9.0**	**9.9**	**10.5**	**11.5**
	10.1	9.6	9.4	9.0	9.9	20.6	40.2	141.3	291.0	390.5
4	**3.2**	**4.3**	**5.5**	**6.5**	**7.7**	**8.3**	**8.9**	**9.8**	**10.5**	**11.5**
	9.7	9.7	9.6	9.2	12.8	30.6	64.8	275.1	392.9	586.5
7	**3.3**	**4.5**	**5.9**	**6.9**	**8.1**	**8.4**	**8.9**	**9.8**	**10.5**	**11.5**
	5.7	6.0	6.7	6.2	14.0	24.7	47.7	234.9	381.7	275.3
14	**3.2**	**4.6**	**6.4**	**7.3**	**8.3**	**8.5**	**8.8**	**9.7**	**10.4**	**11.3**
	5.7	6.0	7.9	9.6	21.3	35.5	63.8	299.9	332.0	298.8
35	**3.2**	**4.7**	**7.1**	**7.9**	**8.5**	**8.6**	**8.8**	**9.6**	**10.4**	**11.4**
	9.1	7.8	12.8	28.5	57.0	56.9	83.2	365.3	369.8	348.2
49	**3.2**	**4.6**	**7.1**	**8.0**	**8.5**	**8.7**	**8.8**	**9.7**	**10.5**	**11.4**
	9.4	19.0	17.4	35.6	127.2	69.5	79.2	410.0	334.1	347.3

Appendix B Figures
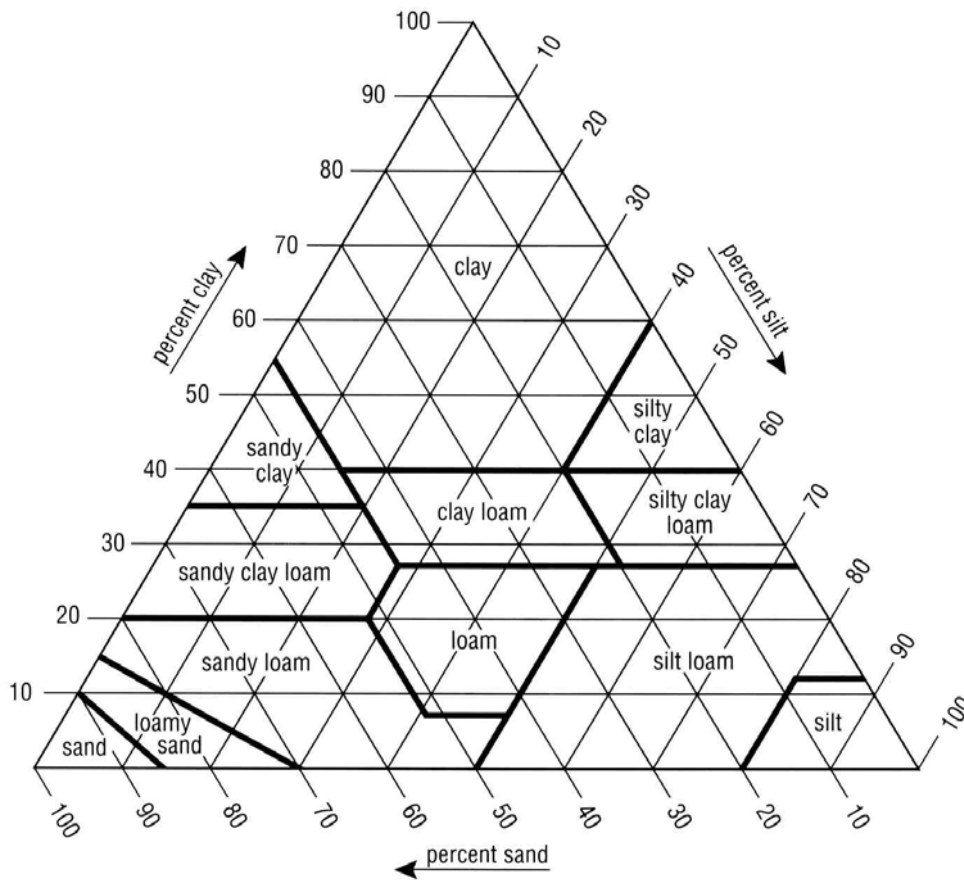
Appendix B.1 USDA Textural Triangel (BRADY and WELL, 2005)